Title	Modeling soil CO_2 and N_2O emissions and estimating carbon budget in agro-ecosystem at regional scale
Author(s)	李，琋
Degree Grantor	北海道大学
Degree Name	博士(農学)
Dissertation Number	甲第12005号
Issue Date	2015-09-25
DOI	https://doi.org/10.14943/doctoral.k12005
Doc URL	https://hdl.handle.net/2115/62865
Type	doctoral thesis
File Information	Li_Xi.pdf

Modeling soil CO_2 and N_2O emissions and estimating carbon budget in agro-ecosystem at regional scale

（土壌からのCO_2およびN_2O排出モデルの構築と地域レベルでの農業生態系炭素収支の見積もり）

Hokkaido University　　Graduate School of Agriculture
Division of Environment Resources　　Doctor Course

XI LI

Acknowledgements

First and foremost, I am heartily thankful to my supervisor Prof. Ryusuke Hatano, whose invaluable guidance, encouragement, supervision, and support for the whole study period enabled me to complete this study. My sincere acknowledgements are also extended to the members of the Advisory Committee: Prof. Munehide Ishiguro, Prof. Takashi Hirano and Assistant. Prof. Yoshitaka Uchida, for their constructive comments and suggestions on this manuscript.

I would like to express my gratitude to Mr. Iwasaki Shinya, Mr. Naoya Kajihara, Mr. Kei Takizawa, who accompanied me to field sampling and their valuable suggestions throughout my study. I deeply appreciate Mr. Kiwamu Ishikura for his kind support in statistics and modeling running and Dr. Chunying Wang for her valuable comments on soil water simulation by HYDRUS-1D. Sincerely thanks also offers to Dr. Nagaaki Sekiya who provided me the relevant data to calculate carbon budget. I deeply appreciate Asst. Prof. Toma Yo of Ehime University for his comments on carbon budget estimation, and his guidance and support for manuscript writing. I also would like to make a special reference to Prof. Sonoko D. Bellingrath-Kimura of Leibniz Centre for Agricultural Landscape Research Institute of Land Use Systems, with her valuable comments on uncertainty analysis and Dr. Lulie Melling of Tropical Peat Research Laboratory Chief Minister's Department whose encouragement for the doctor thesis writing.

I deeply appreciate Ms. Yoshino Nakamura and Ms. Kazumi Ishikuwa, for her kind support in dealing with various official matters related and her friendship.

It is a pleasure to thank all other colleagues in Hokkaido University for their kindness, support, encouragement, and friendship during my study in Japan. Special thanks are due to Asst. Prof. Kanta Kuramochi, Dr. Mariko Shimizu, Dr. Yohei Hamada, Mr. Atfritedy Limin, Ms. Mengjie Li, Mr. Adji Fengky, Mr. Ikabongo

Mukumbuta, Ms. Rina Kartikawati, Ms. Kayuko Ogura, Mr. Kentaro Ookura, Mr. Nagatake Arata, Mr. Kentaro Tanabe, Mr. Motohiro Yoshimura, Mr. Shuusuke Morita, Ms. Fu Yang, Mr. Vecky Varara, Ms. Rina Shirataki, Mr. Daiki Kamei, Mr. Arima Michinobu, Mr. Yuta Nobuoka, Mr. Hirokazu Nakamoto, Mr.Yosuke Morimitsu, and Mr. Priyo Adi Nugroho, Mr. Junki Tomohiro, Ms. Zaimire Abudushalamu, Mr. Hitoshi Tsukasaki, Ms. Fuyuko Hazama, Ms. Sachiko Takahashi, Ms. Hirono Kishimoto, Ms. Chihiro Naito, Dr. Jiang Rui, Dr. Jin Tao.

I would like to express my appreciation to friends in Information and Computational Science, The James Hutton Institute, Scotland, UK and Institute of Biological and Environmental Sciences, University of Aberdeen, UK for their kindness, support and friendship. Special thanks are due to Dr. Jagadeesh Yeluripati, for his comments, and suggestions about Bayesian calibration and guidance to calibrate the model. My grateful thanks are also due to Dr. Edward O. Jones and Pro. Jo Smith, for their guidance on model structure and ECOSSE calibration.

I would like to thank my families and friends in China and Japan for their moral support, love and patience.

I could not have carried out this study without the scholarship provided by the Chinese Government, Japan MEXT and Hokkaido University during the whole study period, for which I am very grateful.

Lastly, I offer my regards and blessings to all of those who supported me in any respect during the completion of the project.

Content

List of Tables

List of Figures

List of Abbreviations

C	Carbon
N	Nitrogen
SOC	Soil organic carbon
SOMD	Soil organic matter decomposition
WFPS	Water filled pore space
HB	Hierarchical Bayesian
CO_2	Carbon dioxide
N_2O	Nitrous oxide
NO	Nitrogen monoxide
CH_4	Methane
GHG	Greenhouse gas
CE	Carbon sequestration efficiency
NBP	Net biome productivity
NPP	Net primary productivity
Rh	Heterotrophic respiration

1. General introduction

Global climate change is becoming a hot issue in contemporary sciences as well as politics. A scientific consensus is forming that the emissions of greenhouse gases (GHGs), including carbon dioxide (CO_2), nitrous oxide (N_2O) and methane (CH_4), from anthropogenic activities may play a key role in elevating the global temperatures. The carbon (C) balance in terrestrial ecosystems has large implications on the variation in atmospheric CO_2 emission. Agriculture profoundly affects global C, water and nutrient cycles, as well as the planetary surface energy balance (Bondeau et al., 2007). Soils are the main source of N_2O emission and nitrogen monoxide (NO) emissions via microbial processes of nitrification and denitrification (Wrage et al., 2001). N_2O emissions currently increasing at a rate of 0.2–0.3% per year at agricultural field due to greater use of nitrogen (N) fertilizers which have enhanced these two processes (Abdalla et al., 2010). Quantifying soil GHGs emissions is an essential task for understanding the atmospheric impacts of anthropogenic activities in terrestrial agro-ecosystems.

CO_2 is released mainly from microbial decay or burning of plant litter and soil organic matter (SOM), which showed less spatial-temporal variable than N_2O emission (Wang and Chen, 2012). N_2O is primarily produced by the microbially-mediated nitrification and denitrification processes in soils (Davidson et al., 1991). Modeling is a useful tool for tracing detailed processes, estimating regional GHGs fluxes, and also predicting changes in the fluxes that will be caused by climate change (Del Grosso et al., 2005). In general, these estimations have been performed using detailed process-based models (Potter et al., 1996) or simple data-oriented models (Bond-Lamberty and Thomson, 2010), and these two approaches compensate for the disadvantages of each. The process-models are developed for tracing detailed processes. Whereas simpler models cannot trace such detailed processes, they are essential for incorporation into other models and require fewer inputs and are easier to handle (e.g., a simple model by Hashimoto et al., 2011).

Soil GHGs are influenced by a suite of climate and soil variables, interacting soil and plant N transformations (either competing or supplying substrates) as well as land management practices (Li et al., 2007). Computer simulation models, which can integrate all of these variables, are required for the complex task of providing quantitative determinations of N_2O emissions. Numerous process-based models have been developed to predict CO_2 and N_2O production (Chen et al., 2008), such as, NEMIS (Hénault et al., 2005), CERES-EGC (Gabrielle et al., 2006a) and DNDC (Li et al., 2005), however, they often require a large amount of input data that is not available at regional scale, which making regional and global emission estimates difficult to achieve (Bell et al., 2012). ECOSSE is a process-based model designed to simulate soil C and N stocks and gaseous emissions from using only data which is commonly available at a regional scale (Bell et al., 2012). Another limitation to the wide-spread use of these models lies in the fact that their predictions are highly dependent on parameter settings, and carry a large uncertainty due to uncertainties in parameter values, driving variables and model structure (Gabrielle et al., 2006a). Even though model parameterization and uncertainty analysis are widely developed in the literature on agro-ecosystem models, they are rarely considered simultaneously (Monod et al., 2006; Makowski et al., 2006).

The advantage of Bayesian statistics is that it can simultaneously take into account the uncertainty analysis and parameterization through calibrating unknown model parameters in terms of probability density functions (pdfs) with 95% confidence interval (CI) (Gallagher and Doherty, 2007; Gabrielle et al., 2006a; Xu et al., 2006); and also it can reduce the uncertainty associated with the parameters (Yeluripati et al., 2009). Different from nonhierarchical Bayesian model, the hierarchical model represents a modeling structure with capacity to exploit diverse sources of information, and yields subunit-specific parameter estimates, but shares commonality in values across systems. The nonhierarchical Bayesian model assumes that there is a "true" parameter value that is incrementally approached with increasing sample size. However, Hierarchical Bayesian (HB) assumes that parameter has distribution of its own; therefore hierarchical model assigns two hyper parameters to yield the posterior distribution of each subunit-specific parameter. It be beneficial to identify such "hyper parameters" to explain variability of parameter. Thus, HB models have been developed in recent years for a number of environmental applications (Borsuk et al., 2001; Agarwal et al., 2005; Cable et al., 2009; Patrick et al., 2009). In general, the current challenge is how to scale up the relatively more robust field-scale model to catchment, regional and national scales, meanwhile, the uncertainty analysis and parameterization should be taken into account simultaneously.

Assessment of soil C stock changes over time is typically based on application of two methods, namely (i) repeated soil inventory and (ii) determination of the net biome productivity (NBP) by continuous measurement of CO_2 exchange in combination with quantification of other C imports and exports (Leifeld et al., 2011). However, soil C inventory has some limitation, such as not providing an annual C budget, not necessarily taking into account dead organic matter C, and placing limitations on extrapolation due to high spatial variability. The NBP is the term applied to the total rate of organic C accumulation (or loss) from ecosystems (Chapin III et al., 2006; Schulze and Heimann, 1998; Buchmann and Schulze, 1999). The main advantages of using NBP to calculate C budget arise from their: (i) spatial explicitness, (ii) flexibility over a range of crops, (iii) reflection of local varieties and field management practices used in the study area and (iv) allowing a simple estimation of annual plant C inputs.

In principal, an indication for the uncertainty in NBP should be provided and thus a direct quantitative evaluation of methods is available. Meanwhile, the NBP value for an agricultural system should be directly comparable with the C stock change measured by repeated sampling of soil, but up to now, there has been few field study that directly compared the two approaches at an agricultural system at the regional scale.

The specific objectives are:

1. To design and produce the model to simulate CO_2 from soils (CO_2-HB) based on simple model theory using soil temperature, soil water and soil information and to quantify uncertainty by developing a suitable calibration method, and to up-scale the CO_2-HB model at regional scale and incorporate it into other model as sub-model.

2. To design and produce the model to simulate N_2O and NO emissions from soils (N-HB model) and to quantify the uncertainty of model simulations by developing a suitable calibration method, and to investigate the model extrapolation and the parameters' variability using soil information.

3. To explore trends and interannual variability of NBP at regional scale, focusing on the spatial and temporal patterns of NPP, crop residue inputs at main land use: upland, paddy and grass from 1959 to 2011 by using relationship-based estimation of plant C inputs and CO_2-HB modeling, and to verify the C stocks change at main land uses from 2005 to 2011 by comparing two methods: (i) repeated soil inventory and (ii) C flux budget (NBP).

There are a total of 8 chapters in this thesis. This introduction (Chapter 1) is followed by a literature review (Chapter 2), where studies on simulating the greenhouse gases (GHGs) emissions in agricultural soils and the agro-ecosystem global warming potential and net biome productivity (NBP) during the last century are reviewed. Chapter 3 describes a general introduction of Ikushubetsu watershed, introduction of monitoring data of GHG gas, introduction and application of Bayesian method to the monitoring data, and application of CO_2-HB model to estimate C change at regional scale. Chapter 4 presents modeling soil CO_2 flux from cropland using soil texture (CO_2-HB model). Chapter 5 presents modeling soil N_2O and NO fluxes from cropland (N-HB model). Based on the estimation done in Chapter 4 and Chapter 5, applying CO_2-HB model to estimate the NBP at regional scale during the last four decades was presented in Chapter 6. Finally, all results are discussed in general and together with outline of further research needs in Chapter 7.

2. Literature Review

2.1 Greenhouse gas (GHG) emissions in agricultural soils

Agricultural lands occupy 37% of the earth's land surface. Agriculture accounts for 52% and 84% of global anthropogenic CH_4 and N_2O emissions (Smith et al., 2007b). Agricultural soils may also act as a sink or source for CO_2. Agriculture releases to the atmosphere significant amounts of CO_2, CH_4 and N_2O (Cole et al., 1997; Haines, 2003; Paustian et al., 2004). CO_2 is released largely from microbial decay or burning of plant litter and soil organic matter (Janzen, 2004; Smith et al., 2004). CH_4 is produced when organic materials decompose in oxygen-deprived conditions, notably from fermentative digestion by ruminant livestock, stored manures and rice grown under flooded conditions (Mosier et al., 1998). N_2O is generated by the microbial transformation of N in soils and manures, and is often enhanced where available N exceeds plant requirements, especially under wet conditions (Smith and Conen, 2004; Oenema et al., 2005).

2.1.1 Mechanism of carbon and nitrogen dynamics in upland agricultural soils

Upland soils constitute the majority of soils in agricultural areas throughout the world. Because these soils tend to be better aerated than wetland soils, oxygen presence plays a key role in the process dynamics and management responses of these systems, and generally promotes higher decomposition rates of organic materials compared to wetland soils. Periodic wet and dry cycles on a seasonal or more frequent basis cause temporary shifts in oxygen (O_2) availability that in turn affect process rates and directions. The landscape position of agriculture upland soils promotes drainage and movement of nutrients and soil particles to lower lying areas, and aspect exposure can have significant effects on temperature and water retention regimes. Location of the soils on the Earth relative to latitude and elevation also plays an important role in the accumulation of soil organic matter (SOM) and associated C/N dynamics (Povirk et al., 2000). Particularly in far, upland soils have experienced dramatic changes since the introduction of agriculture (Dregne, 1982). Losses of SOM in the surface horizons from erosion and accelerated decomposition rates have been pronounced worldwide, and continue to occur especially in areas converted from the native condition within the past 50 to 100 years (Miller et al., 1985).

2.1.2 Carbon cycling in upland agricultural soils

Organic C in upland soil occurs as SOM, dead and living plant material (tops and roots), micro-flora biomass (dead and living), and soil micro-, and macro-fauna (dead and living). Fractionation of C into various designated pools for purposes of analysis by empirical methods and simulation modeling has been attempted for many years. C pools used in the simulation models are mostly conceptual (Ma and Shaffer, 2001; McGechan et al., 2001) and are only approximately correlated with the physical/chemical/biomass pools described above. Soil organic C (SOC) in soils is a continuous (time and space) product of microbial processes, and fractionation into pools probably should be entirely microbial based. In general, the physical C pools are described based on size and include litter or easily recognizable residues (>2 mm in size), a light fraction that can be floated off using dense liquids (0.25 to 2 mm in size), and particulate organic matter that is separated using dispersion and physical separation techniques (0.05 to 2 mm in size) (Jenkinson et al., 1991). Soil microbial biomass C is determined using the chloroform fumigation-incubation (CFI) method (Jenkinson et al., 1991); and more resistant forms of SOM, including humic acid, fulvic acid, and humin, are fractionated using chemical techniques such as the HCl and NaOH methods (Ping et al., 2001). As an approximation, most model-based pools can be compared to the physical/chemical/microbial pools as follows. The fast SOM model pools are similar to the light and/ or particulate pools, the microbial biomass pools are similar to each other, and the slow SOM model pool is similar to the resistant SOM pool. In some cases, the slow residue model pool may be similar to the light SOM pool. The model pools are highly dynamic and initialization depends on the design of the model, the rate coefficients, and the relationships of model C/N components to other parts of the model.

The relative contributions of above- and below-ground higher plant parts to SOC vary depending on the ecosystem involved. Agricultural system receives the majority of its SOC from above-ground plant parts, while grassland and tundra systems receive SOM primarily from root decay (Povirk et al., 2000). Sobecki et al. (2001) present a comparison of standing organic C residues for various ecosystems such as forests, grasslands, tundra/desert, and croplands. Forests have the most above- and below-ground biomass C, with 177 Mg C ha^{-1}, followed by grasslands with 19.8 Mg C ha^{-1}, croplands with 16.4 Mg C ha^{-1}, and tundra/desert with 4.2 Mg C ha^{-1}. Living microorganisms mediate the vast majority of the C/N cycling processes in soils, although these organisms constitute only about 0.3 to 5% of the SOM C. Microbial activity in soils is highly dependent on the presence of C substrates, which is why most activity and associated microbial biomass occurs near the soil surface and immediately after introduction of residues.

Soil inorganic C in the form of CO_2, bicarbonate, and carbonic acid, and soil and rock carbonates constitute most of the remaining C (Monger and Martinez-Rios, 2000). Given a long enough time period, C cycles among all of these pools. Cycling times vary from a few hours for CO_2 and plant materials, to a few weeks for plant material and fresh SOM, to several decades for labile SOM, to thousands of years for stable SOM, and to millions of years for carbonate rocks. Of most concern to agricultural manager and modelers is SOM with short turnover times up to several decades. This material supplies nutrients to the crops and can be managed and replaced, while the older material needs to be protected but is less easily managed. Cycling of C is closely tied to cycles involving other soil nutrients, such as N, phosphorus, sulfur, potassium, and trace constituents (McGill and Cole, 1981).

Upland agricultural soils have been studied extensively over the years under a range of management and climate regimes. For example, long-term plots such as the High Plains Agricultural Laboratory site at Sidney, Nebraska (Lyon et al., 1996), and the Morrow Plots at Urbana, Illinois (Darmody and Peck, 1996), provide evidence of the effects of long-term agricultural management on soil C, fertility, and crop productivity. The decrease in soil C in these plots relative to the native state is quite evident and ranges from 40 to 80%. Disturbances resulting from cultivation (biological oxidation), removal of crop residues, and soil erosion are factor in these losses (Darmody and Peck, 1996). In the case of biological oxidation, disturbance of the soil from tillage has been shown to release significant amounts of CO_2 gas (Reicosky et al., 1995). Buyanovsky et al. (1996) have demonstrated that decomposition of crop residues such as corn, wheat, and soybean returned to the soil makes only a minimal contribution to the more stable (long-term) soil C pool. Most of the C cycling from crop residues takes place in the faster, less stable pools. However, the return of crop residues to the land, rather that removal, has produced significant increase in organic C levels (Buyanovsky et al., 1996).

The introduction of reduced tillage and no-till has had significant impacts on C/N cycling. This is due primarily to decreased mixing of residues in the plow layer and a decrease in aeration plus and increase in soil water content. Soil organic C levels are significantly higher under no-till, especially near the surface (Peterson and Westfall, 1996).

2.1.3 Nitrogen cycling in upland agricultural soils

Considerable work has been published over the past several decades on C/N dynamics in soils (Campbell et al., 1995; Nakane et al., 1997; Janzen et al., 1997). The N and C cycles are closely linked and cannot be effectively studies or modeled separately (McGill and Cole, 1981). This is especially true with upland agricultural soils where good aeration coupled with periodic wet-dry and temperature cycles direct the microbial and plant biological processes and significantly influences the physical processes. In fact, most models simulate N cycling from C cycling. N cycle occurs along with C in all of crop residue and SOM pools and also occurs as inorganic NO_3^- and NH_4^+, urea, and as N_2, N_2O, NO_x, and NH_3 gases. The relative amounts of N found in the soil generally are SOM-N > residue-N > NH_4^+-N > gaseous-N forms. From the standpoints of mobility and negative effects on the environment, NO_3^--N and the gaseous-N forms (N_2O, NO_x, and NH_3) are of most concern.

The N cycle in upland soils is shown in Figure 2.1. N enters the soil symbiotic plants (e.g., legumes) fix N, from animal manures, and from the addition of commercial fertilizer and other organic materials such as sewage sludges and compost. Soil losses of N include removal in crops, nitrate (NO_3^-) leaching, denitrification and gaseous losses as NH_3^-, and losses in surface runoff and erosion (Römkens et al., 1973). The relative N loss amounts are highly variable and any of these major loss components can dominate given the right conditions. These may occur rapidly and major soil N changes can occur within a few hours or days (Shaffer et al., 1994).

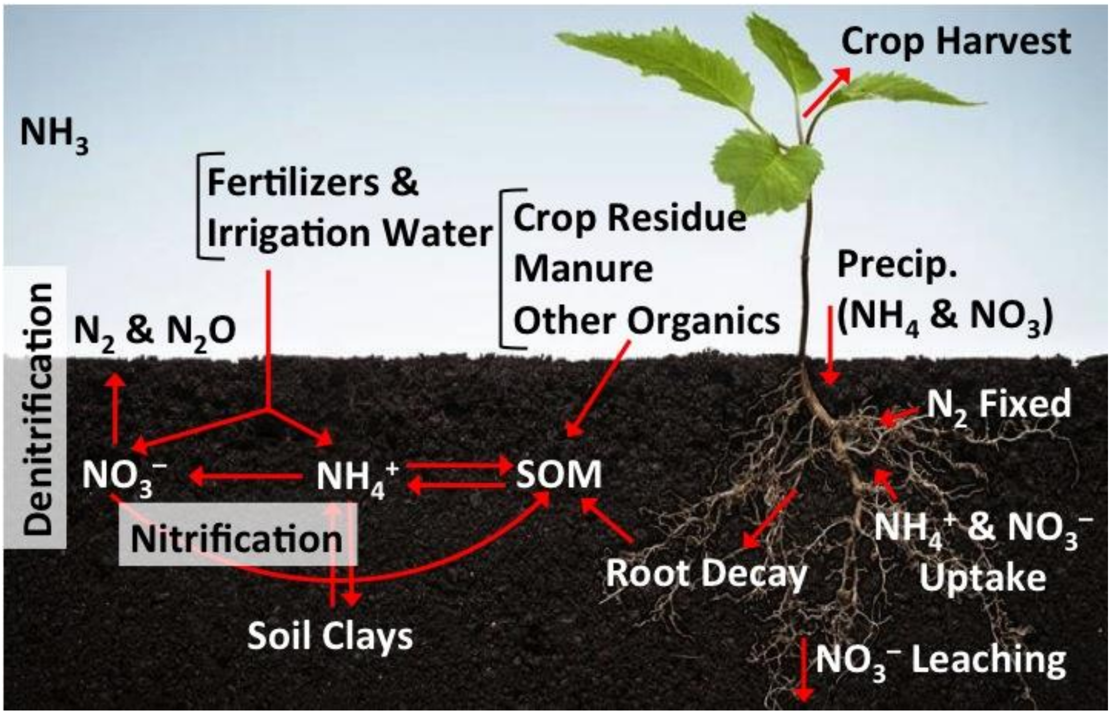

Figure 2. 1 The nitrogen cycle in soils.

Figure 2.1 also depicts N cycling or turnover within the soil where, under aerobic conditions, the microbial processes of mineralization (or ammonification) decompose residues and SOM to NH_4^+ and more stable forms of SOM. CO_2 is the primary by-product, although temporary or localized anaerobic conditions in upland soils can also result in ammonification with the by-product CH_4 being produced instead of CO_2.

The heterotrophic microorganisms (primarily soil fungi along with lesser biomass quantities for bacteria and actinomyces) utilize C and N from the decomposing residues and N from the soil NO_3^- and NH_4^+ pools to produce microbial biomass. This biomass generally ranges from about 250 to 900 kg C ha^{-1} for a range of agricultural soils (Doran, 1987). Rangeland biomass levels in the top 30 cm range from 65 g m^{-2} to 635 g m^{-2}, depending on the type of prairie ecosystem (Reeder et al., 2000). With C-rich residues such as wheat and barley straw C/N is higher than 80, insufficient N is available in the residues to supply the demand of the biomass growth (C/N=6), resulting in temporary net uptake or immobilization of mineral soil NO_3^- and NH_4^+. NH_4^+ then released from microbial biomass when the microbes die. However, crops will not have access to this N source while it is immobilized. In general, decay of residues with C/N ratios greater than about 25 or 30 will cause temporary net immobilization, while lower C/N ratios result in net mineralization. Systems decomposing residues with C/N ratios greater than 30 may become deficient in mineral N and become self-limiting in their ability to decompose these residues. Soil temperature and moisture content are important state variables in the mineralization process and control the microbial rates of growth and death (Melillo et al., 1989).

N has the capacity to cycle fairly rapidly between the inorganic and organic forms within the soil and a few weeks can see the complete turnover of some inorganic/organic N forms. Conversely, some forms of organic N, such as soil humus, may be very stable and have an age of several thousand years. Studies to identify the relative ages for SOM pools have been performed using C isotope ratios (Follett et al., 2015).

Conversion of NH_4^+ to NO_3^- is called nitrification and is mediated by specific genera of aerobic autotrophic microorganisms, namely Nitrosomonas and Nitrobacter (Alexander, 1977). These organisms use CO_2 as a C source, with Nitrosomonas oxidizing NH_4^+ to nitrite (NO_2) and Nitrobacter converting NO_2^- to NO_3^-. Nitrification state variables in upland soil include temperature and water content with a strong dependency on pH. Nitrification rates in uplands soils are generally medium relative to other C/N cycling processes, and 2 to 4 weeks are usually needed in the warmer months to nitrify and application of commercial ammonia-based fertilizer. The nitrification process is not 100% efficient and some conversion of NO_3^- to N_2O and NO_x greenhouse gases can occur (Xu et al., 1998). Nitrification is sensitive to soil pH, with significant reduction in process rats below pH 6.0 and above pH 8.0.

Nitrification inhibitors such as nitrapyrin have been developed that slow the process by enzyme inhibition of Nitrosomonas (Peoples et al., 1995).

Denitrification involves the conversion of NO_3^- and NO_2 to N_2, N_2O and NO_x. The process is mediated primarily by facultative anaerobic bacteria that oxidize organic C and reduces N oxides in the absence of O_2. The key to understanding and simulating denitrification in upland agricultural soils is the transient and localized nature of the anaerobic conditions. Complete reduction of N oxides to N_2 is an anaerobic process, while partial or transient anaerobosis results in the production of N_2O and NO_x. Denitrificaiton tends to be a very rapid pulse process with major losses of soil N possible in a single day given the right conditions (Xu et al., 1998). Ideal pulse conditions involve the occurrence of significant amounts of soil NO_3^-, a fresh C source such as manure or other residue SOM, warm temperature, a precipitation or irrigation event, or temporary flooding (Tiedje, 1988). These conditions are common in the early spring or summer in upland soils and apply to production of the greenhouse gases and N_2 (Tiedje, 1988).

Gaseous loss of NH_3 from upland agricultural soils is primarily a soil surface process. In addition, it is one of the few soil N processes that is abiotic and not directly mediated by microorganism, although they play a key role in NH_4^+ production. NH_3 gas exists in chemical equilibrium with the NH_4^+ ion in soil water, and the reaction is highly dependent on soil pH. Applications of ammonia fertilizer and manure to the soil surface set the stage for major N losses as NH_3 volatilization. The process is enhanced by high pH levels (>8.5) and by wind and high temperatures (Smith et al., 1996). Incorporation of fertilizers and manure into the soil can significantly reduce or eliminate NH_3 volatilization.

Nitrate leaching below the crop root zone of upland soils is a primary mechanism for N loss from these soils and contributes to pollution of underlying shallow aquifers. Nitrate leaching amounts from upland soils vary greatly, but values from less than 25 to greater than 300 kg ha^{-1} yr^{-1} are common depending on management, soil and climate. Leaching of NO_3^- is a pulse process keyed to precipitation and irrigation events, but tied closely to previous N and water management, crop N uptake, and soil texture (Shaffer et al., 1994). NO_3^- is highly soluble in water and move quickly along with the water transport because they are not usually adsorbed by soil particles. Once leached below the root zone, recovery or reduction of NO_3^- is difficult and further downward movement over time can result in contamination of the ground water (Shaffer et al., 1995). Application of a NO_3^- leaching index for annual mass of NO_3^- leached below the crop root zone can be used to help identify potential "hotspot" regions in aquifers (Shaffer et al., 1995). Leaching of NO_3^- can be controlled by applying fertilizers and manure in smaller increments as needed by the crop to reduce the potential leaching risk from precipitation and irrigation, and by managing water applications where appropriate to reduce leaching (Shaffer et al., 1994; Follett et al., 2015). Other mitigation techniques such as planting deep-rooted cover crops can be beneficial.

Plant uptake of NO_3^- and NH_4^+ represents an important sink process in the N cycle and proper accounting is essential for simulation of C/N cycling and NO_3^- leaching in soils (Follett et al., 2015). For agricultural crops on upland soils, typical crop uptake of N is from amount 50 to over 400 kg N ha^{-1} yr^{-1} (Follett et al., 2015). Producers are tempted to pre-apply large doses of commercial fertilizers of manure to help ensure that the crop will not become nutrient deficient. However, this practice runs the risk of losing significant amounts of N to the major sinks such as NO_3^- leaching, denitrification, and NH_3 volatilization. Nitrifier populations have decreased by 16 to 56% in reduced and no-till plots relative to conventional tillage. While denitrifier populations have increased (Lyon et al., 1996). Microbial biomass levels of no-till soils averaged 54% higher in the surface layer compared to plowed soils (Doran, 1987).

2.2 Methods for simulating greenhouse gas (GHG) emissions from soil

A significant number of models for predicting GHG emissions from agricultural lands have been developed. Each of them has been developed for a specific purpose, with their own view and interpretation of the processes and controlling variables for GHG emissions, with its unique strengths, limitations and for different scales, ranged from laboratory, field, regional to global scales. Increased emphasis on up-scaling processes at various scales has been evident in the more recent literature.

2.2.1 Laboratory scale to field scale models

The laboratory-scale models simulate microbial growth, substrate dynamics, solute and gas transport through the soil profile and aggregates, and mostly are used to test the researchers' hypothesis of mineralization, nitrification, denitrification and associated mechanisms of C and N trace gas emissions from soils. The major factors considered at this level are soil water content, soil pH, soil organic C content, ammonium and NO_3^- concentrations and soil temperature. The laboratory models explicitly simulate the denitrification reaction, but only for singular incubation experiments with limited applications outside of these strict boundaries. In addition, the N_2O contribution from soil nitrification is not simulated. Because of the complexity across natural and agricultural ecosystems, the application of laboratory-scale models is very limited. However, the laboratory-scale models serve as the theoretical basis for more complex field-scale models (e.g. DNDC, DAYCENT, ECOSSEs and WNMM) which incorporate soil water dynamics, plant growth, C and N cycling and the impacts of site-specific soil properties, climate and agricultural management practices.

2.2.2 Field to regional models

Field-scale models have received the most attention in last two decades due to the need to simulate 'real world' conditions by integrating generic processes in plant-soil C/N and water cycling and anthropogenic influences (i.e. land use change and management practices). A field-scale model can also be used to develop a decision support system for mitigation (Chen et al., 2005). Review from Langeveld and Leffelaar (1996) outlined several common features within the process-oriented N_2O emission simulation models: soil-air atmosphere and climate interactions, plant growth, C and N cycling, and land use management. In the N cycling component of each model, the contributions of N_2O from both denitrification and nitrification are estimated. These models reviewed in this paper include NGAS-DAYCENT (Mosier et al., 1983; Mosier and Parton, 1985; Parton et al., 1988b; Parton et al., 1988a; Parton et al., 1996; Parton et al., 2001; Del Grosso et al., 2000), DNDC (Li, 2000; Li et al., 1992) , NLOSS (Riley and Matson, 2000), Expert-N (Engel and Priesack, 1993), WNMM (Li et al., 2005), FASSET (Chatskikh et al., 2005) and CERES-NOE (Hénault et al., 2005; Gabrielle et al., 2006b).

Field-scale models such as DNDC, DAYCENT, and WNMM have also been coupled with GIS or have the built-in spatial capability for application at regional scales, to estimate the spatial and temporal variability of GHGs emissions in different landscapes if the detailed spatial information (specifically climate and soil) required by these models is available. With spatially explicit input data, it is possible to explore inter-daily, inter-seasonal, and inter-annual variation of GHG emissions in direct response to soil, climate and sub-regional management practices. Whilst the use of very simplistic approaches such as the IPCC methodology for identifying, climate or annual differences across a region is not possible, regression models such as those developed by Hargreaves et al. (1994) and Sozanska et al. (2002) may work.

If users are only interested in the spatial pattern of annual GHGs emissions from agricultural soils, e.g. for regional or national inventories, it may not be essential to use a detailed field-scale models to simulate specific management interactions in fine detail because of the intensive data requirements. A calibrated regional-scale models may be adequate for such a task whereby a select series of pre-determined simulations are run using the field-scale approach but then articulated as simpler GHGs responses based on regressions. The land use, soil type, topography and climate are generally recognized as the major environmental controlling factors to contribute to the spatial and temporal variations of GHGs emissions from landscapes, and, thus such information is often used for constructing regional-scale models.

2.2.3 Regional scale to global scale models

The regional/global-scale models can produce the monthly, seasonal or annual pattern of GHG emissions for large landscapes or globally by using a few parameters through regression models, scaling approaches, empirical models, or in rare cases, simplistic mechanistic or processed-oriented models such as NASA CASA. In contrast to field and regional scales models, there are few published modelling approaches at the global level: the monthly version of the NASA CASA model (Potter et al., 1996), Bouwman's scaling model (Bouwman et al., 2002), the IPCC scaling model (UNEp, 1995; Gómez et al., 2006) and FAO/IFA model (FAO/IFA 2001). The total amount of global annual N_2O emissions from soils estimated by Bouwman's model is 6.9 Tg N yr^{-1}, while NASA CASA predicted 6.1 Tg N yr^{-1} N_2O emissions globally. In terms of global estimates of N_2O emissions from agricultural lands, the prediction by FAO/IFA model (2.9 Tg N yr^{-1}) FAO/IFA (2001) is higher than that by the NASA CASA model (2.1 Tg N yr^{-1}) (Potter et al., 1996). The FAO/IFA estimation was developed using higher resolution land use and management data than the other approaches.

Some field and regional models have the potential for upscaling to provide global annual N_2O emissions, but the underlying uncertainty is potentially large due to the fact that field and regional models were normally calibrated for localized areas, e.g. several to thousands hectares. Even though many of the processes underpinning the soil C, N and water cycles are generic, when applying some models to different climatic zones or latitude regions in which they were developed, the originally boundary conditions in these models may be exceeded, For example, the findings by Sabey et al. (1959) and Malhi and McGill (1982) indicated that the optimal temperature for soil nitrification process tends to decrease from tropical to cool temperate regions. The DNDC and DAYCENT models are probably the two most prolific models in use today across a variety of scales and environments and continue to be used by a diverse group of users around the globe.

2.3 Existing studies on parameterization and uncertainty in modeling greenhouse gas emissions from soil

Several studies on model comparisons and testing via experimental data indicate that on one hand, in-depth studies via lab and field experiments on the physical, chemical, and biological mechanisms for each process are still needed; on the other hand, significant knowledge gaps exist in the development of reasonable models and the application of appropriate models: (a) limited temporal and spatial experimental data is available for model calibration and verification; (b) multiple processes and complex model structure engender great challenges in model parameterization; and (c) a lack of information on uncertainties from different sources brings difficulty in model selections and applications (Chen et al., 2005; Wu and McGechan, 1998).

2.3.1 Parameterization

Process-oriented models have led to a better understanding of C and N transformation processes, and resulted in complexity and difficulty in model parameterization. There are three categories of model parameters controlling C and N processes: (a) experimentally measureable parameters (e.g., weather data, topographic and soil data, management practices); (b) internal parameters that cannot be directly measured (e.g., nitrification/denitrification rate constant); and (c) the parameters that depend on other processes in an ecosystem (e.g. soil water movement and heat transfer, may be measured at limited sites within a very small region) (Ma and Shaffer, 2001). However, it is neither economical nor practical to conduct continuous field observation in a large area because of the temporal and spatial variability. For these reasons, the response functions of soil water and temperature were used in models to modify the transformation rates (Li et al., 1992).

Consequently, one of the main tasks for parameterization is associated with the second category of parameters. Fortunately, some model developers have prepared a database for the parameters corresponding to specific conditions, especially topography, land cover, and soils. For instant, DNDC provides a graphical user interface (GUI) with geographical information system (GIS) for users to select the study area, where the corresponding county-level database is used to parameterize and initialize the model (Li, 2007). Wu and MCGechan (1988) selected the major parameter values for SOILN model based on a combination of field experiments and literature sources. Some parameters were estimated from short-term experiments, thus it is difficult to achieve good simulation results at any specific site. This means that model calibration is still essential.

Due to the complexity of process-based model, the subjective optimization method (McCuen, 2003) was usually used to manually adjust parameter values based on the modeler's subjective knowledge. The subjective optimization method requires modelers to have a good understanding of both parameters and input data. A limited number of parameters are selected for model calibration, and usually one parameter is adjusted at each model run. Undoubtedly, it is a great challenge for users to apply the model to their own studies.

2.3.2 Uncertainty

The efficacy of mathematical modeling as a tool for estimating GHG emissions from soil depends on the uncertainty. Studies on systematic evaluation of various sources of uncertainties in GHG models are still limited. Most studies currently focus on uncertainty from individual sources, e.g., parameter or input. In addition, the methods are confined to simple sensitivity analysis and Monte Carlo simulations. The sensitivity analysis of PnET-N-DNDC model to changes in environmental factors indicated that the simulated N-trace gas emission varied with measured ranges (Stange et al., 2000). The environmental factors include temperature, precipitation and some model input variables (litter mass, SOC, pH, soil texture, etc.). The sensitivity analysis was conducted by changing one factor and keeping all others constant. Abdalla et al. (2010) and Thorsen et al. (2001) used the Monte Carlo method to analyze the propagation of uncertainty from input data to model output, and found that the magnitude of uncertainty was significantly associated with the investigated temporal and spatial scale, ie., smaller output uncertainty on catchment scale than on gird level. Reth et al. (2005) used the Monte Carlo technique to assesse the uncertainty of model output, where a Gaussian distribution within ± one standard error was used for parameter sampling. Reth et al. (2005) concluded that the uncertainty of DenNit output was about 32% for unlimited nutrient availability and the optimum values of soil temperature, water and pH values. In the comparison of C and N dynamics under conditions of conventional and diversified rotations, 64 parameter combinations were identified to test their impacts on model outcomes (Tonitto et al., 2007).

DNDC has provided an uncertainty analysis tool for SOC, clay, bulk density and pH value. This tool allows for the selection of either Monte Carlo or Most Sensitive Factor (MSF) method (Li, 2007). The MSF method involves running the model twice for each spatial unit with the maximum and minimum parameter values. These two runs generate two gas fluxes to form an interval the theoretically covers the real gas fluxes with a high probability (Li, 2007). Using this uncertainty model, several highly sensitive factors influencing DNDC model were identified. N_2O emission was found to be sensitive to soil clay content, SOC and mean annual temperature; while CO_2 emission was significantly affected by SOC, clay fraction, mean annual temperature and annual precipitation (Li et al., 1992).

The Monte Carlo analysis was also adapted to assess uncertainties in soil N_2O simulations from model input and structure of DAYCENT (Del Grosso et al., 2005). Probability distribution functions (pdfs) of major model inputs (weather, soil texture, and N applications) were assigned to quantify the uncertainty due to model inputs. The structural uncertainty was a synthesis of parametric uncertainty and model residual errors derived by an empirically-based linear mixed effect model (Ogle et al., 2007). Based on the range of confidence intervals of simulated N_2O, they concluded that the total uncertainty was majorly attributed to model structure (80–85%) rather the model input (Del Grosso et al., 2010).

The Bayesian inference based on Markov Chain Monte Carlo (MCMC) has been used to calibrate parameters and quantify parametric uncertainty in the N_2O submodel of CERES-EGC (Lehuger et al., 2009). The uniform probability distributions were assigned as a priori for 11 global parameters. The uncertainty in N_2O simulations was significantly reduced by the site-specific calibration.

HB models have been developed in recent years for a number of environmental applications (Agarwal et al., 2005; Cable et al., 2009; Yeluripati et al., 2009). This approach allows model inferences to be shared across sites (or other subunits, such as species) and yields subunit-specific parameter estimates. While HB model is clearly not the only way to address uncertainty, it stands out as an approach that can accommodate complex systems in a fully consistent framework. (Malve and Qian, 2006) indicated that a hierarchical modeling approach can be used to pool data from different sources to reduce the model uncertainty and improve the parameter accuracy; additionally, a hierarchical model can be used to form a realistic model without over-fitting the data by obtaining sufficient data from the hierarchical probability distribution.

2.4 Assessing greenhouse gases (GHGs) and net biome productivity (NBP) at regional scale

The NBP is the C remaining in the ecosystem when all other fluxes have been accounted for (Schulze and Heimann, 1998; Chapin III et al., 2006). In croplands, due to the removal each year of the crop material, the NBP is estimated by measuring the long-term change in SOC.

For soil C, long-term C cycling is often studied by measuring changes in total SOC over long periods (years to decades; Smith et al., 1997). In many sites, while SOC concentration has been measured over many years, calculation of total SOC concentration has been hindered by the absence of data on soil bulk density and by discrepancies in sampling techniques (e.g. no standardization of soil depth and of soil layers). In the last decade, individual long-term experiments have been brought together into networks such as the Soil Organic Matter Network (SOMNET (Smith et al., 1997), EuroSOMNET (Smith et al., 1997) and LTSE (Richter Jr, 2014)). Such networks allow the impacts of management practices on SOC stocks to be determined and for regional projections of the impact of different management strategies to be explored (e.g. Ogle et al., 2005).

In addition to measurement of changes in bulk SOC, other techniques are now being used to better understand SOC turnover. Various fractionation techniques are being used to isolate different components of SOC (e.g. Six et al., 2011; Del Galdo et al., 2003) to better understand SOC turnover, and to identify sensitive indicators of SOC change. Mathematical methods to test the relationship between measured fractions and model pools are being developed (e.g. Smith et al., 2002; Zimmermann et al., 2007), in order that this information can be incorporated into process-based models.

The main method for interpreting flux (and other) results, and for extrapolating temporally and spatially the data in ago-ecosystem (and other systems), is the use of process-based models (Wattenbach et al., 2010). Process-based models are continually being improved, with the most significant advance in the last decade being the development, and testing of models that simulate all biogenic GHGs. The main hurdle to applying such models at the regional level is data limitation. In recent years, high-resolution, spatially-explicit datasets have become more readily available. National, regional and global databases have been improved and it is now possible to run models for entire sub-continental regions (e.g. Europe, USA) at fine spatial scale such as a 10’ by 10’ grid (Gervois et al., 2008; Wattenbach et al., 2010), at US county level (Parton et al., 2005) or even at 1 km^2 grid scale. Historical climate data have been interpolated to higher spatial resolution and future climate scenarios from global climate models have been downscaled to the same spatial resolution (e.g. Mitchell et al., 2004). Soil data are now available at high spatial resolution (e.g. at 1km^2 for Europe, Jones et al., 2005) and historical land-use data and future land use scenarios are beginning to be constructed at high resolution (e.g. Rounsevell et al., 2006). There are many areas in which these datasets require further improvement, but significant advances have been made in some regions in recent years, including in Europe. In some other regions, however, especially in the developing world, such datasets are poor or non-existent. The development of airborne (satellite data) and ground flux measurements can provide sufficient information to estimate the C balance at large scale, which is a valuable tool to validate regional models (e.g. Gioli et al., 2004; Miglietta et al., 2007).

Improvements in remote sensing capability and products have greatly improved datasets on land use and land cover and enabled improvements in modeling the consequences of recent land use change. All land based sectors use process based models and remote sensing products. Remote sensing data and land information systems for C accounting have been particularly successful when land is converted from forest to other land use (Nobre and Harriss, 2002).

2.5 Research needs in Agro-ecosystem GHG modeling

Significant progress has been made in the simulation modeling of N_2O at all scales, from the laboratory to the globe. N_2O simulation models at the field scale are the most widely used models, not only because they bridge the knowledge gaps between the laboratory level and regional/global level, but also they simulate the entire agro-ecosystems, including water dynamics, C and N cycling and agricultural management, therefore it can be used to develop N_2O mitigation strategies which align closely as the best management practices within the particular industry. These approaches still has many uncertainties, and significant knowledge gaps still exist in the construction of suitable models and need to be addressed: (a) limited temporal resolution of experimental data, particularly N_2O emissions as a function of the quantity, quality and timing of N applied; (b) limited unequivocal data, particularly using isotopes, to separate the N_2O contribution between nitrification and denitrification; (c) the need for a detailed examination of N_2O leakage in the nitrification process; (d) limited data for partitioning N_2O and N_2 in denitrification; (e) a need for development of N_2O emissions from chemo-denitrification and nitrifier denitrification; and (f) detailed analysis of gaseous diffusion of N_2O from depth and its assimilation in the soil profile.

The challenging task is how to scale up the relatively more robust-scale models to catchment, regional and national scales, especially the interaction of biophysical processes between fields. Upscaling is an essential requirement, not only for more accurate regional and national inventories, but also for development of site-specific mitigation practices with increased interest in full GHGs accounting and emissions trading in the agricultural sector.

3. Materials and Methods

3.1 Study site

The study site is the Ikushunbetsu River watershed located in central Hokkaido, Japan, latitude 43°14′N, longitude 141°57′ E, which covers an area of 35,887 ha (Fig. 3.1) (Mu et al., 2008). The 30-year average temperature is 7.4°C, and the annual precipitation is 1154 mm (Japan Meteorological Agency, 2014). The main agricultural land uses are paddy rice (*Oryza sativa* L.), growing onion (*Allium cep* L.) and winter wheat (*Triticum aetivum*). Vegetable such as soybean (*Glycine max* L.) is the minor crop.

The altitudinal range of the Ikushunbetsu River Basin was 20 to 1054m (Digital Map 50m Grid, Geographical Survey Institute, 2001). At the regional scale, there are total 15 soil types, 6 soil textures and 5 major soil types including information of C content (TC) (g kg^{-1}), total N content (TN) (g kg^{-1}), clay content (%), silt content (%), clay + silt content (%) depended on different soils (Table 3.1). The 5 major soil types were according to a basic survey on soil fertility (Hokkaido Central Agricultural Experiment Station, 1971). Brown lowland soils were found along the main stream of the Ikushunbetsu River, surrounded by gray and gley lowland soils. Pseudogleys were distributed on the left side of the Ikushunbetsu River (Fig. 3.2). Other parts have not been identified, but they are thought to be brown forest soils. In each major soil type, the sub-soil type was defined. Grey lowland soils included soils of B-2, Hk-2, A-2, H-2 and forest (for); Brown lowland soils included soils of Ik-2, M-3, Sg-3, To-3 and Tu-3; Gley lowland soils included soils of Ks-3, Mi-2 and Kb-2; Pseudogleys included soils of Ni-3 and Kn-2 (Hokkaido Central Agriculture Experiment Station, 1971) (Fig. 3.3). The type of soil textures across the whole region around 6, they are clay loam (CL), light clay (LiC), silty clay (SiC), silty clay loam (SiCL), sandy loam

(SL) and heavy clay (HC). The main 4 soil textures are classified in this study, included CL, LiC, SiC and SiCL (Fig. 3.4). LiC soils were found along the main stream of the Ikushunbetsu River, surrounded CL, SiC and SiCL.

Land use history was analyzed using 1:25,000 maps from the Geographical Survey Institute (1959, 1966, 1976, 1988, 1994). Fallow land was defined as an area with previous artificial land use, but no cultivation or construction in the ground survey years. Bush land was defined as the fallow land was abandoned more than two years. Ground survey were conducted in 2002, 2005, 2007 and 2011 to locate the land use areas, and the land use distribution was mapped digitally using ArcView 10.0. According to a ground survey conducted in July 2011, the total upland area was 723 ha, paddy field area was 430 ha, grassland area was 320 ha, and bush/fallow area was 673 ha (Fig. 3.5). Among upland field, the main crops are soybean (33 ha), vegetable (19 ha), onion (279 ha) and wheat (392 ha). Cultural conditions and plant biomass components for major crops in Ikushunbetsu river watershed was shown in Table 3.2.

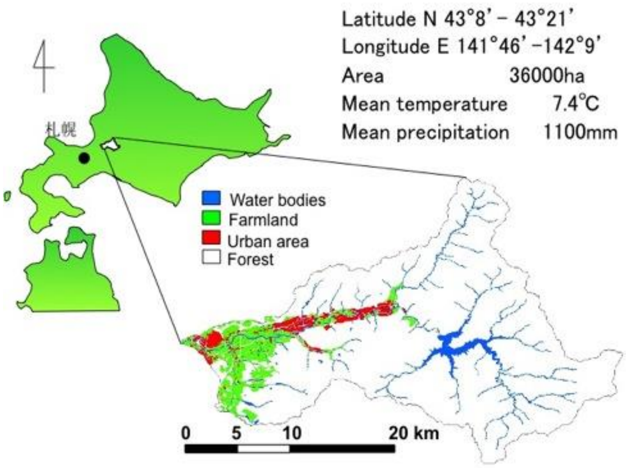

Figure 3. 1 Location and characteristics of the study site.

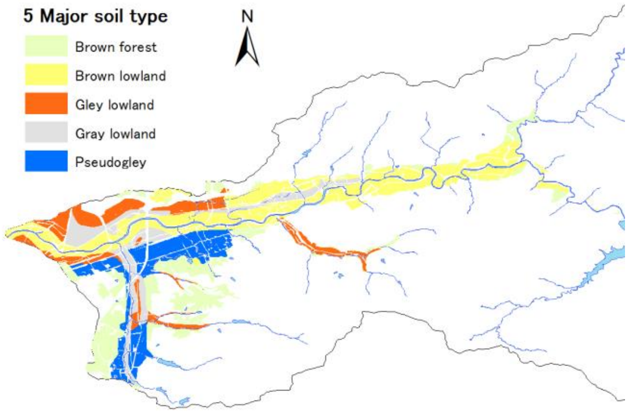

Figure 3. 2 Distribution of 5 main soil types in Ikushunbetsu watershed.

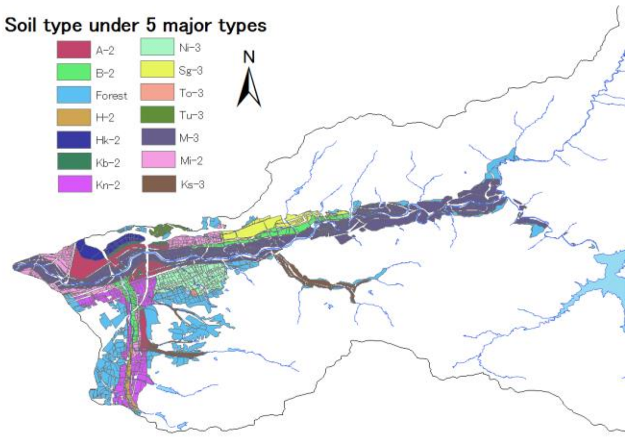

Figure 3. 3 Distribution of sub-soil types under the 5 main soil types in Ikushunbetsu watershed.

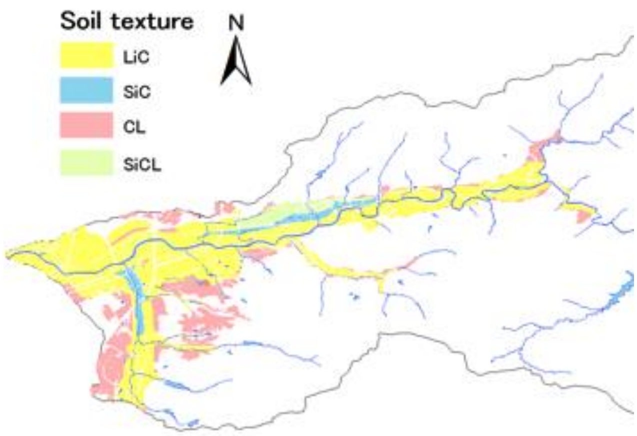

Figure 3. 4 Distribution of soil texture in Ikushunbetsu watershed (LiC: Light Clay; SiC: Silty Clay; CL: Clay Loam; SiCL: Silty Clay Loam.)

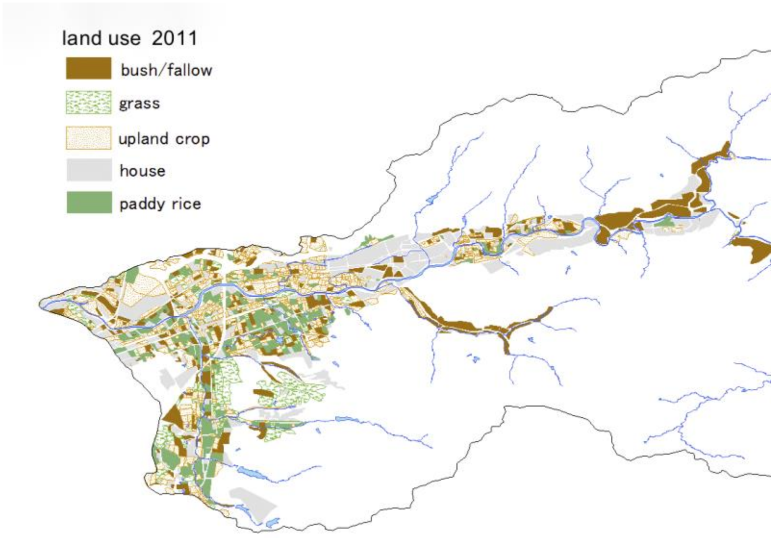

Figure 3. 5 Distribution of major land uses conducted in 2012 in Ikushunbetsu watershed.

Table 3. 1 The general information of soil type at the regional scale.

Sub-soil type[a]	Sand	Silt	Clay	Texture	TC	TN	pH	Soil type
	%	%	%		g kg^{-1}	g kg^{-1}		
B-2	33.8	30.8	35.3	LiC~SiC	16.0	1.4	6.0	Grey lowland
Hk-2	30.1	33.7	36.2	LiC	53.5	3.8	5.7	Grey lowland
Ik-2	28.5	40.9	30.5	SiC~CL	30.9	1.8	6.8	Brown lowland
Ks-3	31.8	32.4	35.8	LiC	62.0	4.6	5.5	Gley lowland
M-3	34.5	30.6	34.9	LiC	28.7	2.5	5.4	Brown lowland
Mi-2	21.9	38.5	39.5	LiC	28.0	2.3	5.4	Gley lowland
Ni-3	27.6	35.9	36.5	LiC	34.0	3.0	5.5	Pseudogley
Sg-3	40.8	30.3	28.9	SL~SiCL	21.3	2.0	5.8	Brown lowland
Kb-2	17.4	44.5	38.1	CL~LiC	55.0	4.0	5.8	Gley lowland
Kn-2	20.2	35.6	44.3	LiC	33.1	2.2	5.5	Pseudogley
To-3	46.6	28.7	24.7	CL	23.4	1.6	6.5	Brown lowland
Tu-3	31.1	39.7	29.2	LiC	27.0	7.2	5.2	Brown lowland
H-2	36.9	31.0	32.0	LiC	22.0	2.0	4.9	Grey lowland
A-2	21.6	42.1	36.3	HC~LiC	64.0	4.9	5.2	Grey lowland
for	32.6	36.4	31.0	CL	-	-	-	Grey lowland

[a] Hokkaido Central Agriculture Experiment Station, 1971.
HC: Heavy Clay; LiC: Light Clay; SiC: Silty Clay; CL: Clay Loam; SL: Sandy Loam; SiCL: Silty Clay Loam.

Table 3. 2 Cultural conditions and plant biomass components for major crops in the Ikushunbetsu watershed of central Hokkaido, Japan.

				Plant biomass component		
Crop	Sowing	Harvesting	Harvested biomass	Non-harvest biomass (removed from the field)	Above-ground residue biomass (returned to the soil)	Below-ground residue biomass (returned to the soil)
Soybean	Mid May to late May	Late September	Grain		Leaves, stalks, pods	Stubble and roots
Potato	Mid May to late May	Late September	Tubers		Leaves and stems	Roots
Buckwheat	Mid June to late August	Late September	Grain		Stems	Stubble and roots
Vegetable	Mid May to late May	Late September	Heada Heart		Leaves	Roots
Onion	Late April to early May	Late September	Bulb		Leaves	Roots
Maize	Mid May to late May	Late September	Ears		Leaves and stalks	Stubble and roots
Greenhouse	Mid May to late May		Heada Heart		Leaves	Roots
Wheat	Mid September to late September	Late July to early August	Grain	Straw	Stubble and busks	Stubble and roots
Grass	Early May	Late September	Grass		Stubble	Stubble and roots
Paddy	Early May	Late September	Rice		Leaves and rice hulls	Stubble and roots

3.2 Data sets

All data were obtained from upland agricultural field sites at the Ikushunbetsu River watershed in central Hokkaido, Japan, latitude 43°14′N, longitude 141°57′E, which covers an area of 35,887 ha (Kimura et al., 2010; Mu et al., 2008). Samples were measured in 15 fields comprising 11 land use types over a period of 9 years from 2003 to 2011 (Fig. 3.6) (Table 3.3). The data set includes information on study site location, dates of study, climate, precipitation, soil type, soil texture, soil temperature, soil water, soil pH, soil NO_3^- and NH_4^+ contents, soil organic C and N contents, CO_2, N_2O and NO emission.

Figure 3. 6 Sampling sites of greenhouse gas in Ikushunbetsu watershed from 2003–2012.

Table 3. 3 General information of 15 experimental sites.

Site_No.	Site	Soil texture	TC mg/g	TN mg/g	C/N ratio	pH	clay %	silt %	sand %
1	B	LiC	19.8	1.8	10.9	5.1	34.7	37.9	27.4
2	BL	LiC	21.7	1.9	11.3	5.9	36.6	57.4	6.0
3	C	CL	24.1	2.2	11.0	5.8	20.4	32.6	47.0
4	D	CL	16.2	1.3	12.1	5.8	20.4	32.6	47.0
5	E	CL	23.3	1.8	12.8	5.3	36.6	57.4	6.0
6	F	CL	26.2	2.2	12.2	5.9	18.6	38.1	43.3
7	G	CL	16.0	1.5	10.4	5.7	23.7	40.1	36.2
8	GL	SiC	32.1	2.8	11.5	5.5	37.3	51.1	11.7
9	P	SiC	27.0	2.1	13.0	6.0	33.9	47.7	18.4
10	R	SiCL	35.3	2.5	14.0	5.2	24.5	47.6	27.9
11	S	LiC	38.7	3.1	12.3	5.8	33.1	42.1	24.7
12	T	LiC	20.6	1.8	11.4	5.8	31.4	36.3	26.2
13	U	LiC	12.3	2.7	4.6	5.7	19.0	40.1	31.0
14	V	CL	31.5	2.6	12.1	5.4	17.9	29.1	53.1
15	W	CL	9.3	1.0	9.2	5.7	36.6	57.4	6.0

TC: the total carbon content. TN: the total nitrogen content. CL: Clay Loam. LiC: Light Clay. SiC: Silty Clay. SiCL: Silty Clay Loam.

3.2.1 Soil properties

TC and TN are the soil total C and total N concentration at 0–20 cm depth, respectively (Kimura et al., 2007). Soil temperature at a depth of 5 cm was recorded using a digital thermometer (CT-220; Custom Corporation, Tokyo, Japan). The content of soil NO_3^- was analyzed by using a Dionex ion chromatograph equipped with a conductivity detector, the content of NH_4^+ was determined by using the indophenol blue colorimetric method (Mu et al., 2008b). In CO_2-HB model, soil water content was expressed as the percentage of water-filled pore space (WFPS) in the top layer from 0 to 5 cm depth, using the measured soil bulk density (g/cm^3) (average of three measuring dates in May, July, and September of each year) and assuming a particle density of 2.65 g/cm^3 (Mu et al., 2008b). In N-HB model, soil water content was expressed as the amount of water (in mm of water depth) present in a layer of soil using depth of soil layer (mm) and soil water content by volume (%). Soil water content by volume (%) was calculated by soil water content by mass (g/g) and bulk density (g/cm^3) (Mu et al., 2008b). Soil water saturation (mm layer^{-1}), field capacity (mm layer^{-1}) and permanent wilting point (mm layer^{-1}) were estimated based on soil texture and organic matter (Saxton and Rawls, 2006). The WFPS was also simulated by using HYDRUS-1D for future regional model up-scaled, as it will be more precisely mentioned. The soil temperature at a depth of 5 cm ranged from 6.73°C to 30.02°C. The measured WFPS (WFPS_measured) ranged from 0.24 to 0.83 with a median of 0.39 (mean: 0.44) and skewness of 1.38. The simulated WFPS (WFPS) ranged from 0.37 to 0.87 with a median of 0.25 (mean: 0.49) and skewness of 0.70 (Table 3.4).

Table 3. 4 Statistics of measured data used in this study. CI indicates confidence interval.

	Median	Mean	SD	95% CI	Skewness	Kurtosis
soil temperature(°C)	21.45	20.47	6.52	6.73 ~ 30.02	–0.46	–0.71
WFPS_measured	0.39	0.44	0.66	0.24 ~ 0.83	1.38	1.28
WFPS	0.25	0.49	0.70	0.37 ~ 0.87	0.70	–0.34
TC (g kg^{-1})	17.00	18.64	11.13	0.90 ~ 38.70	0.15	–1.17
TN (g kg^{-1})	1.67	1.48	0.78	0.10 ~ 3.14	0.07	–1.05
C/N ratio	12.17	12.38	14.27	9.20 ~ 20.78	2.10	7.92
silt(%)	40.60	42.70	8.17	24.80 ~ 57.40	–0.20	–0.36
clay(%)	25.30	27.47	6.28	16.8 ~ 36.70	0.07	–1.31

WPFP_measured is the measured value of water filled pore space. WFPS is the simulated value.

3.2.2 Greenhouse gas (GHG) emission

The GHG measurements were carried out on 15 experimental sites weekly using the closed chamber method throughout the non-snow period (Middle April to Early November) across 9 years from 2003 to 2011(for details, see Kusa et al., 2002; Toma et al., 2007; Mu et al., 2008a,b). GHG fluxes from heterotrophic respiration (Rh) were measured from the bare soils where the soils were not treated with chemical and organic fertilizers or residues, and weeds were removed from the monitoring plots. For use in the CO_2 calibration, the CO_2 emission from heterotrophic respiration (Rh) was used. And in order to decrease the effects of daily weather or temporal variations at the field scale, and to decrease the uncertainty in emissions, which is particularly large during periods of high emissions (Chatskikh et al., 2005; Chatskikh and Olesen, 2007; Chatskikh et al., 2008), the measured CO_2 flux data were aggregated on a monthly basis. Cumulated monthly CO_2 emissions (kg C ha^{-1} $month^{-1}$) were estimated by linear interpolation between measurements on the dates of the corresponding daily fluxes and then divided by the number of days of one month to obtain the daily flux (kg C ha^{-1} day^{-1}) on a monthly basis, with number points N = 154. For use in the N_2O and NO calibration, N_2O and NO emission from both ctrl and fop treatment were used at daily step directly, with number points N = 607.

3.2.3 Land management

An inquiry was carried out to investigate the actual amount of applied N fertilizer and yield in each land use category. Farmers were asked about their management methods for each crop. In addition to these inquires, unpublished data were obtained from Iwamizawa Agriculture Cooperation, Mikasa Branch and Agriculture Improving Center of Central Sorachi. The investigated farm numbers for each type of land use were 12 for paddy rice, 22 for wheat, 10 for onion, 6 for vegetables and 17 for grasslands. Among 15 experiments sites, for some sites, different treatments were conducted with various N-fertilizer amounts supplied to the crop (Table 3.5). Chemical fertilizers or residues were not applied on the ctrl treatments and weeds were removed from the monitoring plots without any crop cultivation. The fop (Fertilizer, Organic matter, Plant) treatments were applied with chemical fertilizer (F), organic matter (O) and crop cultivation (Plant). For some sites, there were not only control treatments but also conducted with fop treatment. There were a total of 26 site/treatment combinations (Table 3.5). Bare soil means no chemical application; no organic fertilizer application and no plant application (for details, see Naser et al., 2007; Mu et al., 2008a,b).

Table 3. 5 Information of land management in 15 experimental sites and 26 site/treatment combinations.

Site	Site_No.	ID	ID_No.	Year	Crop type	Treatment	N fertilizer	Crop Residue
							kg N ha^{-1} yr^{-1}	kg N ha^{-1} yr^{-1}
B	1	B_ctrl	1	2003	None	ctrl	0	0
		B_fop	2	2003	Wheat	fop	140	104
BL	2	BL_ctrl	3	2006, 2007	Onion	ctrl	0	0
		BL_fop	4	2006, 2007	Onion	fop	180	57
C	3	C_ctrl	5	2003	None	ctrl	0	0
		C_fop	6	2003	Maize	fop	110	14
D	4	D_ctrl	7	2003, 2005	None	ctrl	0	0
		D_fop	8	2003	Wheat	fop	140	104
E	5	E_ctrl	9	2003	None	ctrl	0.0	0.0
		E_fop**		2008	Onion	fop	165	42
F	6	F_ctrl	10	2003	None	ctrl	0	0
		F_fop	11	2003	Wheat	fop	112	104
G	7	G_ctrl	12	2003	Soybean	ctrl	0	0
GL	8	GL_ctrl	13	2006–2009	None	ctrl	0	0
		GL_fop	14	2006–2009	Onion	fop	237	45
		Verification		2010–2011*	Onion	fop	237	45
P	9	P_ctrl	15	2006–2007	None	ctrl	0	0
		P_fop	16	2007	Onion	fop	200	70
R	10	R_ctrl	17	2006–2007, 2009	None	ctrl	0	0
		R_fop	18	2005	Potato	fop	94	22
				2007	Potato	fop	32	22
				2009	Potato	fop	196	122
		Verification		2010, 2011*	Potato	fop	196	122
S	11	S_ctrl	19	2006	None	ctrl	0	0
T	12	T_ctrl	20	2007, 2008	None	ctrl	0	0
		T_fop	21	2007, 2009	Buckwheat	fop	106	16
U	13	U_ctrl	22	2007	None	ctrl	0	0
		U_fop	23	2007	Maize	fop	146	235
V	14	V_ctrl	24	2009	None	ctrl	0	0
		V_fop	25	2007	Soybean	fop	57	57
				2009	Maize	fop	79	14
		Verification		2010, 2011*	Maize	fop	79	14
W	15	W_ctrl	26	2009	None	ctrl	0	0
		Verification		2010, 2011*	Onion	fop	342	45

ctrl: bare soil without any fertilizer, organic matter and plant residue treatment. fop: Planted soil with fertilizer, organic matter and plant residue treatment.
* Data for verification
**No detailed data of NO flux, therefore didn't included in the database.

3.2.4 WFPS simulation

It is difficult to calculate WFPS at the regional scale, therefore the daily WFPS was simulated in order to make the CO_2-HB model future up-scaled possible. WFPS was calculated from the simulated daily soil water content and measured soil bulk density (Mu et al., 2008b). HYDRUS-1D was calibrated using 9 years (2003–2011) of daily soil water content data in the 0–5 cm soil layer at 15 sites. The HYDRUS-1D model required input of the potential evaporation (PE) to perform surface flux simulation. PE was calculated from the average daily values of air temperature (ºC), humidity (%), wind speed (km d^{-1}), and solar radiation (hr) using the Penman-Monteith Combination Equation (Jensen et al., 1990). Daily meteorological data were obtained from the Japan Meteorological Agency (http://www.jma.go.jp/jma/). Water flow conditions were chosen to allow the surface water layer to increase from precipitation and decrease from infiltration and evaporation for the upper boundary. Free drainage was selected for the lower boundary. The most important factor for successful application of unsaturated flow theory to actual field problems is obtaining the parameters for the governing transfer equation (Dixon, 1999). The hydraulic parameters used in this study for hydraulic conductivity function were predicted using textural characteristics by Van Genuchten et al. 1992. WFPS calculated by HYDRUS was used for HB calibration after values obtained by HYDRUS simulation were found to be significantly correlated with the measured values of WFPS (R^2 = 0.68, P < 0.001, Fig. 3.7).

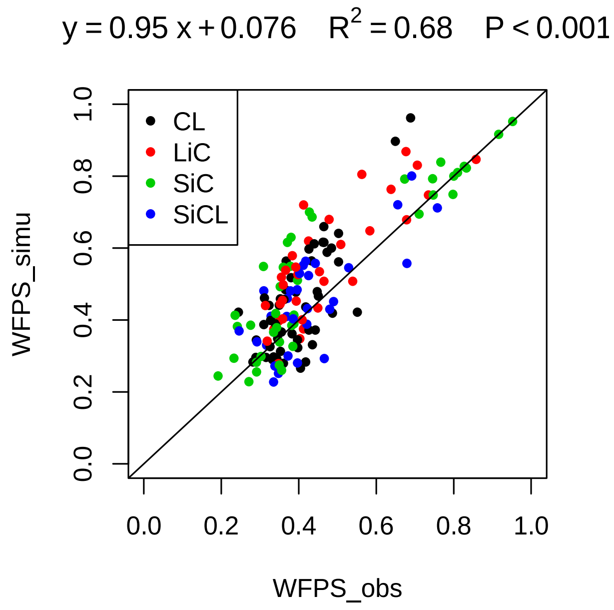

Figure 3. 7 Comparison between predicted and measured water-filled pore space (WFPS).

3.3 Bayesian calibration theory

To estimate the soil gas flux, a Bayesian approach was developed to calibrate the parameters. Bayesian methods are used to estimate model parameters by combining two sources of information: prior information about parameter values and observations on output variables. The prior information is based on expert knowledge, literature review or by measuring parameters directly in the field or laboratory. In our case, the observations on output variables are field measurements. Here Bayesian theory is briefly describe,

$$p(\theta|y) = \frac{f(y|\theta)\pi(\theta)}{g(y)} \qquad (3.1)$$

where θ is the parameter that we are estimating and y represents the observed data. Both θ and y are considered to be random variables. $p(\theta|y)$ is the posterior distribution which represents the probability of the model parameter (θ) values given the observed data (x), $g(y)$ is the unconditional probability of the observed data, $\pi(\theta)$ is the prior distribution, and $f(y|\theta)$ is the conditional probability of the observations on θ, termed the likelihood function.

The likelihood function for all observation can be expressed as:

$$f(y|\theta) = \prod_{i=1}^{N} \frac{1}{\sqrt{2\pi\sigma_y^2}} e^{-\frac{(y_i-(\mu_y)_i)^2}{2\sigma_y^2}} \tag{3.2}$$

where, y_i is the i–th observed data and $(\mu_y)_i$ is the predicted values, N is the number of data points. σ_y is the standard deviation that corresponds to observed data.

Different from nonhierarchical Bayesian model (Bayesian pooled model), the hierarchical model assigns two hyper parameters α and β to yield the posterior distribution of parameter (θ), which is different from Eq. 3.1:

$$p(\theta,\alpha,\beta|y) = \frac{\prod_{j=1}^{n} f(y_j|\theta_j)\pi(\theta_j|\alpha,\beta)u(\alpha)v(\beta)}{g(\theta|\alpha,\beta)} \tag{3.3}$$

where j is the class number, θ_j indicates that each individual class can have a different parameter, but all are linked through hyper parameter. $\mu(\alpha)$ and $v(\beta)$ are the prior distribution of hyper parameters.

To generate a representative sample of parameters from the posterior distribution, the Markov Chain Monte Carlo (MCMC) method was used (Congdon, 2007). For calibration, three parallel Markov chains were started from three different starting points: the default parameter value and its lower (θ_{mix}) and upper bounds (θ_{max}). Convergence was checked with the diagnostic method proposed by Gelman and Rubin (1992), which is based on the comparison of within-chain and between-chain variances and is similar to a classical analysis of variance. Convergence is reached when the variance between chains no longer exceeds the variance within each individual chain.

Total 10,000 iterations of sampling from the prior distribution within each chain was conducted to obtain the posterior probability distributions, discarding the first 2,000 iterations as non-representative "burn-in" of chains to avoid the influence of the initial values and using the remaining 8,000 iterations to evaluate the posterior distribution of parameters (Van Oijen et al., 2005).

3.4 CO_2-HB model

The CO_2-HB runs on a daily weighed time step, which has been developed, based on Rh to simulate soil CO_2 emission with data that can drive the model on a range of spatial scales and as a sub-model incorporated into other models.

3.4.1 CO_2-HB model structure

Simple greenhouse gas (SG) models were used to estimate GHG fluxes (Hashimoto et al., 2011). The model structure developed for CO_2 flux (kg C ha^{-1} day^{-1}) in this study is based on the SG model, which can be generally described using response functions of $h(T)$ and g(WFPS) as follows:

$$CO_2=exp(\beta_1)h(T)g(\mathrm{WFPS}) \tag{3.4}$$

where β_1 is a constant, and T is the soil temperature at a depth of 5 cm (ºC).

$h(T)$ is the response function of soil temperature and can be described as an exponential function as follows:

$$h(T)=exp(\beta_2 T) \tag{3.5}$$

where β_2 is the parameter.

g(WFPS) is the response function of WFPS in the top soil layer at a depth of 0–5 cm. The following function was adopted from the DAYCENT (Parton et al., 1996) and SG models (Hashimoto et al., 2011):

$$g(WFPS) = \left(\frac{WFPS-\beta_3}{\beta_4-\beta_3}\right)^{\beta_6}\left(\frac{WFPS-\beta_5}{\beta_4-\beta_5}\right)^{\frac{-\beta_6(\beta_4-\beta_5)}{(\beta_4-\beta_3)}} \tag{3.6}$$

where β_3, β_4 and β_5 are the parameters which are the minimum, optimum, and maximum values of WFPS, respectively (*i.e.*, $\beta_3 < \beta_4 < \beta_5$), and β_6 is the parameter controlling the curvature of the function.

3.4.2 Hierarchical model

This study mainly focused on using the HB model to predict CO_2 flux across various soil textures. The HB model is summarized as follows:

$$CO_{2ij} \sim N(\mu_{y\,ij}, \sigma^2_y) \tag{3.7}$$

$$\mu_{y\,ij} = exp(\beta_{1,j})\, exp\left(\beta_{2,j}T_{ij}\right) \left(\frac{WFPS_{ij}-\beta_{3,j}}{\beta_{4,j}-\beta_{3,j}}\right)^{\beta_{6,j}} \left(\frac{WFPS_{ij}-\beta_{5,j}}{\beta_{4,j}-\beta_{5,j}}\right)^{\frac{-\beta_{6,j}(\beta_{4,j}-\beta_{5,j})}{(\beta_{4,j}-\beta_{3,j})}} \tag{3.8}$$

$$\beta_{k,j} \sim N(\mu_{\beta k}, \sigma^2_{\beta k}) \tag{3.9}$$

where CO_{2ij} is the i-th observation of CO_2 flux for the j-th texture class and i-th data, i is the data point number ranging from 1 to N, and j is the texture class number (j=1, CL; j=2, LiC; j=3, SiC; j=4, SiCL). N is the total number of data points. k is the k-th number of the parameter, k=1, …, 6, denoted as $\beta_{1,j}$, …, $\beta_{6,j}$, respectively. $\beta_{k,j}$ is the texture-specific model parameter which consists of the constant ($\beta_{1,j}$), the parameter ($\beta_{2,j}$) for $h(T)$, and the parameters ($\beta_{3,j}$, $\beta_{4,j}$, $\beta_{5,j}$, $\beta_{6,j}$) for g(WFPS). σ^2_y is the variance of the model error. $\mu_{\beta k}$ and $\sigma^2_{\beta k}$ are the mean and variance for $\beta_{k,j}$. $\mu_{\beta k}$ and $\sigma^2_{\beta k}$ are defined as hyper parameters. Note that the hierarchical notation in Equations 3.7–3.9 indicates conditional distributions, *i.e.*, CO_{2ij} is normally distributed conditional on $\mu_{y\,ij}$ and σ^2_y, and $\beta_{k,j}$ is normally distributed conditional on $\mu_{\beta k}$ and $\sigma^2_{\beta k}$. In the HB method, all of the hyper parameters also need the prior information along with the other parameters (*e.g.*, σ_y). The non-informative or vague prior information of $\mu_{\beta k}$, $\sigma_{\beta k}$, and σ_y in Equations 3.7–3.9 are as follows:

$$\mu_{\beta k} \sim N(0{,}10\ 000) \tag{3.10}$$

$$\sigma_{\beta k}, \sigma_y \sim Unif(0, 100) \tag{3.11}$$

where N(0, 10 000) is the normal distribution of $\mu_{\beta k}$ with mean 0 and variance 10,0 000 and $Unif$(0, 100) is the uniform distribution of $\sigma_{\beta k}$ and σ_y with lower (0) and upper (100) limits.

3.4.3 Nonhierarchical Bayesian model (Bayesian pooled model)

To evaluate the goodness-of-fit of hierarchical Bayesian (HB) models, we also applied the Bayesian pooled model across all soils. Rather than Equations 3.7–3.11, the Bayesian pooled model can be described as:

$$CO_{2i} \sim N(\mu_{y\,i}, \sigma^2_y) \tag{3.12}$$

$$\mu_{y\,i} = exp(\beta_1)\, exp(\beta_2 T_i)\, (\frac{\mathrm{WFPS}_i - \beta_3}{\beta_4 - \beta_3})^{\beta_6} (\frac{\mathrm{WFPS}_i - \beta_5}{\beta_4 - \beta_5})^{\frac{-\beta_6(\beta_4-\beta_5)}{(\beta_4-\beta_3)}} \tag{3.13}$$

CO_{2i} is the i-th observation of CO_2 flux, i is the data number ranging from 1 to N, and N is the total data number. β_k (k = 1, …, 6) are the model parameters, which consist of the constant (β_1); parameter (β_2) for $h(T)$, and parameters (β_3, β_4, β_5, and β_6) for g(WFPS). CO_{2i} is normally distributed conditional on $\mu_{y\,i}$ and σ^2_y. σ^2_y is the variance of the model error. The vague prior distributions of β_k and σ_y are as follows:

$$\beta_k \sim N(0, 10\,000) \tag{3.14}$$

$$\sigma_y \sim Unif(0,100) \tag{3.15}$$

where N(0, 10 000) is the normal distribution of β_k with mean 0 and variance 10,000, and $Unif$(0, 100) is the uniform distribution of σ_y with lower (0) and upper (100) limits.

3.4.4 Model evaluation and comparison

The goodness of fit of the HB models and the Bayesian pooled version were compared. The HB models and the Bayesian pooled version were evaluated by comparing the prediction of CO_2 flux to the observed values using the root mean square error (RMSE) to quantify the mismatch between the predictions and the mean values of the measurements. In addition, we used an evaluation method developed specifically for evaluating both HB and Bayesian pooled models, the deviance information criterion (DIC) (Spiegelhalter et al., 2002).

Some authors suggest using the posterior mean deviance $\overline{D}=E[D(\theta)]$ as a measure of model fit, where $D(\theta)$ is the deviance defined as:

$$D(\theta) = -2*likelihood = -2logp(x|\theta) \tag{3.16}$$

However, more complex models will fit the data better and thus will have a smaller $\overline{D}$; therefore, a measurement of model complexity was introduced to counterbalance

$\bar{D}$.

Model complexity was measured by estimating the effective number of parameters, *pD*.

$$pD = E[-2logp(x|\theta)] - \left(-2logp\left(x\middle|\bar{\theta}(x)\right)\right) = \bar{D} - D(\bar{\theta}) \quad (3.17)$$

where $\bar{\theta} = E[x|\theta]$. In this case *pD* can be described as: *pD*=[mean value evaluated at the posterior distribution of deviance] – [deviance evaluated at the posterior mean of the parameters].

Therefore, DIC is defined as:

$$\text{DIC} = D(\bar{\theta}) + 2PD = \bar{D} + pD \quad (3.18)$$

Both RMSE and $\bar{D}$ decrease as the model complexity (number of parameters) increases. In contrast, the DIC considers both the goodness of fit ($\bar{D}$) and a penalty for model complexity (*pD*), and it is specifically designed to overcome the difficulty in determining the effective number of parameters and degrees of freedom to assign to hierarchical models. A small DIC is estimated to be the model that would predict a replicate dataset that has the same structure as the currently observed data.

3.4.5 Calculations and statistics

HB calibration was applied to the CO_2-HB model by using data of total 15 experimental sites. Bayesian calibration was performed with the statistical package R (R Development Core Team, 2005), particularly its R2jags package (Plummer, 2003). Convergence diagnostic analysis and model evaluation and comparison were performed with the R 'boa' package (Smith et al., 2007b). Simple linear regression analysis was applied between the mean values of estimated parameters and soil properties. Akaike's information criterion (AIC) (Akaike, 1987) for the different simple linear regressions was compared to choose the best variables (soil properties) for the estimated parameters. A smaller AIC value indicates a better predictor variable. Regression analysis was applied between the estimated parameters and the best variables. In HB statistics, a significant difference at the 10% level among parameters was defined when the 90% CIs of the posterior distribution of the parameters failed to overlap each other (Scheibehenne and Pachur, 2015; Kraft et al., 2010; Lu et al., 2012). The goodness of fit of the effect of soil temperature and WFPS on daily CO_2 flux was tested by comparing the model performance with that obtained with the HB model structure including only the response function of soil temperature $CO_2=exp(\beta_1)h(T)$ and including only the response function of soil WFPS $CO_2=exp(\beta_1)g(\text{WFPS})$.

3.5 N-HB model

The N-HB model runs on a daily time step, which has been developed, based on process theory of nitrification and denitrification to simulate soil N gaseous emission with data that can drive the model on a range of spatial scales.

3.5.1 Nitrification process

Nitrification in N-HB is simulated according to the amount of ammonium (NH_4^+) in the soil layer, and is modified according to the temperature, soil water content and soil pH. The amount of N nitrified, N_n (in kg N ha^{-1}), is calculated using the expression for nitrification developed by Bradbury et al. (1993), and modified by Bell et al. (2012) *i.e.*

$$N_n = N_{NH_4}\left(1-e^{-Nitri_{rate}.m_t.m_w.m_{pH}}\right)\left(1-\frac{N_{NH_4}}{c_{max}+N_{NH_4}+N_{FERT}}\right) \quad (3.19)$$

where $Nitri_{rate}$ is the nitrification rate, N_{NH_4} is the amount of NH_4^+ in the soil (kg N ha^{-1}), m_t is a rate modifier due to soil temperature, m_w is a rate modifier due to soil water content, and m_{pH} is a rate modifier due to soil pH, N_{FERT} is N in NH_4^+ and urea in the added fertilizer (kg N ha^{-1}), C_{max} is a set for a range of soil types, but can be calibrated using data showing the maximum flux rate of N_2O as an indication of the maximum rate of nitrification at high NH_4^+ levels (Bell et al., 2012).

Conversion of NH_4^+ to NO_3^- by nitrification is accompanied by gaseous losses of N due to partial and complete nitrification. The gaseous losses as NO and N_2O are calculated using a linear relationship.

The equations of the response functions of nitrification with the associated unitless response function (m_t, m_w, m_{pH}) as follows:

$$m_t = \frac{T_1}{\left(1+\exp\left(\frac{T_2}{T_{air}}+T_3\right)\right)} \tag{3.20}$$

where m_t is the temperature rate modifier for nitrification. m_t is taken from Bradury et al. (1993). T_1, T_2 and T_3 are parameters, and T_{air} is the daily air temperature (°C).

$$m_{pH} = pH_{cons} + \frac{tan^{-1}\left(3.14 \times pH_{modif}(pH - pH_{Tr})\right)}{3.14} \tag{3.21}$$

where m_{pH} is the pH rate modifier for nitrification. m_{pH} is taken from Parton et al. (1996). pH_{cons} is the constant, pH_{modif} controls the modifier shape and pH_{Tr} are pH threshold for pH rate change.

$$m_w = 1 - \frac{(1-m_{w0})(\theta_f - \theta_c - \theta_i)}{\theta_f - \theta_i} \tag{3.22}$$

$$m_w = 1 - \frac{(1-m_{w0})(\theta_c - \theta_f)}{\theta_s - \theta_f} \tag{3.23}$$

where m_w is the water rate modifier for nitrification. m_w is calculated by the equation presented by Bradbury et al. (1993). m_{w0} is the soil water rate modifier for decomposition at permanent wilting point and saturation. θ_c is the amount of water held in a particular soil layer above the permanent wilting point (mm layer^{-1}), θ_i is the amount of water held between field capacity and –100 kPa (mm layer^{-1}), and θ_f is the amount of water held between field capacity and the permanent wilting point (mm layer^{-1}). θ_s is the water content between saturation and permanent wilting point. Below field capacity, the rate modifier is assumed to follow a linear increase (Eq. 3.22). When above field capacity, the rate modifier is assumed to follow a linear decline to the minimum rate of m_{w0} (Eq. 3.23).

The amount of gas emitted as N_2O during nitrification, N_{n,N_2O} (kg N ha^{-1}), is given by

$$N_{n,N_2O}=\left(\left(n_f\times\frac{\theta_c}{\theta_f}\right)+\left(n_{gas}\left(1-n_{no}\right)\right)\right)N_n \quad (3.24)$$

where n_f is the proportion of N_2O, which is produced due to partial nitrification at soil water field capacity, θ_c is the amount of water in a particular soil layer above the permanent wilting point (mm layer^{-1}), and θ_f is the amount of water held between field capacity (mm layer^{-1}) and the permanent wilting point. N_2O produced from partial nitrification increases with ratio of θ_c and θ_f. The proportion of full nitrification gaseous loss to N_2O and NO is n_{gas}, and n_{no} is the proportion of NO loss due to full nitrification. Similarly, the amount of gas emitted as NO during nitrification, $N_{n,NO}$ is given (kg N ha^{-1}) by

$$N_{n,NO} = n_{gas} \times n_{NO} \times N_n \quad (3.25)$$

3.5.2 Denitrification process

Total denitrification in N-HB is simulated as a proportion of the NO_3^- content of the layer, modified according to water content and biological activity of the soil (as described by CO_2 release during decomposition). The denitrified N is then divided into N_2, N_2O and NO according to the soil water content and NO_3^- content of the soil. The total loss of N due to denitrification is given by:

$$N_d = D_P \times m'_{NO_3} \times m'_w \times m'_b. \quad (3.26)$$

where N_d is the amount of N emitted from the soil during denitrification (kg N ha^{-1}); m'_{NO_3} is the effect of soil NO_3^- content on the denitrification, m'_w is the effect of soil water content on the denitrification, and m'_b is the effect of biological activity on denitrification. D_p is the potential denitrification rate. D_p varies as a function of soil texture and soil biological activity, and is considered as site-specific parameter (Hénault et al., 2005).

The equations of the response functions of denitrification with the associated unitless response function (m'_{NO3}, m'_w, m'_b) as follows:

$$m'_{NO_3} = \frac{N_{NO_3}}{N_{d50}+N_{NO_3}} \tag{3.27}$$

where m'_{NO_3} is the NO_3^- modifier for denitrification. m'_{NO_3} is based on the work of Hénault and Germon (2000). N_{d50} is soil NO_3^- content at which denitrification is 50% of its full potential. N_{NO_3} is the amount of NO_3^- in the soil (kg N ha^{-1}).

$$m'_w = 0, \frac{\theta_c}{\theta_f} < w_1 \tag{3.28}$$

$$m'_w = \left[\frac{\frac{\theta_c}{\theta_f} - w_1}{1 - w_1}\right]^{w_2}, \frac{\theta_c}{\theta_f} \geq w_1 \tag{3.29}$$

where m'_w is the water modifier for denitrification. m'_w is calculated by the equation presented by Bradbury et al. (1993). θ_c is the amount of water held in a particular soil layer above the permanent wilting point (mm layer^{-1}), and θ_f is the amount of water held between field capacity and the permanent wilting point (mm layer^{-1}). w_1 is the soil water threshold for denitrification. w_2 is the exponent of power function for denitrification.

$$m'_b = BioAct \times CO_2 \tag{3.30}$$

where m'_b is the biological activity modifier. m'_b is based on the relationship developed by Bradbury et al. (1993). *BioAct* is the rate for soil biological activity. CO_2 is the amount of CO_2 produced during mineralization (kg C ha^{-1} timestep^{-1}). This acts as a surrogate measure of the soil biological activity.

The N lost by denitrification, N_d, is partitioned into N_2 and N_2O using simple linear relationships. The amount of N_2 gas lost by denitrification, N_{d,N_2} (kg N ha^{-1}), is given by:

$$N_{d,N_2} = P_w \times P_{NO_3} \times N_d \tag{3.31}$$

where N_{d,N_2} is amount of N_2 gas lost by denitrification (kg N ha^{-1}), P_w is the proportion of denitrification into N_2 according to the soil water content, P_{NO_3} is the proportion of denitrification into N_2 according to the soil NO_3^- content.

The amount of N_2O gas lost by denitrification, N_{d,N_2O} (kg N ha^{-1}), is similarly calculated by:

$$N_{d,N_2O} = N_d(1 - (P_w \times P_{NO_3})) \tag{3.32}$$

$$P_w = P_{N_{2,f}} \times \frac{\theta_c}{\theta_f} \tag{3.33}$$

$$P_{NO_3} = 1 - \left(\frac{N_{NO_3}}{P_{NO_3,f} + N_{NO_3}}\right) \tag{3.34}$$

$P_{N_2,f}$ is the proportion of denitrification into N_2 according to soil water content. $P_{NO_3,f}$ is NO_3^- content of the soil at which N is released in equal of N_2 and N_2O in denitrification process. N_{NO_3} is the amount of NO_3^- in the soil (kg N ha^{-1}).

For a full description of ECOSSSE model refer to Smith et al. (2010c).

3.5.3 N-HB model structure

The modules simulate the production of N_2O in soils through both nitrification (N_{n,N_2O}) and denitrification (N_{d,N_2O}) pathways. N_2O was calculated according to

$$N_2O = N_{n,N_2O} + N_{d,N_2O} \tag{3.35}$$

N_{n,N_2O} can be further described by Eqs. (3.24) and (3.25). N_{d,N_2O} can be described by Eqs. (3.32). Therefore, the equation can be further written as follows:

$$N_2O = \left(\left(\frac{n_f\theta_c}{\theta_f}\right) + \left(n_{gas}(1 - n_{NO})\right)\right)\left(\frac{N_{n,NO}}{n_{gas}.n_{NO}}\right) + \left(1 - \left(P_w.P_{NO_3}\right)\right)N_d \tag{3.36}$$

The module simulates the production of NO in soils only through nitrification, and was calculated using Eqs. (3.19) and (3.25).

Therefore, the equation can be further written as follows:

$$NO = n_{gas}.n_{NO}.N_{NH_4}\left(1 - e^{-Nitri_{rate}.m_t.m_w.m_{pH}}\right)\left(1 - \frac{N_{NH_4}}{c_{max} + N_{NH_4} + N_{FERT}}\right) \tag{3.37}$$

Parameter of n_{gas} and n_{NO} used here are regarded as the mean value of posterior distribution from the result of HB calibration of N_2O flux module (Eqs. (3.36)).

The N_2O and NO sub-models in this study involves a total set of 19 parameters [θ_1 ,…, θ_{19}]. Prior information was gathered on all parameters from reviewing literature, which was assigned uniform distributions within their likely range derived from the literature data (Table 5.1). A total of 15 parameters [$\theta_1, \ldots, \theta_6$] and [$\theta_{11}, \ldots, \theta_{19}$] were calibrated as site-specific parameters, and other 4 parameters [$\theta_7, \ldots, \theta_{10}$] were calibrated as global parameters for all sites (Table 5.1).

The hierarchical model structure for the N-HB model is given by as follows:

$$N_2O_{ij} \sim N(\mu_{N_2O,ij},\ \sigma_{N_2O}), \tag{3.38}$$

$$NO_{ij} \sim N(\mu_{NO,ij},\ \sigma_{NO}), \tag{3.39}$$

where N_2O_{ij} and NO_{ij} are the i-th observation of N_2O and NO flux at j-th class and i-th data, i is the data number ranging from 1 to N, j is the sites class number, N is the total data number. After the HB calibration on N_2O module, the average value of posterior distribution of θ_9 and θ_{10} was set as a constant to put in NO flux module.

$$\theta_{k,j} \sim N(\mu_{\theta k},\ \sigma_{\theta k}) \tag{3.40}$$

where $\theta_{k,j}$ is the class-specific model parameter for N_2O and NO, k is the k-th number of parameter, k=1,…,6 for N_2O and k=11,…,19 for NO, respectively. $\theta_7, \ldots, \theta_{10}$ are the parameters for N_2O module considered as global-parameters, σ_{N_2O} and σ_{NO} are variance of the model error for N_2O and NO. The hyper parameters α and β ($\mu_{\theta k}$ and $\sigma_{\theta k}$ in Eq. (3.41) and Eq. (3.42) described the density of parameter $\theta_{k,j}$, $\mu_{\theta k}$ and $\sigma_{\theta k}$ are mean and variance for $\theta_{k,j}$. There are two hyper parameters plus 15 site-specific parameters. In HB method, all the hyper parameters also need a prior distribution along with the other parameters (*e.g.* σ_{N_2O} *and* σ_{NO}). The vague prior distribution of hyper parameters $\mu_{\theta k}$ and $\sigma_{\theta k}$; σ_{N_2O} *and* σ_{NO} are as shown:

$$\mu_{\theta k} \sim N(0,10\ 000) \tag{3.41}$$

$$\sigma_{\theta k},\ \sigma_{N_2O},\ \sigma_{NO} \sim Unif(0,\ 100) \tag{3.42}$$

where N(0, 10 000) is the normal distribution of $\mu_{\beta k}$ with mean 0 and variance 10 0 000 and *Unif*(0, 100) is the uniform distribution of $\sigma_{\beta k}$, σ_{N_2O} and σ_{NO} with lower (0) and upper (100) limits. Equations 3.36 & 3.37 were fit to the observed data to estimate model parameters ($\theta_{k,j}$) and the hyper parameters using the HB approac

Table 3. 6 Description of 19 parameters of N_2O and NO flux module. The prior probability distribution is defined as uniform between bounds θ_{min} and θ_{max} which were extracted from literature reviews.

Gas module		Parameter vector θ=[θ_1,...,θ_{19}]				Default value	Prior probability distribution		
		Parameter	Symbol	Description	Unit		$\theta_{min}(i)$	$\theta_{max}(i)$	References
N_2O flux module	Site-specific	θ_1	N_{d50}	Soil nitrate content at which denitrification is 50% of its full potential	kg N ha^{-1} layer^{-1}	16.5	5	20	(Stanford et al., 1995), (Maag and Vinther, 1999), (Gabrielle, 2006), (Lehuger et al., 2009), (Bell et al., 2012)
		θ_2	w_1	soil water threshold for denitrification	%	0.62	0.5	1	(Gabrielle, 2006), (Hénault and Germon, 2000), (Johnsson et al., 1991), (Lehuger et al., 2009), (Bell et al., 2012), (Parton et al., 2001), (Frolking et al., 1998)
		θ_3	w_2	Exponent of the power function for denitrification	uniteless	1.74	1.3	2.5	(Stanford et al., 1975), (Smith et al., 1998), (Johnsson et al., 1991), (Maag and Vinther, 1996), (Maag and Vinther, 1999), (Skopp et al., 1990), (Lehuger et al., 2009), (Bell et al., 2012)
		θ_4	$BioAct$	Rate for soil biological activity	uniteless	0.005	0	0.01	(Bradbury et al., 1993), (Bell et al., 2012)
		θ_5	$P_{NO3,f}$	NO_3 content of the soil at which N is released in equal of N_2 and N_2O	uniteless	200	150	250	(Frolking et al., 1998), (Bell et al., 2012)
		θ_6	D_P	Potential denitrification rate	kg N ha^{-1} layer^{-1}	Site–specific	0	1	(Parton et al., 1996), (Parton et al., 2001), (Bell et al., 2012)
	global	θ_7	nf	Proportion of N_2O produced due to partial nitrification at filed capacity	uniteless	0.02	0.01	0.4	(Bell et al., 2012)
		θ_8	$P_{N2,f}$	Denitrification proportioned into N_2 according to water content	uniteless	0.5	0	1	(Frolking et al., 1998), (Bell et al., 2012)
		θ_9	n_{gas}	Proportion of full nitrification lost as gas	uniteless	0.02	0.01	0.09	(Bell et al., 2012)
		θ_{10}	n_{no}	Proportion of full nitrification gaseous loss that is NO	uniteless	0.4	0.1	1	(Frolking et al., 1998), (Bell et al., 2012)
NO flux module	Site-specific	θ_{11}	$Nitri_{rate}$	Nitrification rate	kg N ha^{-1} layer^{-1}	0.6	0	1	None information
		θ_{12}	T_1	Parameter for air temperature	uniteless	47.9	45	55	(Bradbury et al., 1993)
		θ_{13}	T_2	Parameter for air temperature	uniteless	106	90	110	(Bradbury et al., 1993)
		θ_{14}	T_3	Parameter for air temperature	uniteless	18.3	15	25	(Bradbury et al., 1993)
		θ_{15}	pH_{cons}	Constant for pH modifier	uniteless	0.56	0.2	0.7	(Parton et al., 1996)
		θ_{16}	pH_{modif}	Shape of pH modifier	uniteless	0.45	0.2	0.7	(Parton et al., 1996)
		θ_{17}	pH_{Tr}	pH threshold for pH rate change	uniteless	5	4	6	(Parton et al., 1996), (Mortland, 1970), (Gilmour, 1984)
		θ_{18}	m_{w0}	Soil water rate modifier for decompostition at permanent wilting point	%	0.2	0.1	0.3	(Bell et al., 2012)
		θ_{19}	$Cmax$	Maximum rate of nitrification possible	uniteless	50	40	60	(Parton et al., 1996)

3.5.4 Calculations and statistics

HB calibration was applied to the N-HB model by using data of total 15 experimental sites. Bayesian calibration was performed with the statistical package R (R Development Core Team, 2005), particularly its R2jags package (Plummer, 2003). Convergence diagnostic analysis and model evaluation and comparison were performed with the R 'boa' package (Smith et al., 2007b). Simple linear regression analysis was applied between the mean values of estimated parameters and soil properties. Analysis of association was used to reveal how well the trends in the measured values were simulated, and indicate whether the model was showing the correct response to changes in conditions; this was calculated using the coefficient of determination (R^2) and correlation coefficient (r), and the significance of the correlation was quantified using an F test (Smith et al., 1997). The degree of coincidence was calculated as the root mean squared error ($RMSE$) and the significance was quantified where standard errors were available by comparing to the calculated value for $RMSE$ at the 95% confidence interval of the measurements around the mean (Smith et al., 1997). Bias in the model was analyzed by calculating the mean difference (M) and then undertaking a t test to check for significance in M. Also bias was analyzed by calculating relative error (E) and compare to the E value at the 95% confidence interval of the measurements.

3.6 C budget calculation

3.6.1 Measurements of the net biome productivity

NBP is the total rate of organic C accumulation in (or loss from) ecosystems (Chapin III et al., 2006; Schulze and Heimann, 1998; Buchmann and Schulze, 1999), Based on studies by Ciais et al. (2010), NBP is quantified as

$$NBP = NPP - Rh - CH_4 - H + I \qquad (3.43)$$

NPP is the net primary production (NPP) using crop-level yield statistics and crop-specific allometric relationships developed by Koga et al. (2011). Rh is the soil heterotrophic respiration (Rh), which is calculated based on soil temperature (T, 5 cm depth) and water-filled pore space (WFPS, 5 cm depth), and soil texture classes (Li et al., 2015). CH_4 losses from croplands are expected to be a significant component in paddy rice, but in other cropland systems on well aerated soils it is negligible or even a net sink (i.e. methane oxidation outweighs methane production) (Smith et al., 2010), thus, CH_4 is the CH_4 emission from paddy field in this study. CH_4 flux in a paddy rice field showed a high correlation with the applied amount of straw and was calculated by a function of the amount of straw residues (Naser et al., 2007). H is the harvested component of NPP (TC_h). I is the C input into the soil as residue C, which is plant residue C include above-ground residue biomass (TC_a) and below-ground biomass (TC_b), and C input from manure, which was only considered in grassland (2.41 Mg C ha^{-1} yr^{-1}, Kimura et al., 2010). The ratio of NBP/NPP is defined as the C sequestration efficiency (CE) (Ciais et al., 2010).

We consider the loss of dissolved C to be of minor importance of the NBP determination in this study. C lost in fires was considered to be low/negligible in northern Japan. Part of the organic material produced during NPP is lost via emission of volatile organic compounds (VOC), we consider VOC as being negligible here because VOC losses in croplands are relatively small compared to losses from forest (Smith et al., 2010). We consider surface runoff and erosion as being negligible here given the non-hill slopes, permanent soil coverage and level surface at our site (Leifeld et al., 2011).

3.6.2 Estimation of net primary production, carbon harvest and residue carbon inputs

For each crop, crop-level NPP and plant C inputs from plant residues to the soil were calculated using crop yield (Table 3.8) and crop-dependent plant parameters (Table 3.7), which were developed by (Koga et al., 2011). Crop yield production (kg ha^{-1} yr^{-1}) in 1994, 2002, 2005, 2007, 2009 and 2012 were from the total yield production (t) per year and planted area (ha) in Iwamizawa city (Ministry of Agriculture, Forestry and Fisheries, Japan). Crop yield production (kg ha^{-1} yr^{-1}) in 1959, 1966, 1976 and 1988 were estimated by the total yield production (t) per year and planted area (ha) in Hokkaido (Ministry of Agriculture, Forestry and Fisheries, Japan).

$$\mathrm{NPP} = TC_h + TC_r + TC_a + TC_b \tag{3.44}$$

$$\text{Plant C input} = TC_a + TC_b \tag{3.45}$$

where TC_h, TC_r, TC_a and TC_b were the quantities of C (Mg C ha^{-1} yr^{-1}) found in harvest biomass, non-harvested biomass removed from the field (wheat straw in this study), above-ground residue biomass and below-ground residue biomass, respectively. These, in turn, were calculated as follows:

$$TC_h = Y \times \frac{D_h}{100} \times \frac{C_h}{100} \tag{3.46}$$

$$TC_r = Y \times \frac{D_h}{100} \times R_r \times \frac{C_h}{100} \tag{3.47}$$

$$TC_a = Y \times \frac{D_h}{100} \times R_a \times \frac{C_a}{100} \tag{3.48}$$

$$TC_b = Y \times \frac{D_h}{100} \times R_b \times \frac{C_b}{100} \tag{3.49}$$

where Y was the crop yield on a fresh weight basis (Mg ha^{-1} yr^{-1}) obtained from crop yield statistics (Table 3.8), D_h was the dry matter content in harvested biomass (%), R_r, R_a and R_b were the dry weight ratios of non-harvested biomass removed from the field, above-ground residue biomass and below-ground residue biomass to harvested biomass, respectively, and C_h, C_r, C_a and C_b were the dry weight-based C contents (%) of harvested biomass, non-harvested biomass removed from the field, above-ground residue biomass and below-ground residue biomass, respectively.

Crops such as fruits, melon and pumpkin which are lack of details of crop-dependent plant parameters (Table 3.7), their NPP (Mg C ha^{-1} yr^{-1}) and C in harvest (Mg C ha^{-1} yr^{-1}) were estimated from dry weight of total plant (Mg C ha^{-1} yr^{-1}) and dry weight of main plant using the empirical linear regression (Matsumoto, 2000). Dry weight of total plant (Mg C ha^{-1} yr^{-1}) and dry weight of main product (Mg C ha^{-1} yr^{-1}) were estimated from total crop production (kg ha^{-1} yr^{-1}), water content of main product (%) and the ratio of by product to main product

(Eq. 3.50 and 3.51). We used the water content of plant (%) and ratio of main product and by product were developed (Table 3.7).

NPP (Mg C ha^{-1} yr^{-1}) = (Crop production of each land use type (kg C ha^{-1} yr^{-1}) $\times$ (100 – Water content of each main product (%))/100 $\times$ (1 + Ratio of by product to main product) $\times$ 0.446 – 0.00067) $\times$ 0.001 (3.50)

C in harvest (Mg C ha^{-1} yr^{-1}) = (Crop production of each land use type (kg C ha^{-1} yr^{-1}) $\times$ (100 – Water content of each main product (%))/100 $\times$□0.446 – 0.00067) $\times$ 0.001 (3.51)

The crop residue was defined as that part of the crop not harvested as product, including root. The amount of total crop residue for a given land use type was calculated using the ratio of the by product to the main product (Eq. 3.44).

C in residue (kg C ha^{-1} yr^{-1}) = (C in harvest (kg C ha^{-1} yr^{-1})) $\times$ Ratio of by product to main product) $\times$ 0.001 (3.52)

Table 3. 7 Crop-specific allometric relationships and C contents used to estimate crop NPP, C harvest and plant C inputs.

Crop		Ratio of plant biomass to harvested biomass in dry weight			C content (%)					
	Dry biomass content in harvested biomass (%)	Non-harvested biomass (removed from the field)	Above-ground residue biomass (returned to the soil)	Below-ground residue biomass (returned to the soil)	Harvested biomass (C_h)	Non-harvested biomass (removed from the field)	Above-ground residue biomass (returned to the soil)	Below-ground residue biomass (returned to the soil)	main product water content[d]	by prod/main prod[d]
	D_h	R_r	R_a	R_b	C_h	C_r	C_a	C_b	%	% (DW base)
Soybean	85[a]	-	1.14(27)[a]	0.298(27)[a]	56(2.1)[a]	-	43.5(3.7)[a]	37.9(10)[a]	-	-
Potato	22.1(4.5)[a]	-	0.0845(33)[a]	0.0827(23)[a]	43.4(1.4)[a]	-	33.3(12)[a]	37(11)[a]	-	-
Buckwheat	86.5[d]	-	1.2[b]	0.17[b]	45[c]	-	45.8[b]	45.8[b]	-	-
Vegetable	28[d]	-	0.7[b]	0.04[b]	45[c]	-	33.2[b]	39.4[b]	-	-
Onion	16[d]	-	0.12[b]	0.005[b]	45[c]	-	39.3[b]	40.4[b]	-	-
Maize	19.1(14)[a]	-	1.47(13)[a]	0.422(67)[a]	47.5(1.3)[a]	-	45.2(2.4)[a]	26.4(23)[a]	-	-
Greenhouse	28[d]	-	0.7[b]	0.04[b]	45[c]	-	33.2[b]	39.4[b]	-	-
Fruits	-	-	-	-	-	-	-	-	89.70	0.44
Melon	-	-	-	-	-	-	-	-	74.70	1.50
Pumpkin	-	-	-	-	-	-	-	-	94.70	0.53
Wheat	86.5[a]	0.986(16)[a]	0.831(18)[a]	1.1(37)[a]	44[a]	43.5(2.1)[a]	45.2(2.4)[a]	25.3(26)[a]	-	-
Grass	28[d]	-	0.1[b]	0.55[b]	45[c]	-	43.4[b]	43.8[b]	-	-
Paddy	95[d]	1.2 [b,e]	1.42[b]	0.27[b]	45[c]	38.1[e]	38[b]	38[b]	-	-
Bush Fallow	-	-	-	-	-	-	-	-	-	-

[a] Data from Koga et al. (2011)

[b] Data from Ogawa (1988)

[c] The C content of crop dry matter was assumed to be 45% from Matsumoto (2000) when there is no detailed data of C content in harvested biomass, above-ground residue biomass and below-ground residue biomass.

[d] Guidelines for cultivation of green manure crops in Hokkaido, Hokkaido Government of Agriculture, Hokkaido Agricultural Development and Extension Association.

[e] Data from Naser (2006)

Table 3. 8 Crop yield (Mg C ha^{-1} yr^{-1}) data in the Ikushunbetsu watershed from 1959 to 2011.

Year	1959[a]	1966[a]	1976[a]	1988[a]	1994[b]	2002[b]	2005[b]	2007[b]	2009[b]	2012[b]
Soybean	1.5	0.7	1.8	1.9	2.4	2.1	2.3	2.7	2.2	2.7
Potato					24.2	28.6	28.6	31.4	26.9	25.8
Buckwheat					0.7	0.9	0.8	0.7	0.7	0.9
Vegetable	22.6	27.0	51.2	53.5	55.2	61.5	62.2	64.5	56.6	63.4
Onion	65.5	46.9	56.2	50.2	42.2	53.1	51.0	37.4	37.4	50.0
Maize					10.2	11.3	10.8	10.4	10.4	11.2
Greenhouse					55.2	61.5	62.2	64.5	56.6	63.4
Fruits					8.9	7.3	8.5	8.5	8.5	8.5
Melon					18.4	18.4	20.2	21.1	21.1	22.3
Pumpkin					19.8	15.3	14.6	10.8	11.2	12.8
Wheat	2.0	1.2	3.1	4.1	3.9	4.5	4.7	5.0	3.4	4.9
Grass	21.3	21.5	30.9	42.2	34.8	33.9	34.4	33.5	32.8	32.9
Paddy	3.1	3.9	4.5	4.9	5.3	5.4	6.0	5.4	4.9	5.7
Bush / Fallow	38.4	38.4	38.4	38.4	38.4	38.4	38.4	38.4	38.4	38.4

[a] Crop yield were estimated from the total yield production (t) per year and planted area (ha) in Hokkaido (Ministry of Agriculture, Forestry and Fisheries, Japan).
[b] Crop yield were estimated from the total yield production (t) per year and planted area (ha) in Iwamizawa city (Ministry of Agriculture, Forestry and Fisheries, Japan)

3.6.3 Soil heterotrophic respiration

Soil heterotrophic respiration (Rh) was from decomposition of soil organic matter decomposition (SOMD) in uplands, which was simulated based on soil temperature (*T*, 5 cm depth), water-filled pore space (WFPS, 5 cm depth) and soil texture (Li et al., 2015). Soil temperature was calculated by air temperature based on the empirical equation (Kimura et al., 2010). We converted the gravimetric soil water content data simulated by HYDRUS-1D to WFPS after making the assumption, based on local soil textural data, that bulk density of the clay loam (CL), light clay (LiC), silty caly (SiC) and silty caly loam (SiCL) was 1.22 (±0.15) g/cm, 1.15 (±0.12) g/cm, 1.12 (±0.11) g/cm and 1.09 (±0.00) g/cm, respectively. Gravimetric soil water content in each soil texture was simulated by HYDRUS-1D in the 0–5 cm soil layer (Li et al., 2015).

3.6.4 Uncertainty in net biome productivity

Uncertainty classes were assigned to individual budget terms depending on the accuracy of the data source using a similar classification scheme as proposed by (Vogt et al., 2013). The overall uncertainty of the NBP ($E_{\Delta NBP/\Delta t}$) was calculated as the square root of the sum of the error (*E*) squares.

$$E_{\Delta NECB/\Delta t} = \mathrm{sqrt}[(E_{NPP})^2 + (E_{Rh})^2 + (E_{CH4})^2 + (E_H)^2 + (E_I)^2] \tag{3.53}$$

The uncertainty associated with the NPP (E_{NPP}) is estimated based on standard deviations for TC_h, TC_r, TC_a and TC_b. Uncertainty of TC_h, TC_r, TC_a and TC_b were calculated based on standard deviations of crop-specific plant parameters (Table 3.7). The uncertainty of C harvest and plant C inputs was based on standard deviation of crop-specific plant parameters (Table 3.7). The uncertainty of manure C inputs is estimated to be low (10%) (Kimura et al., 2011). The uncertainty of (E_{Rh}) is considered to be the 95% confidence interval of the simulated value (Li et al., 2015). The uncertainty of CH_4 emissions (E_{CH4}) is estimated to be high (90%) due to straw application in paddy rice field (Naser et al., 2007). The Temporal uncertainty of NPB was estimated as the inter-annual variation between 1959 and 2011.

3.6.5 Soil inventory

There are total 51 soil sampling sites across land use of upland, paddy and grass at Ikushunbetsu river watershed. Sampling points at regional scale were drawn on a map and the main soil type of was determined using ArcGIS. Soil properties sampling were conducted every two years from 2002 to 2011, with the number of sampling points N=51 drawn on an ArcGIS map (Fig. 3.8). The land use change from paddy to upland occurs at only 3 soil-sampling sites from 2005–2011. There are 4 soil-sampling sites at grass, 15 at paddy, 29 at upland from 2005–2011. The first soil inventory took place on September 2005 and the second one on September 2011. For each soil inventory, in the soil depth (0–30 cm), each soil depth was divided into 2 or 3 layers, volumetric soil samples were taken by hand with steel cores (100 cm^3) in each layers with 5 replications. Soil samples were sieved over 0.5 mm mesh to remove stones and coarse roots and dried as dry soil. Total C (TC) (mg C kg^{-1}) was analyzed by TC analyzer (NC-1000, Sumika Chemical Analysis Service, Ltd., Osaka, Japan). Bulk Density (BD) (Mg m^{-3}) was measured in 2007, 2009 and 2011. There was no data record of BD in 2005, therefore, the average value from 2007–2011 was used to calculate BD in 2005. The change of soil C stock at non land-use change at individual land use (upland, paddy, grass) from 2005–2011 was compared with the C budget change from NBP method.

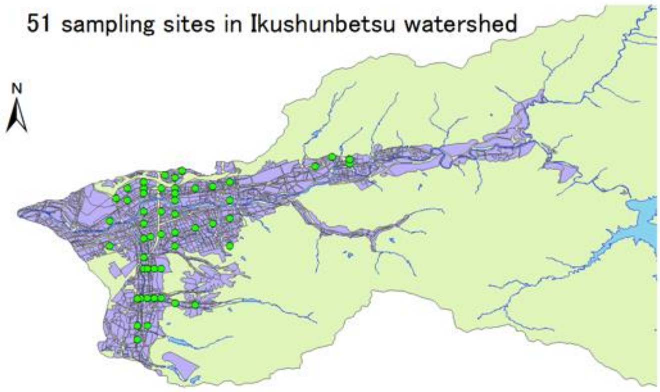

Figure 3. 8 Sampling sites for soil properties (N=51) in Ikushunbetsu watershed.

3.6.6 Calculations and statistics

Correlations between each weather variable and residue production (Mg C ha^{-1} hr^{-1}) were determined using the Pearson correlation. To determine which combination of weather variables could best predict the observed temporal pattern of residue C input rates (i.e., as an indicator of primary productivity), and growing season (Beginning of April until middle of September) weather data were used as independent variables in a suite of backward stepwise regression (in R).

4. Modeling soil carbon dioxide (CO_2) flux from cropland (CO_2-HB model)

4.1 Introduction

Soil emits CO_2 mainly through microbial decay of plant litter and soil organic matter (SOM) (Wang and Chen, 2012), and quantitative studies on soil CO_2 flux from SOM is basic and essential for understanding C and N cycle. CO_2 flux estimation have provided insights into the factors controlling soil CO_2 flux, which are mainly soil temperature and soil water, and shown that the importance of these factors varies depending on soil type (Jenkinson et al., 1991; Raich and Potter, 1995; Hashimoto et al., 2011). Hashimoto et al. (2011) developed a simple greenhouse gas (SG) model based on three functions, namely soil physico-chemical properties, soil temperature, and soil water, and calibration revealed that the physico-chemical properties of the soil were less sensitive than soil temperature or soil water upon simultaneous application of these functions. The SG model is a complete pooled model created as one single model across all soil textures and sites; therefore, it neglects the inherent variation among CO_2 fluxes. As data often arrive with a multilevel structure (e.g., soils with different textures, with sampling performed on-site), the effect of soil water on soil gas flux (CO_2, N_2O, and CH_4) is considered to depend on soil texture or clay content (Parton et al., 1996). Because the effect of soil water and soil temperature on CO_2 flux varies across different soil textures, thus, this chapter simulates CO_2 flux from soil at a daily time resolution, addresses the uncertainties associated with CO_2 flux estimation by the HB method, and quantifies the response of CO_2 flux to environmental factors with soil texture-specific estimation using a hierarchical structure.

4.2 Results

4.2.1 Hierarchical Bayesian calibration

The median, mean, and standard deviation values, in addition to the 95% confidence interval levels of the posterior probability distribution of the parameters (β_1, β_2, β_3, β_5, and β_6) estimated for the best fit of the HB model for each soil texture are summarized in Table 4.1. Daily CO_2 fluxes for each soil texture were predicted from the mean values, together with the soil temperature and WFPS. The HB model captured a large part of the measured variation in CO_2 fluxes (Fig. 4.1), with an R^2 of 0.64 (P<0.001). The plots of the predicted against measured CO_2 fluxes for each soil texture were distributed around the 1:1 line (Fig. 4.1), indicating that the HB model could produce reliable predicted values for each soil texture. The value of R^2 for CL, LiC, SiC, and SiCL were 0.58 (P<0.001), R^2 =0.55 (P<0.001), R^2 =0.48 (P<0.001), and R^2=0.57 (P<0.001), respectively. The HB model accurately predicted the direction, timing, and magnitude of changes in CO_2 flux, and more than 90% of the predicted CO_2 flux values were distributed within the 95% confidence interval of the measured data (Fig. 4.2). The measured CO_2 flux showed clear seasonality, with high levels in summer and low levels in spring and autumn (no observation was conducted in winter), showed a good correspondence with the seasonality of soil temperature (Fig. 4.2). The resulting posterior area-specific export described by the 95% confidence interval can provide both point and interval estimations of CO_2 flux at different times. Taking the peak CO_2 flux at SiCL in the summer of 2008 as an example, the mean value was calculated as 28.9 kg C ha^{-1} day^{-1}, the median value was 23.2 kg C ha^{-1} day^{-1}, and the 95% confidence interval ranged from 10.2 to 69.7 kg C ha^{-1} day^{-1}.

Table 4. 1 Characteristic values for posterior probability distributions of the parameters fit for hierarchical Bayesian (HB) CO_2 flux model for each soil texture. A uniform distribution was assumed for every prior distribution.

Soil texture	Function	Parameter	Median	Mean	SD	2.50%	97.50%
CL*(j=1)*		$\beta_{k,i}$					
	constant	$\beta_{1,1}$	1.470	1.491	0.253	1.040	1.982
	h(T)	$\beta_{2,1}$	0.067	0.065	0.011	0.046	0.087
	g(WFPS)	$\beta_{3,1}$	–1.405	–1.327	0.477	–1.968	–0.277
		$\beta_{4,1}$	0.553	0.547	0.066	0.410	0.679
		$\beta_{5,1}$	2.252	2.254	0.561	1.075	2.959
		$\beta_{6,1}$	13.522	14.014	9.051	1.870	35.947
LiC*(j=2)*							
	constant	$\beta_{1,2}$	1.637	1.658	0.225	1.035	1.897
	h(T)	$\beta_{2,2}$	0.074	0.073	0.011	0.063	0.104
	g(WFPS)	$\beta_{3,2}$	–1.241	–1.191	0.518	–1.975	–0.139
		$\beta_{4,2}$	0.474	0.468	0.064	0.325	0.575
		$\beta_{5,2}$	2.344	2.326	0.498	1.213	2.970
		$\beta_{6,2}$	14.417	14.991	10.239	2.344	40.463
SiC*(j=3)*							
	constant	$\beta_{1,3}$	0.892	0.938	0.228	1.008	1.837
	h(T)	$\beta_{2,3}$	0.059	0.057	0.012	0.019	0.065
	g(WFPS)	$\beta_{3,3}$	–1.142	–1.142	0.478	–1.964	–0.234
		$\beta_{4,3}$	0.544	0.541	0.042	0.443	0.614
		$\beta_{5,3}$	2.175	2.203	0.531	1.158	2.958
		$\beta_{6,3}$	18.822	18.314	11.994	5.169	47.582
SiCL*(j=4)*							
	constant	$\beta_{1,4}$	1.658	1.670	0.188	1.264	1.997
	h(T)	$\beta_{2,4}$	0.060	0.059	0.010	0.044	0.082
	g(WFPS)	$\beta_{3,4}$	–1.401	–1.320	0.504	–1.973	–0.182
		$\beta_{4,4}$	0.610	0.602	0.045	0.537	0.697
		$\beta_{5,4}$	2.325	2.308	0.546	1.087	2.961
		$\beta_{6,4}$	13.723	14.194	7.290	2.105	29.207

$\beta_{1,j}$ is the constant; $\beta_{2,j}$ is the parameter for soil temperature function *h(T)*; $\beta_{3,j}$, $\beta_{4,j}$ and $\beta_{5,j}$ are minimum, optimum and maximum values of WFPS, respectively. $\beta_{6,j}$ is the parameter controlling curvature of soil moisture function.

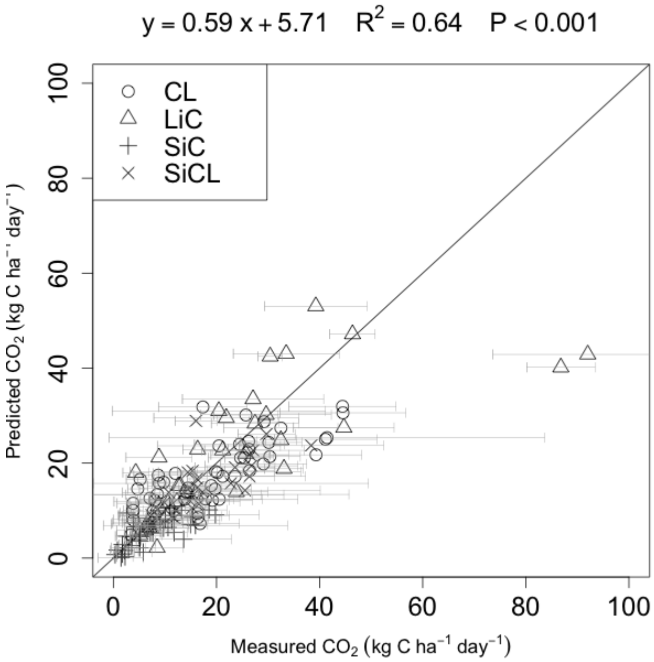

Figure 4. 1 Comparison between CO_2 flux predicted by hierarchical Bayesian (HB) model and measured CO_2 flux. Bars indicate standard deviation for measured value.

Daily CO_2 fluxes predicted by HB generally followed the pattern of the measured fluxes; however, some discrepancies were observed, especially regarding the high spike of CO_2 prediction, *e.g.*, in LiC measured in the summer of 2010 (Fig. 4.2). There were some further discrepancies between the measurements and predictions, particularly for SiC soils, where the model underestimated CO_2 flux in 2008 and failed to reproduce the wide fluctuations in 2006. High CO_2 peaks with high standard deviations explain the large discrepancies. The upper range of the 95% CI included high values, suggesting that the HB model exhibited high uncertainty for high CO_2 flux values (Wang et al., 2010). CO_2 flux had a larger confidence interval (95%) in the summer months of the study years (Fig. 4.2), indicating that the uncertainty of prediction increased with increased temperature.

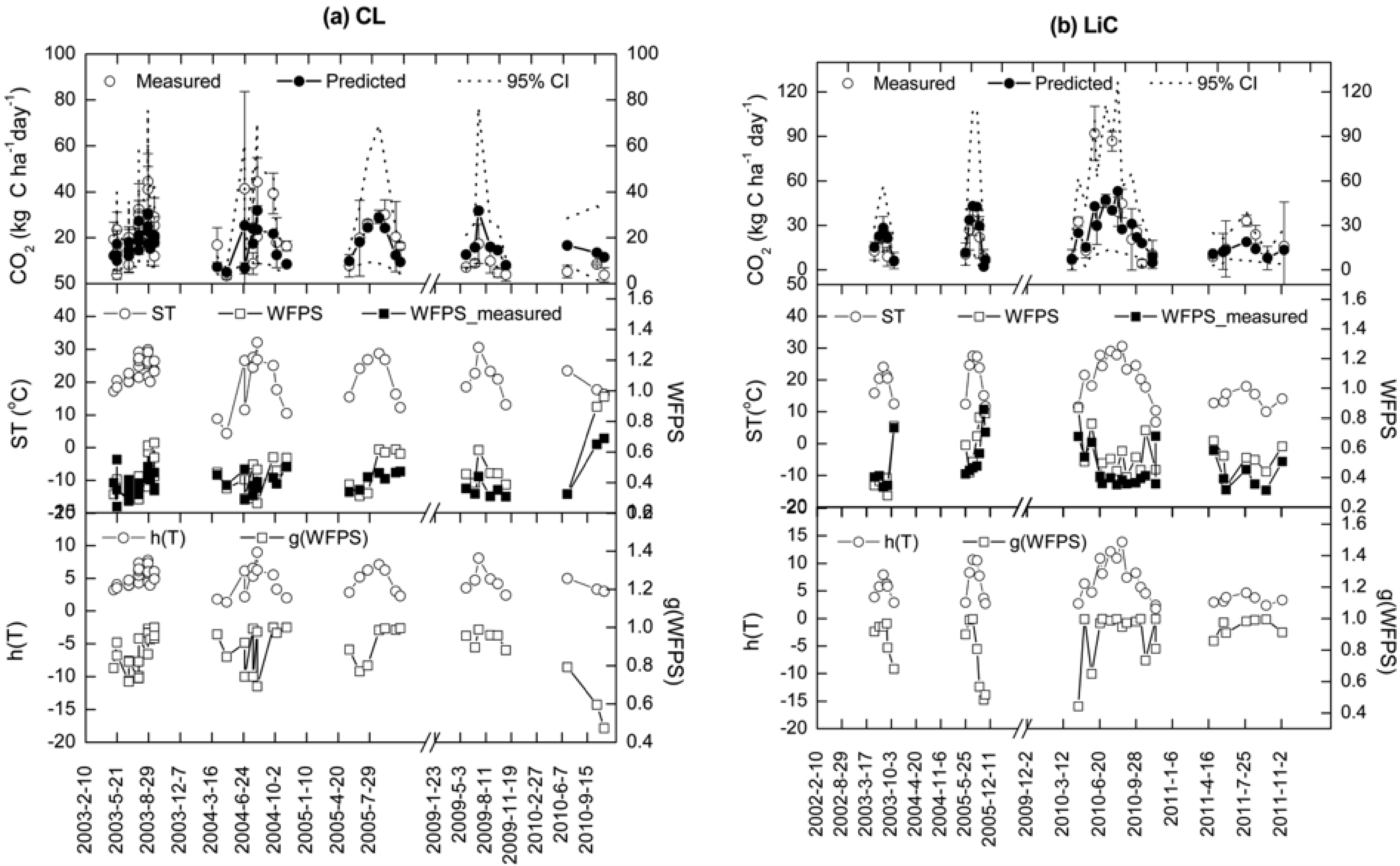

(a) CL
(b) LiC
Measured
Predicted
95% CI
CO2 (kg C ha-1 day-1)
ST
WFPS
WFPS_measured
ST (°C)
h(T)
g(WFPS)

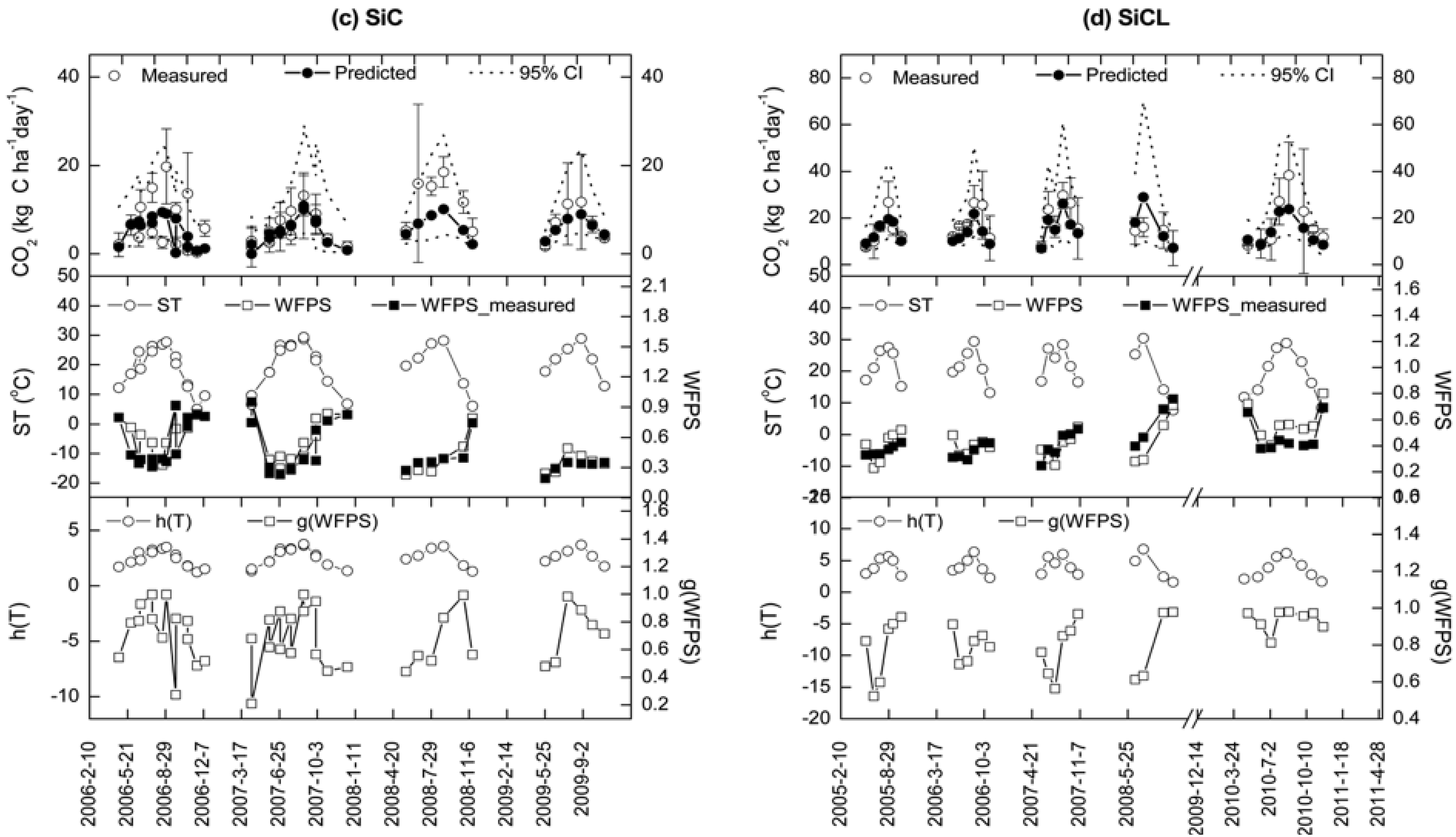

Figure 4. 2 Change in CO_2 flux, water-filled pore space (WFPS), measured value of WFPS (WFPS_measured) and functions of soil temperature [h(T)] and WFPS [g(WFPS)] for each soil texture of (a) CL, (b) LiC, (c) SiC and (d) SiCL. Bars in measured CO_2 flux indicate standard deviation. Predicted CO_2 flux was estimated by the hierarchical Bayesian (HB) model. 95% CI of CO_2 flux was the range of quantile between 2.5% and 97.5% of the posterior distribution of the predicted CO_2 flux at each sampling time.

Figure 4.3 shows the posterior density intervals of the estimated parameters after calibration with texture-specific estimation. Such representation makes it possible to visualize differences between parameter pdfs across textures, whereas the shape of the intervals reveals the dispersion and symmetry of the marginal distribution. For the parameters β_3, β_5, and β_6, the posterior density intervals overlapped, indicating a lack of credible differences among soil textures. A significant difference was found for SiC-LiC and SiC-SiCL in β_1 and LiC-SiCL in β_4. For β_2, though the posterior density intervals did not all overlap, and there were no clear differences among soil textures.

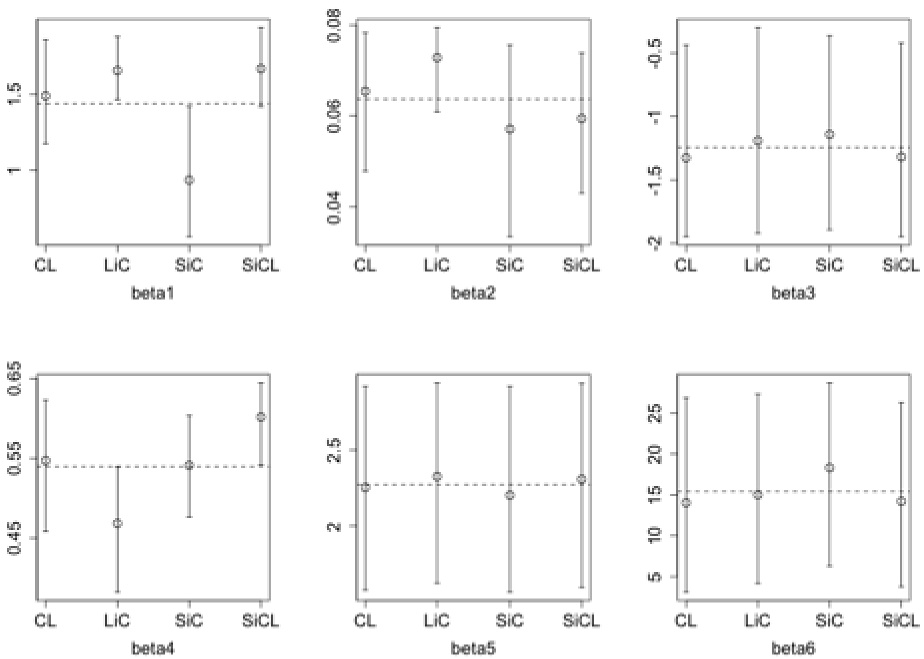

Figure 4. 3 Posterior density intervals of calibrated parameters (β_1 to β_6). Open circles indicate the mean posterior estimate for soil-specific estimation. Error bars are 90% posterior density intervals. Dashed line indicates the mean value over all soil textures.

Table 4.3 shows that the AIC for C:N ratio 2.60 was the smallest among predictor variables of β_1 and also smaller than the AIC for no predictor variables. Therefore, the C:N ratio was the best predictor variable for β_1. In the same manner, the best predictor variables for β_2, β_3, β_4, β_5, and β_6, were silt content, clay content, total C content, C:N ratio, and clay content, respectively. The regression analysis is shown in Figure 4.6, and a significant, positive correlation between clay content and parameter β_3 was found.

4.2.2 Model evaluation and comparison

The HB model achieved better performance than the Bayesian pooled model (Table 4.2), which showed higher RMSE and DIC values than the HB model. In addition, R^2, which represented the fit of the model prediction to the measured values, was lower in the Bayesian pooled model (0.39) than in the HB model (0.64). However, the HB model required a higher effective number of parameters (*pD*) (21.6) than the Bayesian pooled model (5.1). These findings indicate that the HB model provided better predictions but with increased model complexity. Table 4.2 also shows the goodness of fit of the effect of soil temperature and WFPS on daily CO_2 flux. The HB model with only the $h(T)$ function explained 61% of the variability in the measured CO_2 flux, whereas 21% of the variability in the measured CO_2 flux was explained by the HB model with only the g(WFPS) function. DIC was also smaller in the full HB model (996) than in the HB model with only the $h(T)$ function (1018) or only the g(WFPS) function (1131).

Table 4. 2 Root mean square error (RMSE); deviance information criterion (DIC) of nonhierarchical Bayesian model (Bayesian pooled model) and hierarchical Bayesian (HB) model of CO_2 flux and determination coefficient (R^2) of the correlation between measured and predicted values. $exp(\beta_1)h(T)$ and $exp(\beta_1)g(\mathrm{WFPS})$ represent HB model structure including only the response function for soil temperature and including only the response function for WFPS.

Model	RMSE	DIC			R^2
		pD	$\overline{D}$	DIC	
Bayesian Pooled	10.6	5.1	1168	1173	0.39
Hierarchical Bayesian					
$exp(\beta_1)h(T)g(\mathrm{WFPS})$	8.37	21.6	974	996	0.64
$exp(\beta_1)h(T)$	8.77	14.0	1004	1018	0.61
$exp(\beta_1)g(\mathrm{WFPS})$	14.3	16.2	1115	1131	0.21

Table 4. 3 The value of Akaike's Information Criterion (AIC) for selecting the best variables for estimated parameters. Smaller AIC value shows better predictor variable.

	silt	clay	silt+clay	TC	TN	C:N	No predictor variables
β_1	5.70	5.34	4.85	7.66	7.65	2.60	5.66
β_2	–28.08	–23.38	–24.96	–26.42	–26.88	–23.31	–25.28
β_3	–3.55	–14.24	–6.01	–3.22	–2.92	–8.24	–4.81
β_4	–8.08	–7.69	–7.04	–12.43	–11.21	–8.19	–9.00
β_5	–7.93	–7.46	–7.88	–6.91	–6.91	–9.62	–8.91
β_6	19.01	14.99	15.68	21.75	21.70	15.96	19.76

4.2.3 Behavior of response functions of CO_2 flux to soil temperature and soil water [*h*(*T*) and *g*(WFPS)]

Different soil textures showed different tendencies for the response function *h*(*T*) (Fig. 4.4). Light silt and clay soils showed the highest value for parameter β_2 of the response function *h*(*T*) (Table 4.1) and also demonstrated the steepest increase of *h*(*T*) with increased soil temperature, followed by CL and SiCL, whereas SiC showed only a slight increase in h(T). Parameter β_2 was negatively correlated with the silt content, although the R^2 of 0.7 was not significant (Fig. 4.6). The Q_{10} value calculated as $Q_{10} = exp(10\beta_2)$ was highest for LiC (2.08, with 1.87–2.83 of 95% confidence interval (CI)), followed by CL (1.92, with 1.58–2.40 of CI), SiCL (1.80, with 1.55–2.26 of CI), and finally SiC (1.77, with 1.21–1.92 of CI).

Different soil textures also showed different tendencies for the response function *g*(WFPS) (Fig. 4.5). Light clay soils showed the lowest optimal WFPS (0.468) for *g*(WFPS) (the value of parameter β_4 in Table 4.1) and a steep decrease of *g*(WFPS) with increases in WFPS over the optimal value, which occurred rapidly in soils containing less clay and silt at above-optimal WFPS levels. In contrast, SiCL soils had the highest value of optimal WFPS (0.602) and a steep increase of *g*(WFPS) with increases in WFPS below the optimal values. The optimal WFPS for *g*(WFPS) of CL and SiC was 0.547 and 0.541, respectively. However, the change in *g*(WFPS) with WFPS was more gradual for CL than for SiC, possibly because CL had a lower value for parameter β_3 (–1.327) than SiC (–1.142), thus indicating that insufficient parameter constraints resulted in the low sensitivity of *g*(WFPS) in CL.

4.3 Discussion

4.3.1 Suitability and benefits of Bayesian calibration

Evaluation of the performance of the HB model and the Bayesian pooled models

(Table 4.2), and comparison of the predicted and measured CO_2 flux (Fig. 4.2), show that the HB model provided much better predictions by providing texture-specific parameter estimates, except for the highest peaks with high experimental error which are underestimated in some cases. The HB model thus showed good performance in fitting the soil texture data and in providing reasonable prediction intervals. Prediction intervals are influenced by the combined effects of measurement error, variability in local climate, and soil conditions, and also from the uncertainty inherent in fitting models with finite data sets. When measurements are available across multiple soil types, the HB model provides a basis for pooling this information, thereby reducing the overall uncertainty while still maintaining soil-specific model estimates (Yang et al., 2011). Moreover, the HB model can be applied across different sites and different types of soils, as reflected in the lower RMSE and DIC values, although the model was of a higher complexity and required a higher effective number of parameters.

4.3.2 Effect of soil temperature

Both field and laboratory incubation studies have shown that the activity of soil microorganisms to decompose SOM generally increases with temperature and moisture (Drewnik, 2006; Kim et al., 2010); these effects can also be described by models (Xu and Qi, 2001). Additionally, several studies have shown that soil respiration increases exponentially with temperature when soil water or other factors are not limiting (Raich and Potter, 1995; Kätterer et al., 1998). Although soil temperature and moisture both significantly affect CO_2 flux, as the seasonality of soil temperature explains the high variation of CO_2 flux and CO_2 flux decreased when soils were both dry and wet (Fig. 4.2), the HB model with only the $h(T)$ function explained 61% of the variability in the measured CO_2 flux (Table 4.2), indicating that soil CO_2 flux is primarily dependent soil temperature and that the control of soil water is weak, as previously indicated by another study (Hayakawa et al., 2014; Smith et al., 2005).

Although numerous investigations have evaluated the influence of texture on microbial activity and SOMD (Hayakawa et al., 2014), the influence of soil texture on soil CO_2 flux is seldom revealed by models. The calibration of the HB model in this study suggest that the effects of soil temperature and soil WFPS on CO_2 flux are complex and change with different soil conditions, and that their effects on CO_2 flux are confounded by each other.

The optimized function of soil temperature [$h(T)$] was mildest in SiC soils among the four textures (Fig. 4.4). The Q_{10} values for each soil texture were in the range of previously reported values (Lenton and Huntingford, 2003, Hashimoto, 2005). Although parameter β_2 for soil temperature did not show significant differences among soil textures (Fig. 4.3), β_2 was found to decrease linearly with silt content (Fig. 4.6). The estimation of only four values representing the four soil textures means that the simple linear regression is restricted, and the R^2 value of 0.7 obtained here is not significant (Fig. 4.6). However, our study with a small number of soils revealed that SOMD may be influenced by soil texture. Other studies have revealed that fine-textured soils can absorb organic matter and prevent it from being decomposed by microorganisms (Hassink, 1993; Chevallier et al., 2004), possibly through two mechanisms: (1) physically confining microorganisms in small pores, which makes them less active and protects them against grazing by the soil fauna; and (2) physically protecting nonliving soil organic matter from decomposition by surface adsorption. These may be reasons why temperature sensitivity is low in SiC soil, which had the highest total C and silt and clay content. However, the effect of soil texture on SOMD was undetectable (Hassink, 1993), perhaps because of the confounding effects of variability in substrate availability, microbial biomass (MBC), enzyme activity, and other biochemical characteristics among different soils. Trasar-Cepeda et al. (2007) showed that decomposition activity was highest in the soil containing the highest amount of OM because the enzyme activity was highest in the soil with the highest OM. Although the amount of organic matter appears to be important, Trassar-Cepeda et al. (2007) indicated that because only a small number of soils was studied, no conclusions can be reached about which soil properties cause the variations of Q_{10} value.

Similar to most models of soil C dynamics, we simply assumed that SOM decomposition is nearly equally sensitive at different temperatures, but this assumption is contrary to kinetic theory (Davidson et al., 2006; Kirschbaum, 1995). Some studies observed that temperature sensitivity is far greater at a low temperature than at high temperature (Kirschbaum, 1995); additionally, the decomposition rate of low-quality substrates has a stronger temperature dependence than that of high-quality substrates (Bosatta and Ågren, 1999). For simplicity, the temperature function used here adopts a simple exponential temperature response. This simplification may lead to errors in the estimation of soil CO_2 fluxes at low and high temperatures, although this limitation likely had a small effect on the study period because 95% of the measured soil temperature ranged from 6.73 to 30.02 °C (Fig. 4.4).

$h(T)$ exhibited high uncertainty, probably because the posterior distribution of CO_2 flux had a larger upper interval, particularly in the high-temperature range (Fig. 4.4). Indeed, occasional high CO_2 fluxes were observed in our study at high temperatures (*e.g.*, in October 2010 in LiC soils; Fig. 4.2), as also observed in recent studies (Yang et al., 2011). In addition, the estimation of Q_{10} from the exponential equation often showed high uncertainty; however, this type of uncertainty is ignored in traditional models.

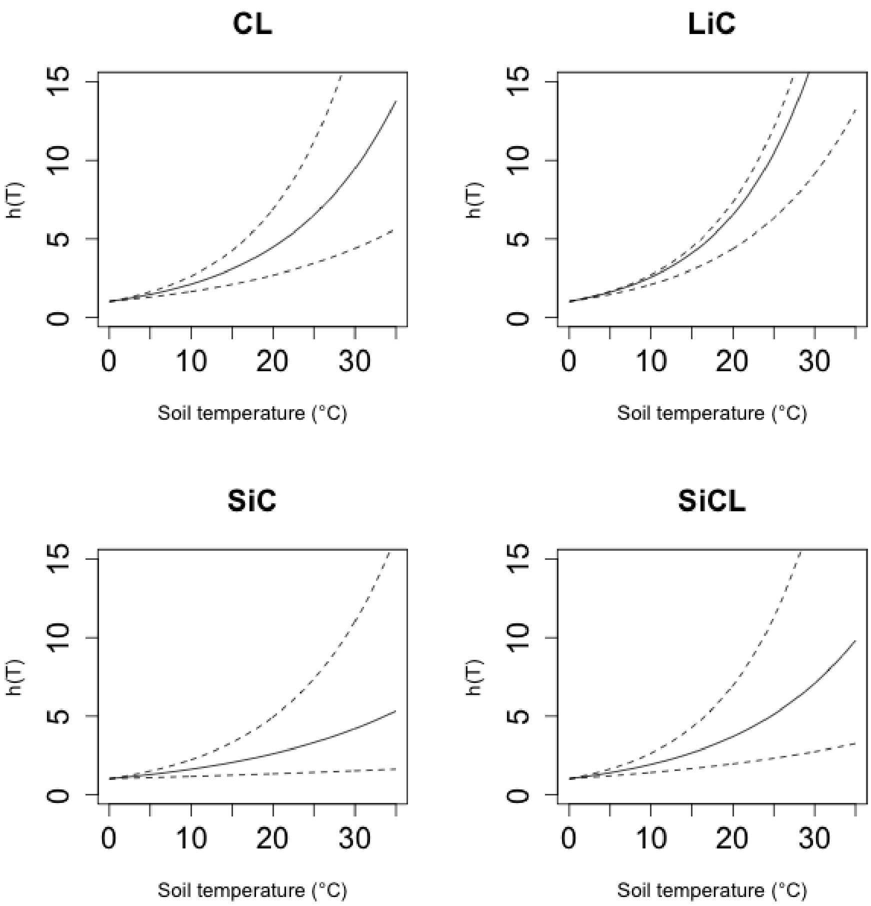

Figure 4. 4 Optimized functions of soil temperature [$h(T)$] predicted by the hierarhical Bayesian (HB) model for each soil texture. Dashed line indicates 95% confidence interval.

4.3.3 Effect of soil water

In general, three phases of the response of CO_2 flux to soil water can be identified in many experiments and models (Davidson et al., 2000; Howard and Howard, 1993; Abdalla et al., 2010; Linn and Doran, 1984; Skopp et al., 1990). (1) When soils are relatively dry, biological activities were limited through limitation of soluble organic C-substrates, and then increase strongly with water availability. (2) There is a range of near-optimum soil water content where CO_2 is maximally emitted because the macropore spaces are mostly air-filled, thus facilitating O_2 diffusion, and the micropore spaces are mostly water-filled, thus facilitating diffusion of soluble substrates. (3) Above the field capacity and approaching saturation, oxygen deficiency inhibits aerobic respiration. Therefore, the shape and curve of the response function of soil water for CO_2 become similar (Fig. 4.5), and this is a better way of expressing soil water content in relation to microbial activity (Rovira, 1953). According to the HB model, WFPS values in the range of 0.47 to 0.60 led to more optimal conditions for CO_2 flux for all textures in this study (Fig. 4.5), which was comparable to the optimum WFPS in other studies (0.34 to 0.56) (Howard and Howard, 1993; Hashimoto et al., 2011). However, some soil types showed different curvature in the relationship. Indeed, differences in the relationship between CO_2 flux and soil water for different types of soil have been found in several studies (Howard and Howard, 1993; Singh and Gupta, 1977).

Soil texture influences the effect of WFPS on SOMD and disturbance of the soil can impact the effect of WFPS on soil CO_2 flux (Fig. 4.5). No significant difference among soil textures was found in parameters of β_3, β_5, and β_6, except for the significant difference of β_4 between LiC and SiCL (Fig. 4.3). Del (2000) found that water is held more tightly with a higher clay and silt content; therefore, soil with a lower clay and silt content requires a lower water content to induce water stress on biological activity. The HB model revealed a higher minimum water content (parameter β_3) in fine-texture soils with significant $R^2 = 0.94$ (Fig. 4.6). Parameters β_4, β_5, and β_6 were positively associated with total C content, C:N ratio, and clay content, respectively, although the correlations were not statistically significant. Howard and Howard (1993) found that soil with a large organic matter content will have a lower degree of saturation than soil with a low organic matter content. However, there was no significant relationship between saturation (parameter β_5) and total C content in this study.

LiC soil exhibited a sharper decrease of *g*(WFPS) after the optimum WFPS (parameter β_4) compared with other soils, which is unrealistic when only considering the effects of soil water on microbial activity because WFPS of approximately 0.47 is not sufficiently high to limit microbial activity or gas diffusion in soils. This phenomenon could be derived from the low CO_2 flux from wet LiC soil when the snow melts in the end of April and early May, resulting in high soil water and low temperature. The soil water content has a lower effect on CO_2 flux at a lower temperature than at a higher temperature (Douglas and Tedrow, 1959), and the spring soil respiration is controlled by temperature rather than moisture (Smith et al., 2003). Xu and Qi (2001) also found that the decrease in soil respiration rate at high soil water levels was mainly caused by the low temperature rather than by the moisture itself. This sharp decrease may indicate that correlations between soil water and CO_2 flux can easily be confounded by other factors (Xu and Qi, 2001; Davidson et al., 1998), and that soil water is not necessarily the single most important factor.

The optimized function of the water-filled pore space [*g*(WFPS)] showed higher uncertainty, higher than that of *h*(*T*) (Fig. 4.4 and 4.5). When the best-fit functions were compared among soil textures, the range of *g*(WFPS) in LiC was larger than that in other soils because LiC soils had the largest range of CO_2 flux (4.3–92.0 kg C ha^{-1} day^{-1}) among soils.

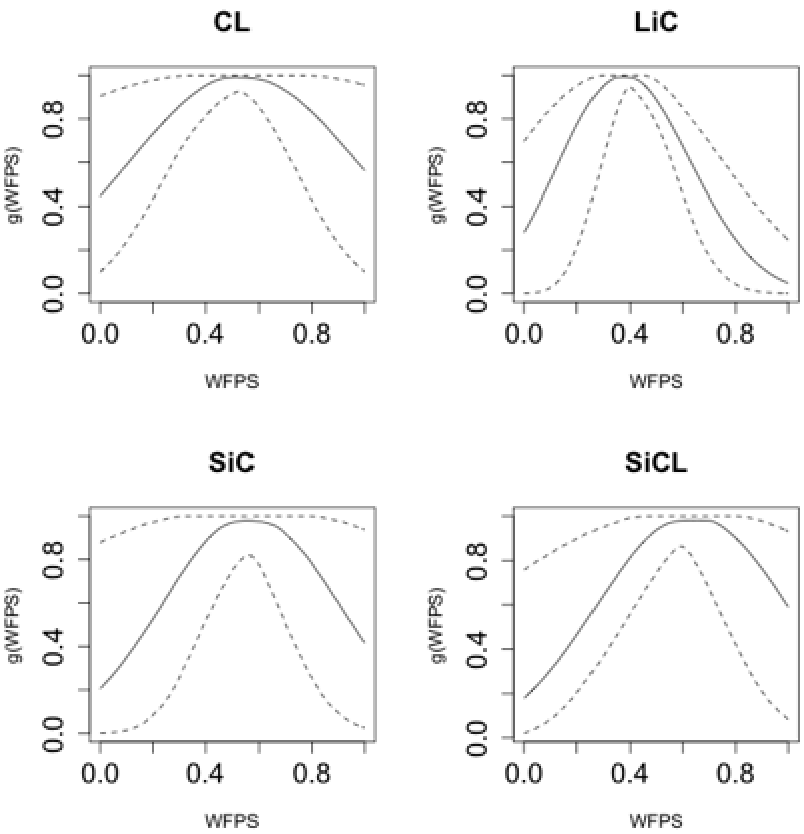

Figure 4. 5 Optimized functions of soil water-filled pore space [*g*(WFPS)] predicted by hierarhical Bayesian (HB) model for each soil textures. Dashed line indicates 95% confidence interval.

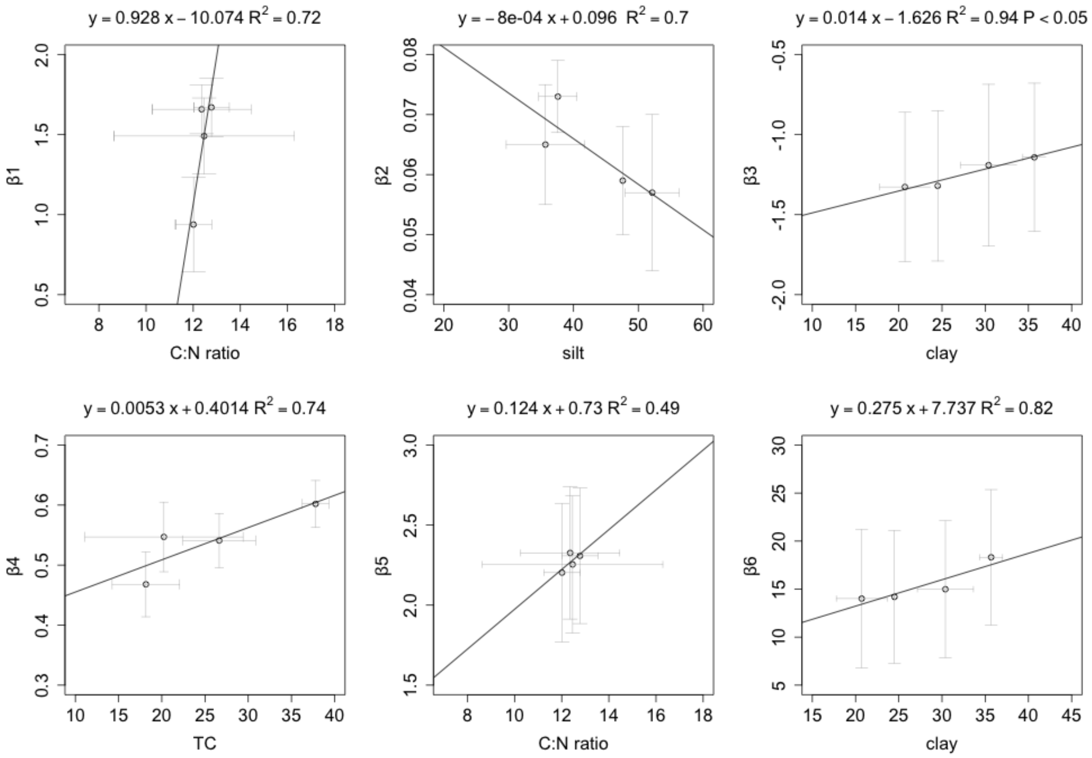

Figure 4. 6 Simple linear regression of estimated parameters calibrated by the hierarchical Bayesian (HB) model with soil properties (C:N ratio, silt content, clay content, and total C content). Bars indicate standard deviation.

4.3.4 Model limitation and improvement

Our results confirmed previous findings showing that soil temperature and moisture are key factors affecting daily CO_2 flux, and that their effects on CO_2 flux are dependent on soil texture. Compared to the SG model constructed by Hashimoto et al. (2011), the HB model not only has the advantage of being simple but also reveals that soil texture should be regarded as a possible scaling factor when up-scaling the model from the site to the regional scale. Thus, the HB model simulates daily CO_2 fluxes at various sites using minimal input data consisting only of soil texture, daily soil temperature, and WFPS, and its results have the potential for extrapolation to the regional scale in soils with similar texture in Hokkaido.

Regarding the application and limitations when up-scaling the model from the site to regional scale, first, the limited data for low CO_2 flux from wet soil (*e.g.*, WFPS range from 0.55 to 0.65) from the end of April until early May resulted in an unrealistic function shape (*e.g.*, LiC), which may overemphasize the effects of soil water on CO_2 flux when the same parameter function is applied to the soils of similar texture. However, this effect was weak during early spring because the effect of soil water is strongly masked by soil temperature (Smith et al., 2003; Xu and Qi, 2001). Therefore, even in early spring, CO_2 flux can be reliably predicted when both functions of soil temperature and moisture are considered in the model, and the soil water function could not constrain CO_2 flux prediction when the HB model was extrapolated to a larger scale. Second, although the temperature effect described by exponential function $h(T)$ and soil water function g(WFPS) is widely and reliably used in gas flux model stimulation (Parton et al., 1996; Del Grosso et al., 2000), the estimated parameters were constrained by the limited amount of data measured in this study. Therefore, the estimated parameters could be applied at the regional scale in Hokkaido for the same seasonal pattern and soil texture, but it is not appropriate to scale up the HB model to a longer temporal scale and larger spatial scale across different soil types, as the parameter functions obtained in this study may be limited in distinguishing the effects of soil temperature and moisture on a larger temporal scale, especially under low-temperature and wet conditions such as those occurring in early spring. The estimated parameters should be considered as site- or soil-specific parameters rather than global parameters.

Although the small number of studied soils and season patterns limits the application of the model to other fields, the results obtained are sufficient to establish a reliable methodology and provide conclusions that may be generalizable to other soils and climate. This study proposed a method to predict the influence of soil texture on the effects of soil temperature and moisture on CO_2 flux, and soil texture could thus be regarded as an up-scaling factor for future research on regional extrapolation. To enhance the reliability and applicability of the HB model on a larger scale and for other soils, future studies should evaluate data across more soils types, especially for coarse soils and seasonal patterns cover snow season and snow melting period.

4.4 Conclusion

We accurately predicted the daily CO_2 flux and quantified the effect of environmental factors on CO_2 flux with consideration of uncertainty using a HB model. Our results confirm previous findings that soil temperature and WFPS are key factors affecting daily CO_2 flux and demonstrate that the effects on CO_2 flux vary with soil texture. The parameter values resulting from the multi-dataset procedure could then be applied to sites sharing the same soil texture. The posterior distributions estimated by CO_2-HB model encompass all of our current measurements, and CO_2-HB model could quantify the uncertainty of CO_2 flux by 95% confidence interval. The HB model structure requires minimal input data for soil texture and simulates daily CO_2 flux using daily soil temperature and WFPS, which may allow the model to be easily applied to the observed CO_2 fluxes.

5. Modeling soil nitrous oxide (N_2O) and nitrogen monoxide (NO) flux from cropland (N-HB) model

5.1 Introduction

There are two general approaches to estimating direct N_2O and NO fluxes from soils in agro-ecosystems. In an empirical model, N_2O and NO fluxes are proportional to some easily quantifiable factors, and is ignoring complex processes and environmental factors in N cycle (Lokupitiya and Paustian, 2006). The process-oriented ecosystem models attempt to simulate many or all of the complex components of N cycle; therefore, process-based models have a unique potential to predict N_2O and NO emissions from arable soils (Butterbach-Bahl et al., 2004; Gabrielle et al., 2006a). However, model testing is often limited by a lack of field data to which the simulations can be compared (Desjardins et al., 2010). The input data requirement for process-based models is also often very high, which leads to the limited use in regional or national predictions from agricultural land (Beheydt et al., 2007; Bell et al., 2012). The model designed and produced to simulate soil N gaseous emissions from soils using only data which is available at national or regional scale where only a minimum amount of meteorological, land-use and soil input data is needed (Smith et al., 2010).

A remaining obstacle to the extrapolation of the N_2O model is that some parameters should be measured or estimated on sites (Lehuger et al., 2009). In traditional model development, parameters of N_2O and NO emissions modules in process-based models are considered universal, because variability of these parameters are not well known in different soils and land managements. However, both theory and observation suggest that the assumption of commonality in parameter values across systems may not always be valid (Borsuk et al., 2001). For ecological modeling, parameter uncertainty estimates is essential (Beck, 1987), and a Bayesian approach provides such information (Malve and Qian, 2006). In the Bayesian framework, the problem of parameter estimation using cross-system data can be viewed as a hierarchy. HB models represent a modeling structure with capacity to exploit diverse sources of information, and yields subunit-specific parameter estimates (Clark, 2005), but shares commonality in values across systems. The HB approach is, therefore, a practical compromise between entirely site-specific and globally common parameter estimate, which could be the potential strategy to deal with model extrapolation and parameters' variability (Lehuger et al., 2009).

Therefore, this chapter designs and produces the model to simulate N_2O and NO emissions from soils using only data which is available at regional scale and to quantify the uncertainty of model simulations by developing a suitable HB calibration method, and to investigate the model extrapolation and the parameters' variability using soil information.

Table 5. 1 Description of 19 parameters of N_2O and NO flux module. The prior probability distribution is defined as uniform between bounds θ_{min} and θ_{max} which were extracted from literature reviews. The posterior parameter distributions are characterized by the mean values of the posterior, their standard deviation (SD), and 95% CI for 15 experimental sites.

Gas module		Parameter vector $\theta=[\theta_1,...,\theta_{19}]$				Default value	Prior probability distribution			Posterior probability distribution			
		Parameter	Symbol	Description	Unit		$\theta_{min}(i)$	$\theta_{max}(i)$	References	Mean	SD	0.025	0.975
N_2O flux module	Site-specific	θ_1	N_{d50}	Soil nitrate content at which denitrification is 50% of its full potential	kg N ha^{-1} $layer^{-1}$	16.5	5	20	(Stanford et al., 1975), (Maag and Vinther, 1999), (Gabrielle, 2006), (Lehuger et al., 2009), (Bell et al., 2012)	13.0	2.91	8.28	17.7
		θ_2	w_1	soil water threshold for denitrification	%	0.62	0.5	1	(Gabrielle, 2006), (Hénault and Germon, 2000), (Johnsson et al., 1991), (Lehuger et al., 2009), (Bell et al., 2012), (Parton et al., 2001), (Frolking et al., 1998)	0.67	0.16	0.50	0.98
		θ_3	w_2	Exponent of the power function for denitrification	uniteless	1.74	1.3	2.5	(Stanford et al., 1975), (Smith et al., 1998), (Johnsson et al., 1991), (Maag and Vinther, 1996), (Maag and Vinther, 1999), (Skopp et al., 1990), (Lehuger et al., 2009), (Bell et al., 2012)	1.94	0.32	1.43	2.47
		θ_4	$BioAct$	Rate for soil biological activity	uniteless	0.005	0	0.01	(Bradbury et al., 1993), (Bell et al., 2012)	0.005	0.003	0.000	0.01
		θ_5	$P_{NO3,f}$	NO_3 content of the soil at which N is released in equal of N_2 and N_2O	uniteless	200	150	250	(Frolking et al., 1998), (Bell et al., 2012)	184	25.7	151	242
		θ_6	D_P	Potential denitrification rate	kg N ha^{-1} $layer^{-1}$	Site–specific	0	1	(Parton et al., 1996), (Parton et al., 2001), (Bell et al., 2012)	0.49	0.29	0.03	0.97
	global	θ_7	nf	Proportion of N_2O produced due to partial nitrification at filed capacity	uniteless	0.02	0.01	0.4	(Bell et al., 2012)	0.003	0.003	0.000	0.010
		θ_8	$P_{N2,f}$	Denitrification proportioned into N_2 according to water content	uniteless	0.5	0	1	(Frolking et al., 1998), (Bell et al., 2012)	0.34	0.21	0.02	0.78
		θ_9	n_{gas}	Proportion of full nitrification lost as gas	uniteless	0.02	0.01	0.09	(Bell et al., 2012)	0.07	0.02	0.03	0.10
		θ_{10}	n_{no}	Proportion of full nitrification gaseous loss that is NO	uniteless	0.4	0.1	1	(Frolking et al., 1998) , (Bell et al., 2012)	0.86	0.02	0.83	0.89
NO flux module	Site-specific	θ_{11}	$Nitri_{rate}$	Nitrification rate	kg N ha^{-1} $layer^{-1}$	0.6	0	1	None information	0.50	0.29	0.03	0.97
		θ_{12}	T_1	Parameter for air temperature	uniteless	47.9	45	55	(Bradbury et al., 1993)	49.9	2.89	45.2	54.7
		θ_{13}	T_2	Parameter for air temperature	uniteless	106	90	110	(Bradbury et al., 1993)	99.7	5.84	90.5	109
		θ_{14}	T_3	Parameter for air temperature	uniteless	18.3	15	25	(Bradbury et al., 1993)	20.0	2.9	15.3	24.8
		θ_{15}	pH_{cons}	Constant for pH modifier	uniteless	0.56	0.2	0.7	(Parton et al., 1996)	0.45	0.14	0.21	0.69
		θ_{16}	pH_{modif}	Shape of pH modifier	uniteless	0.45	0.2	0.7	(Parton et al., 1996)	0.45	0.14	0.21	0.69
		θ_{17}	pH_{Tr}	pH threshold for pH rate change	uniteless	5	4	6	(Parton et al., 1996), (Mortland, 1970), (Gilmour, 1984)	5.00	0.58	4.06	5.94
		θ_{18}	m_{w0}	Soil water rate modifier for decompostition	%	0.2	0.1	0.3	(Bell et al., 2012)	0.28	0.04	0.14	0.30
		θ_{19}	$Cmax$	Maximum rate of nitrification possible	uniteless	50	40	60	(Parton et al., 1996)	40.2	0.21	40.0	40.8

5.2 Results

5.2.1 Posterior parameter distributions

Figure 5.1 shows boxplots of the posterior parameter distributions in N_2O (θ_1 to θ_6) flux module after HB calibration. The y-axis corresponding to the prior range of parameter variation, and the x-axis represented 15 sites. The priors allow for uncertainty. Such representation made it possible to visualize differences between parameter pdfs across sites, while the shape of the boxplot revealed the dispersion and symmetry of the marginal distributions.

Figure 5.1 demonstrates that the posterior distributions of some parameters in N_2O flux module became narrower compared to the uniform prior distributions (corresponding to y-axis), which was due to the efficiency of the HB calibration procedure. Van Oijen et al. (2005) and Lehuger et al. (2009) revealed that the choice of an uniform distribution for the prior had little influence for posterior pdfs, as the measured data gradually became much more dominant than the prior distribution in the calibration process. For example, the posterior distributions of the soil water threshold triggering denitrification (θ_2) had a narrow range for all sites compared to the prior range (corresponding to y-axis) suggesting that the HB calibration drastically reduced its uncertainty. Conversely, NO_3^- content of the soil at which N is released in equal of N_2 and N_2O (θ_5) remained spread across their prior range of variation (corresponding to y-axis), and centered around their prior mean values. This means that the calibration did not significantly reduce their uncertainty. In addition, some posterior distributions were flattened on one of the prior bounds (corresponding to y-axis), implying that their optimal values were outside the prescribed range. This was particular true for soil biological activity (θ_4), for the site number of 2, 3 and 8 (Site BL, C, GL, respectively). We should therefore reconsider the prior ranges for these parameters. The posterior distributions of parameters (θ_{11}–θ_{19}) in NO flux module are not variable across sites revealed that these parameters in nitrification may be considered universally constant (Figure of posterior distributions of some parameters in NO flux module was not showed here).

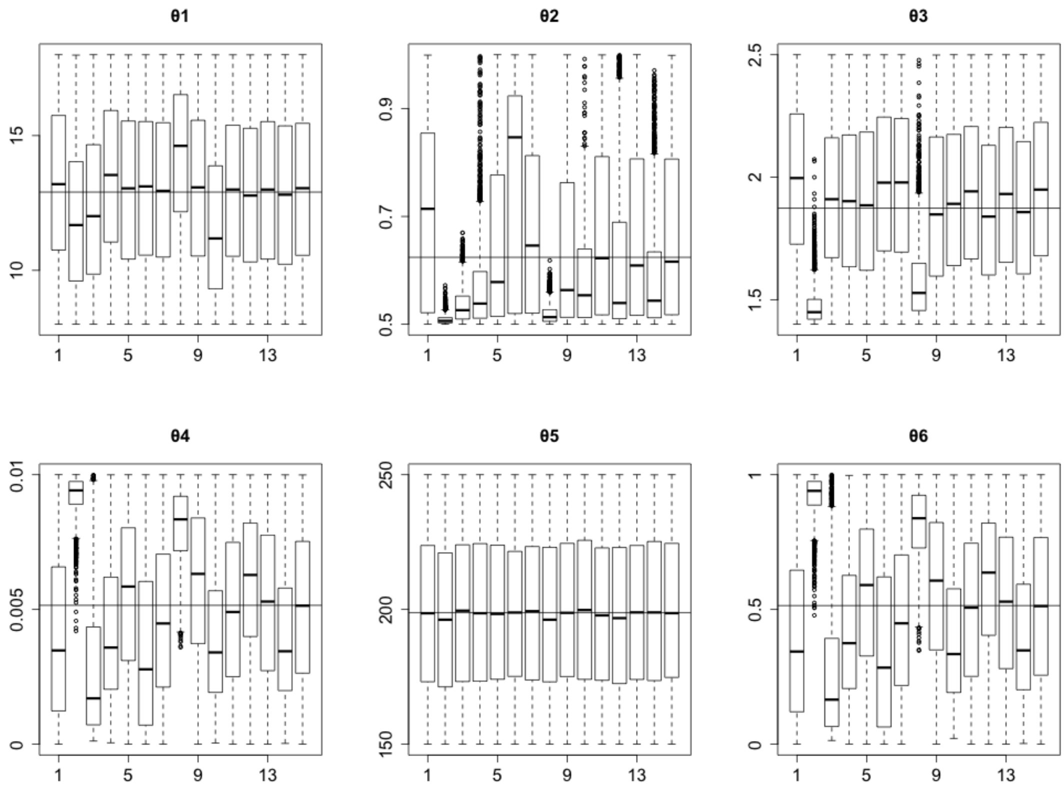

Figure 5. 1 Posterior distribution of the 6 calibrated parameters (θ_1 to θ_6) in N_2O flux module represented as boxplots over the prior range of variation (corresponding to the range of the y-axis). The boxplots are computed from hierarchical Bayesian calibration with 15 experimental sites. The horizon line represents the global cross-sites parameter. The boxplots depict the median (solid line), the *2nd* and *3rd* quartiles (bars), the *1st* and *4th* quartiles (dotted line), and the extreme values (excluding outliers). The x-axis present 15 sites.

Figure 5.2 and Figure 5.3 depicts the ranges of response functions of the N_2O and NO flux resulting from the N-HB model calibrations. These response functions of N_2O (Fig. 5.2) were more variable than function of NO (Fig. 5.3), which matches with the higher variability of parameters in N_2O flux module (Fig. 5.1) than that of NO (Figure of posterior distributions of some parameters in NO flux module was not showed here). The calibrated response of denitrification to biological activity (m'_b) was highly variable, along with the response of denitrification to soil NO_3^- content (m'_{NO_3}) and the response of denitrification to soil water content (m'_w). Response of denitrification to soil water content (m'_w) varied widely, as a consequence of the large variations of soil water threshold for denitrification (θ_2). Hénault et al. (2005) showed that the denitrification was highly sensitive to the soil water threshold, θ_2, and that this parameter dependent on soil type. The response functions of NO had a similar shape across the sites (Fig. 5.3) corresponding to the low variation of posterior distribution of calibrated parameters in NO module, which lead to the conclusion that the parameters for NO module could be considered to be universal.

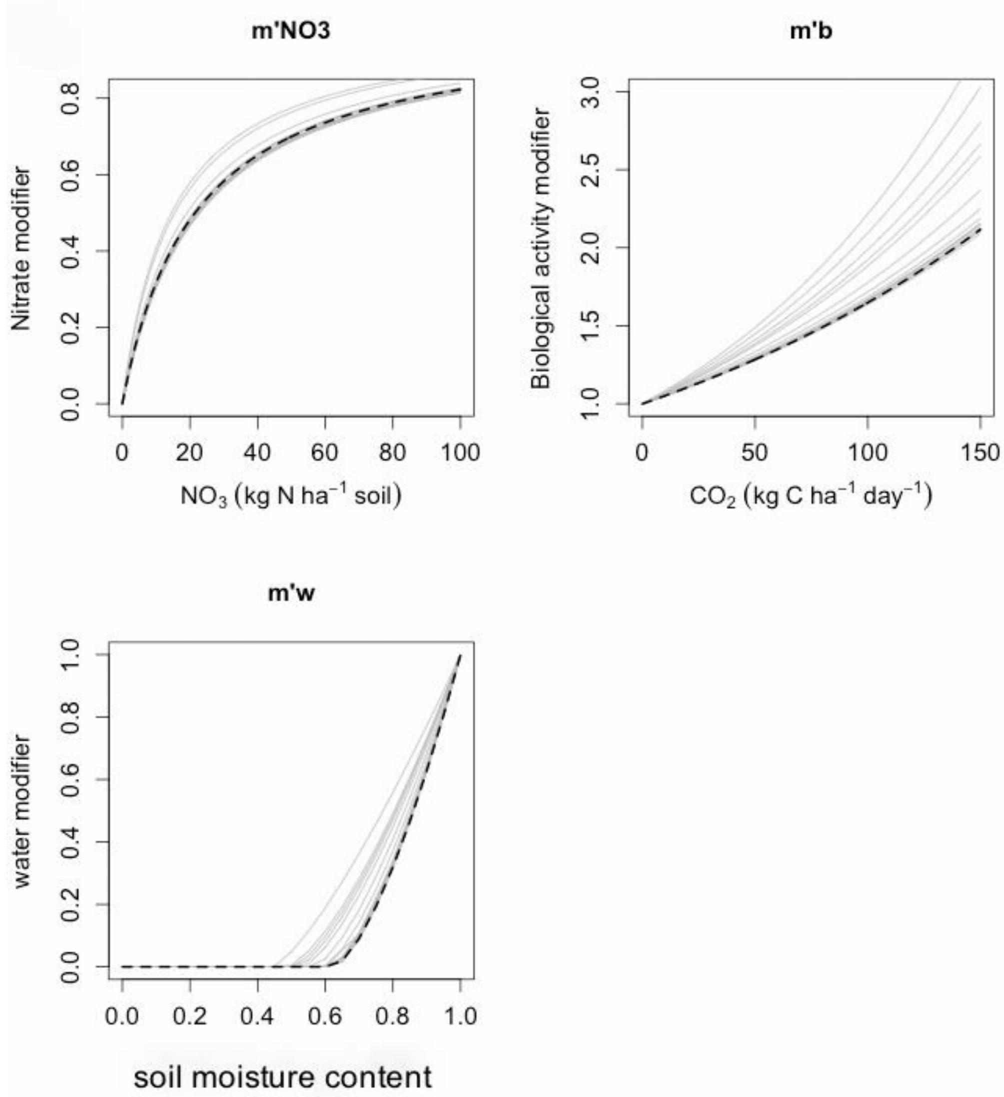

Figure 5. 2 Response functions of the N_2O flux module traced with different sites: mean of the posterior for each study site calibration (line), and the global cross-sites posterior for the 15 experimental sites calibration (dashed line).

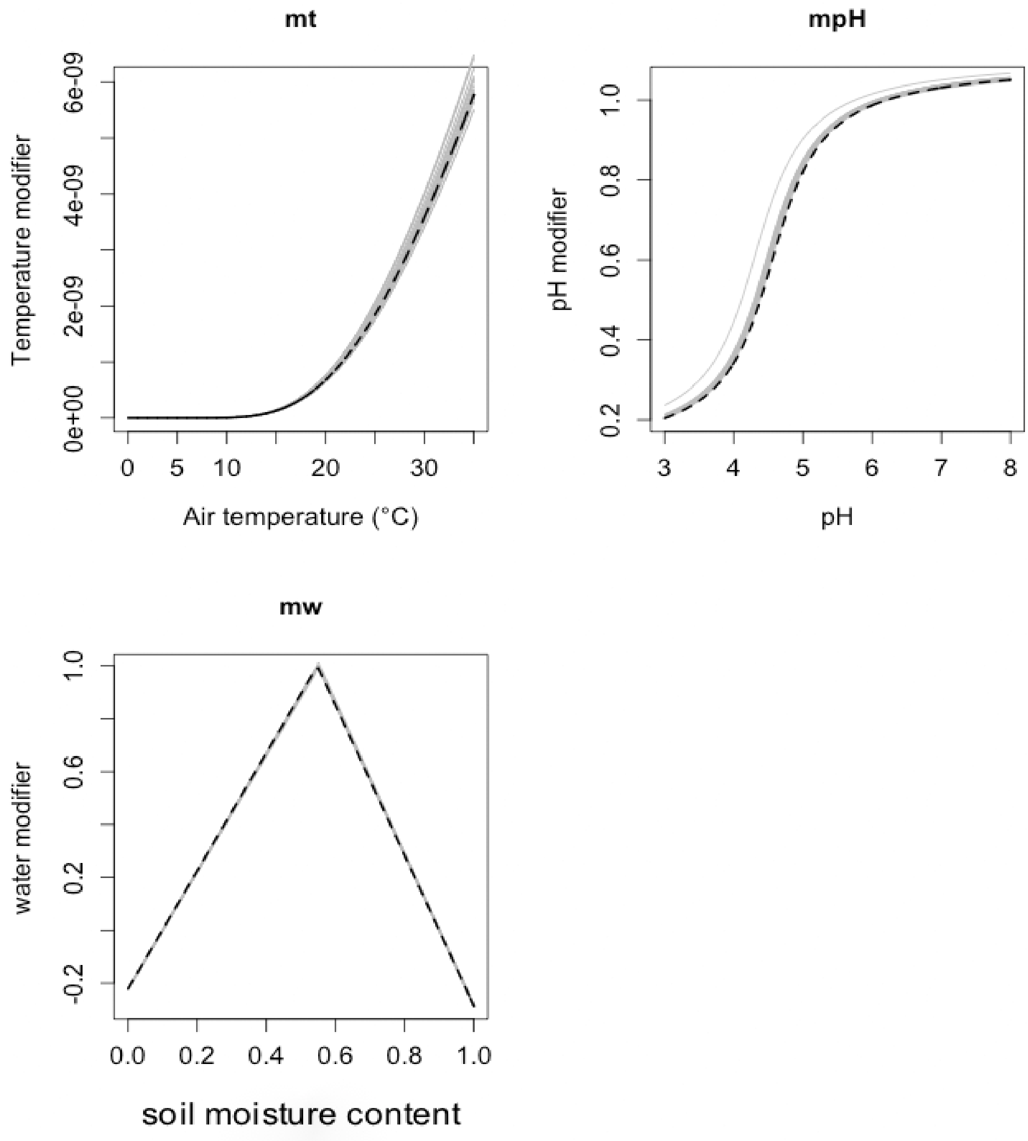

Figure 5. 3 Response functions of the NO flux module traced with different sites: mean of the posterior for each study site calibration (line), and the global cross-sites posterior for the 15 experimental sites calibration (dashed line).

5.2.2 N_2O and NO simulation

Under the hierarchical approach, each different fifteen experimental sites had its own parameter set (data not shown here), the mean posterior probability for the globally common model was summarized in Table 5.1. Table 5.2 summarized the *R* squared (R^2), and the root-mean-square error (*RMSE*) of N_2O and NO fluxes simulated by N-HB model. The HB calibrated model's *RMSE* over the 15 sites ranged from 0.8 to 22.0 kg N ha^{-1} day^{-1} for N_2O, from 0.9 to 37.5 kg N ha^{-1} day^{-1} for NO. Although the R^2 at none of the 15 sites was high on a daily time step, the model simulation could predict the N_2O and NO across the 15 sites (Table 5.2). Comparison of simulated and measured soil state variables of site_GL was displayed in the Figure 5.5, which indicated that the model adequately simulated the direction, timing and magnitude of the measured data. The peaks of N_2O and NO fluxes were correctly predicted following fertilizer addition, and there was no mistiming of the model response for fertilizer application.

Table 5. 2 Sample size (*N*), *R* squared (R^2) and root mean square errors (*RMSE*) computed with the predicted and measured N_2O and NO fluxes at 15 sites.

Site	Site_No.	*N*	N_2O kg N ha^{-1} day^{-1}		NO kg N ha^{-1} day^{-1}	
			R^2	*RMSE(%)*	R^2	*RMSE(%)*
B	1	34	0.35	2.38	0.35	7.82
BL	2	112	0.36	21.98	0.20	16.64
C	3	29	0.33	1.02	0.31	0.90
D	4	62	0.50	0.93	0.62	3.08
E	5	96	0.28	0.80	No data	
F	6	31	0.36	4.51	0.22	2.66
G	7	24	0.21	7.32	0.32	37.53
GL	8	339	0.42	1.22	0.46	1.23
P	9	83	0.08	1.45	0.28	12.58
R	10	267	0.12	1.78	0.30	1.66
S	11	17	0.37	0.88	0.41	1.47
T	12	84	0.17	1.78	0.08	1.30
U	13	46	0.29	1.34	0.24	7.85
V	14	220	0.34	2.11	0.32	1.86
W	15	84	0.48	1.77	0.16	3.78

The model performance of N_2O and NO simulation applied across 15 sites for calibration and verification were shown in Table 5.2 and Figure 5.4. Simulation of N_2O flux showed appropriate correlation corresponding to observations on a daily time-step, with R^2 value of 0.38 in calibration and 0.27 in validation. Although this correlation (R^2) was weak, it was statistically significant, with *RMSE* value smaller than $RMSE_{95}$. Simulation of the NO flux showed better correlation corresponding to observations on a daily time-step, with R^2 value of 0.49 in calibration and 0.55 in verification, and it was statistically significant.

Table 5. 3 Model performance for calibration (2003–2009) and verification (2010–2011); and model performance efficiency through the years 2003–2011.

	N_2O			NO		
	Calibration	Verification	Model performance	Calibration	Verification	Model performance
Year Data	2003–2009	2010–2011	2003–2011	2003–2009	2010–2011	2003–2011
R^2	0.38	0.27	0.35	0.49	0.55	0.51
r = Correlation Coeff.			0.57			0.70
T value			17.26			23.92
Critical *T* value at *P*=0.05			2.13			2.13
Significant association?			Yes-Good			Yes-Good
RMSE = Root mean square error of model	0.57	0.28	1.77	0.43	0.23	2.14
RMSE (95% Confidence Limit)	27.74	22.5	28.19	24.19	20.18	19.39
Significant total error?	No-Good	No-Good	No-Good	No-Good	No-Good	No-Good
M = Mean Difference			0.00			0.00
T value			–0.01			–0.20
Critical *T* value at *P*=0.05			1.96			1.96
Significant bias?			No-Good			No-Good
E = Relative Error			–0.55			–0.03
E (95% Confidence Limit).			19.63			9.79
Significant bias?			No-Good			No-Good
Number of Values			607			607

R^2 is the coefficient determination. *r* is the correlation coefficient and the significance was quantified using an *F* test at 95% confidence limit. *RMSE* is the root mean squared error and the significance was quantified by *RMSE* at the 95% confidence limit. *M* is the mean difference and then undertaking a *t* test to check for significance. *E* is the relative error and compare to the *E* at 95% confidence limit.

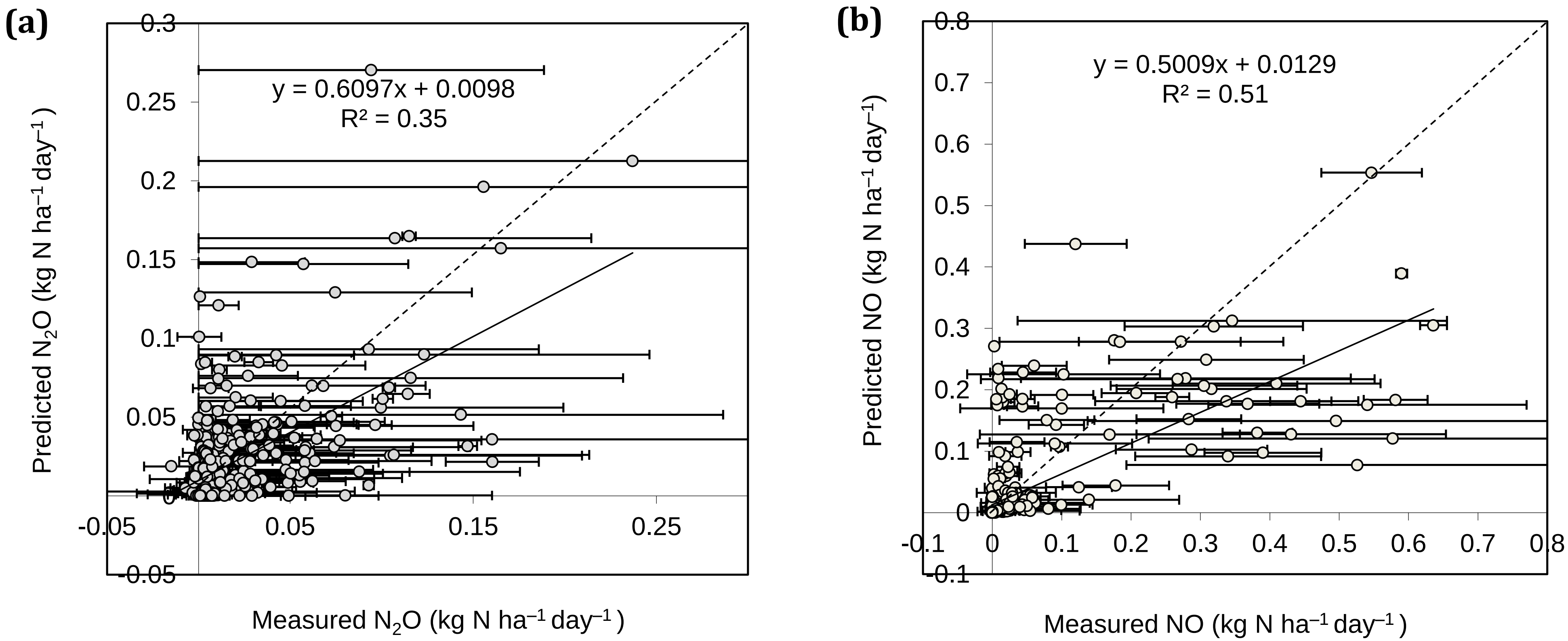

Figure 5. 4 Predicted vs. Observed N_2O (a) and NO (b) flux in study sites for calibration and verification (2003–2011) from N-HB model performance. Bar indicate S.D. (n=3) for observed data.

Figure 5.5 shows the simulated daily N_2O and NO fluxes for GL (Site_No. 8). The model could predict daily N_2O and NO fluxes well, except for the fluxes with high experimental error, which it failed to predict in some cases. Here, some discrepancies between measurements and simulations remained, due to uncertainty on both sides. The two N_2O spikes measured in 2009 May and July had a large experimental error, but did not appear to constrain the calibration as much as the more frequent lower N_2O fluxes with much lower standard deviations. The same failed estimation were found in NO fluxes simulation in 2008 May, which with much higher standard deviations.

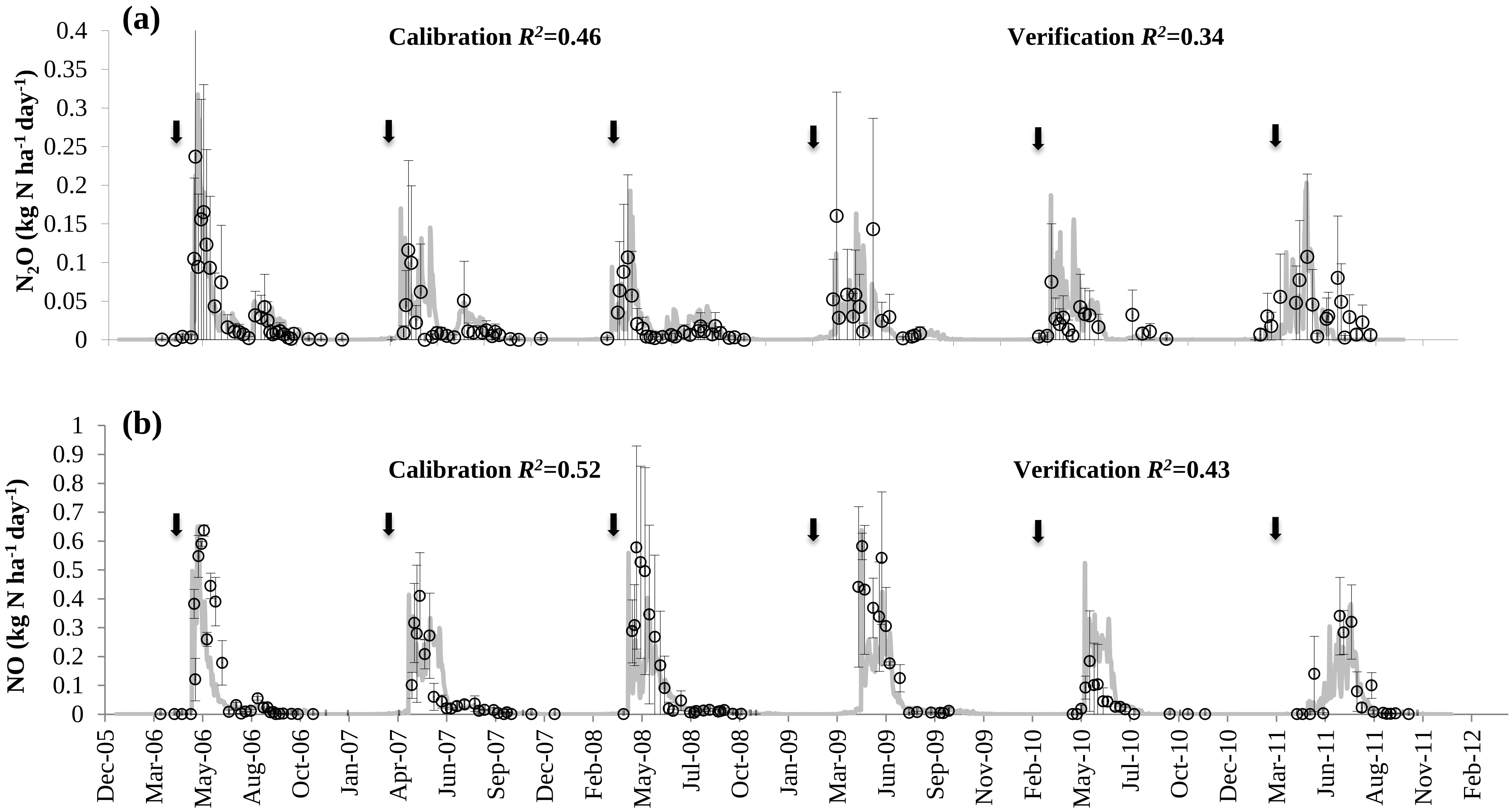

Figure 5. 5 Simulated vs. Observed N_2O (a); NO (b) at Site GL (Site_No.8). Arrows indicates fertilizer application.

5.3 Discussion

5.3.1 Spatial variability of model parameters

We sought to calibrate model parameters by hierarchical structure in order to minimize model error and simultaneously on all datasets to find parameter values that would be universally applicable, expressed by the mean value of posterior distribution. Such values would be extremely useful to apply the model to new soil conditions and to spatially extrapolate it. Measurements of denitrification show extreme higher spatial and temporal variability with typical coefficients of variation exceeding 100% compared with nitrification, which lead to large uncertainty in denitrification simulation (Hénault et al., 2005). The parameters in denitrification revealed by HB calibration in this study are highly variable, which suggested that the simulation of N_2O flux using the universal parameters for denitrification is not appropriate and the site-specific parameterization of denitrification process in process-based model is required (Heinen, 2006; Lehuger et al., 2009). In contrast, HB calibration revealed that parameters in nitrification and response function of NO are less variable, therefore, nitrification process could be parameterized on universal basis.

Heinen (2006) concluded that defining a set of denitrification response functions to soil NO_3^- and soil water (Fig. 5.2), and parameter values for denitrification that would equally apply to sandy, loamy and peat soil types was not easily possible. Our HB calibration gave further evidence to that response functions for denitrification (Eqs. 5.9, 5.10, 5.11, 5.12) were highly variable, and the soil NO_3^- at which denitrification is 50% of its full potential (θ_1), soil water threshold for denitrification (θ_2), exponent of soil water power function in denitrification (θ_3), soil biological activity (θ_4) in these functions were in large variations in pdfs across sites. Parameters of denitrification are required to be site-specific due to the fact that soil structure and aggregate characteristics exert a major influence on denitrification (Gabrielle et al., 2006a).

In our study, non-linear relationships between the soil water threshold for denitrification and soil texture was found, however, our result indicated that the exponent of the power function for soil water (θ_3) decrease linearly with soil silt content (P<0.05) (Table 5.4). Some authors have suggested that the threshold of soil water for an existing denitrification activity (θ_2) was especially sensitive, and it could vary with soil texture or corresponds to the soil's field capacity (Hénault et al., 2005; De Klein and Van Logtestijn, 1996). Generally, the soil water content has a complex effect on denitrification by controlling aeration, diffusion of substrates and microbial activity, which also indicated by the variable denitrification response functions for soil water in this study (Fig. 5.3). Results from previous studies investigated the relationships among soil water, texture and denitrification rate are not consistent or even contradictory. Several studies (Sexstone et al., 1988; Weier et al., 1993) found that a stronger effect of soil water content on denitrification rate in clay loam, compared to a sandy loam. Groffman and Tiedje (1991) indicated that when soil water content increased, denitrification rates increased more sharply in coarse soil than in a finer-texture soil.

Denitrification response function to CO_2 was highly variable, however, the linear relationship between the soil biological activity with soil sand contents (Table 5.4), which conflicted with the concept that fine-texture soils can absorb organic matter and prevented it from being decomposed by microorganisms (Sorensen, 1975). The denitrification-CO_2 production relationship was more complicated. Fine-texture soils have smaller pores thus are more easily become anaerobic than the coarse soils, which was likely to favor denitrification (Groffman and Tiedje, 1991). Therefore, denitrification response factor to CO_2 production cannot be considered as simple isolated SOMD in denitrification simulation.

Denitrification response function for NO_3^- varied less from site to site, compared with denitrification response function for CO_2 production and soil water (Fig. 5.3). We also observed the soil NO_3^- content at which denitrification is 50% of its full potential (θ_1) was not very sensitive at different sites (Hénault et al., 2005).

Our study indicated that the potential denitrification rate (θ_6) decrease linearly with soil sand content (P<0.05) (Table 5.4). Hénault et al. (2005) suggested that parameter potential denitrification rate (θ_6) could be used for comparing soil capacities for denitrification. θ_6, was widely used in process-based model: NEMIS (Hénault et al., 2005), CERES-EGC (Gabrielle et al., 2006a) and ECOSSE model (Bell et al., 2012), which varied as a function of soil texture and soil biota, and was calculated on site by experimentally creating optimal conditions for denitrification in the soil (Bell et al., 2012). Hénault et al. (2005) reported that potential denitrification rate was also a seasonal variable, which is different in summer season from autumn, winter or spring season with the assumption that there is little anaerobic denitrification during summer because the soil is too dry. Although potential denitrification rate measured on a few French soils seemed to be positively influenced by the organic C in the soil, no model could include this because of the weak observed relation (Wheatley and Williams, 1989). Our study didn't test the seasonal variability and there was no relation between potential denitrification rate and organic C content was found, however, the result indicated that potential denitrification rate, θ_6, in soil includes implicitly different soil characteristics, which decrease linearly with soil sand content (P<0.05) (Table 5.4). It is possible that potential denitrification rate assessments based on soil texture or establish a dataset of potential denitrification rate, θ_6 , based on soil classification.

As Bayesian calibration assumes that there is a 'true' parameter value that is incrementally approached with increasing sample size, the hierarchical approach differs from this assumption in the sense that a parameter can varies, that equals hierarchical approach admits that parameter has its own variability. Thus, hierarchical approach identifies two "hyper parameters" to described the posterior distribution of each subunit-specific parameter variability. Figure 5.1, demonstrated posterior distribution of calibrated parameters represented as boxplots over the prior range (range of y-axis). In this case, the posterior density describes parameters' variability. For example, variability in soil water threshold for denitrification (θ_2) in this study is accomplished by conditioning on two hyper parameters α and β ($\mu_{\theta 2}$ and $\sigma_{\theta 2}$ for θ_2) in Eq. (5.22) (posterior distribution of hyper parameters was not shown here). Hyper parameter $\mu_{\theta 2}$ and $\sigma_{\theta 2}$ have the estimation error, while the individual parameter $\theta_{2,j}$ have distributions that depend on data for the jth individual site and for the entire sites. Two hyper parameters $\mu_{\theta 2}$ and $\sigma_{\theta 2}$ define a conditional distribution of the $\theta_{2,j}(\pi(\theta_{2,j}|\mu_{\theta 2},\sigma_{\theta 2}))$, and this distribution does not collapse with increasing sample size. Unlike the hierarchical model, the nonhierarchical model does not admit variability in θ_2. It simply expresses our posterior belief in values of θ_2 (Eq. 3.1), which collapses to a point estimate with large sample size (Clark, 2003). The spread in parameter distributions (Fig. 5.1) describes the parameters' variability by hierarchical model that could have been missed by the nonhierarchical model.

Table 5. 4 The linear regression relation between calibrated parameter and soil texture.

Linear regression relation	R^2	*P* value
θ_3=–0.0071×silt+2.1816	0.21	0.08
θ_4=–0.0008×sand+0.0728	0.53	0.002
θ_6=–0.007756×sand+0.727487	0.52	0.002

5.3.2 Model application

We have established a database on N_2O fluxes for central Hokkaido, Japan and sought to calibrate the model parameters on different sites in order to minimize the uncertainty and to find the parameter values that would be universally applicable. Generally, the parameters with less variability would be regarded as the global parameters and be extremely useful for spatial extrapolation, however, the parameters with the large variability need to be parameterized on site-specific basis. The simple linear relationship of calibrated parameters and soils provide a pre-requisite for simulation over space. Ensuring the accurate parameterization is a pre-requisite to develop the model with the purpose of providing predictions over a large domain in space and time. Although the studied soil types in this study are limited, our HB approach developed in this study is universal rather than the calibrated parameter itself. The HB approach is the recommended strategy to improve the model simulations at separately field scale, and to find the universal values of parameters to spatially extrapolate the model. When attempting at simulating N_2O fluxes in a new site where no measured data available, following strategy is suggested. Firstly, the user should make the calibrated parameter sets based on the variability range of parameters refers to the previous studies of used model. Hence the most important/sensitive parameters must be identified before. Take the ECOSSE used in this study as an example. The less variable parameters, such as parameters of nitrification may serve as the default values for the spatial extrapolation of the model at regional scale regardless of soil types or soil physic-chemical characteristics. Secondly, the user should check if calibrated parameters sets, especially for high variability parameters, already exist for similar soil types, based on soil taxonomy or physic-chemical characteristics, such as the soil nitrate content at which denitrification is 50% of its full potential (θ_1), soil water threshold for denitrification (θ_2), exponent of soil water power function in denitrification (θ_3), soil biological activity (θ_4) and potential denitrification rate (θ_6) in this study. If these parameters are not exist for similar soil types, these parameters derived from the multi-dataset calibration may be used to encompass a wide range of space and time condition at regional scale, though at the cost of a larger error between simulations and observations with site-specific sets.

Our results do not provide robust evidence that the parameters of N_2O fluxes could be estimated from soil texture. It is difficult to apply the liner relation to other soils due to the limited breadth of input soil textures, however, it agrees with other models' result that the soil or landscape characteristics could control these parameters. Such as potential denitrification rate (θ_6), though several studies revealed that it varies as a function of soil texture, how θ_6 changes in soil taxonomy is still unknown (Hénaul and Germon, 2000; Bell et al., 2012). Therefore, it will be interesting to apply HB calibration across different soils and establish a database of parameters based on soil taxonomy.

5.4 Conclusion

N-HB model was successfully applied to simulate N_2O and NO emission from agriculture field. The parameters were calibrated against sites to improve model simulations at field scale and to find universal values of parameters described by the mean value of posterior parameter distributions to spatially extrapolate the model. The posterior parameter encompassing all our observations at the study sites gave us the possibility of quantifying the real parameter variability. Parameters for nitrification could be considered universal while parameters for denitrification were much less constant across sites.

Based on our result, we recommended a strategy to develop a HB approach across more soil types globally. The spatial variability of parameters for soil classification could deal with model extrapolation; and could serve as prior information to infer the parameters of the N_2O module to decrease uncertainty in N_2O simulation.

6. Carbon balance at regional scale during the last four decades

6.1 Introduction

The C balance in terrestrial ecosystems has large implications on the variation in atmospheric CO_2 emission. Soil have the potential to sequester organic matter and thus to significantly contribute to the terrestrial C sink. Agriculture profoundly affects global C, water and nutrient cycles, as well as the planetary surface energy balance (Bondeau et al., 2007) . Assessment of soil C stock changes over time is typically based on application of two methods, namely (i) repeated soil inventory and (ii) determination of the NBP by continuous measurement of CO_2 exchange in combination with quantification of other C imports and exports (Leifeld et al., 2011).

Long-term trends in agricultural productivity and residue inputs to soil, driven by technological and management changes, impact the magnitude and direction of change in soil C storage (Johnsson et al., 1991). Because of the high net primary productivity (NPP) of many agricultural crops, relative to non-cropland vegetation, agricultural systems can substantially increase short-term C exchanges between the land surface and the atmosphere in regions converted to agricultural land use. Interannual variability and changes in crop species distribution, as well as interannual variability in net ecosystem C storage, may have significant implications for estimating short-term changes in terrestrial C balances, for both atmospheric-based estimates of regional C cycling and ground-based soil C inventories. Spatial and temporal variability of C inputs present significant challenges for estimating the C balance in agricultural ecosystems. A large proportion of NPP (about 40–50% of above ground biomass in grain crops) is removed as yield and thus the long-term C balance in croplands is instead governed by the amount of crop residues, which is remained on the field.

In principal, an indication for the uncertainty in NBP should be provided and thus a direct quantitative evaluation of methods is available. Meanwhile, the NBP value for an agricultural system should be directly comparable with the C stock change measured by repeated sampling of soil, but up to now, there has been few field study that directly compared the two approaches at an agricultural system at the regional scale.

The first goal of our study was to explore trends and interannual variability of NBP at regional scale, focusing on the spatial and temporal patterns of NPP, crop residue inputs and NBP at the main land use: upland, paddy, grass from 1959 to 2011. Secondly, verifying the ecosystem C budget change estimated by NBP at individual land use (upland, paddy, grass) from 2005 to 2011, by comparing the soil C change estimated by repeated soil inventory.

6.2 Results

6.2.1 Land use Change from 1959 to 2011

Urban area was the largest artificial land use, occupying about 28% of the landscape throughout the study year (Fig. 6.1a). Urban area slightly increased from 24% in 1959 to 28% in 2011. The grassland increased from 38 ha in 1959 to 320 ha in 2011. In cropland, paddy area declined from 1254 ha in 1959 to 430 ha in 2011, upland area keeps stable from 1959 to 1994, and then decline from 977 ha in 1994 to 723 ha in 2011, bush/fallow area keeps slightly increase from 1959 to 1994 and then increased from 270 ha in 1994 to 673 ha in 2011. The main land use type in cropland was shown in Fig. 6.1b. In upland crop, the area of soybean and vegetable declined slighted from 1959 to 2011, onion showed decrease from 1994, while wheat (+other upland crop) increased from 132 ha in

1959 to 392 ha in 2011.

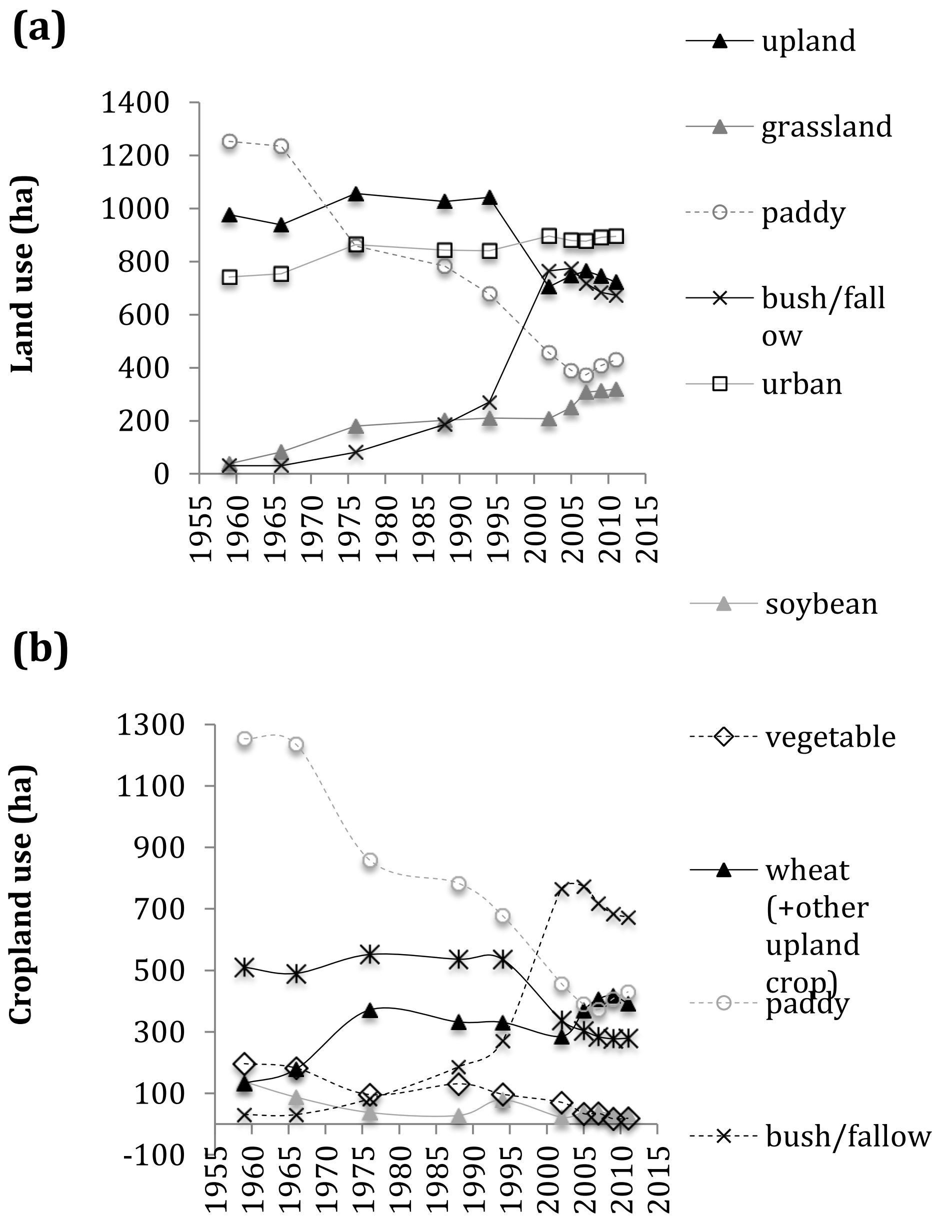

Figure 6. 1 Land use change from 1959 to 2011. (a) The main land use change. (b) The cropland use change.

6.2.2 Regional annual net primary production, carbon harvest and carbon inputs from plants

Average yield of soybean, vegetable, wheat, paddy and grass showed an overall increasing trend, and yield of onion showed an overall decreasing trend over the period of 1959–2011, although there were considerable variations from year to year. Average yield of buckwheat, maize, greenhouse and melon showed slightly increasing trend, and yield of fruits, potato remained relatively stable, while yield of pumpkin showed a decreasing trend from 1959 to 2011 (see Table 3.8). Crop-dependent NPP, C harvest and plant C inputs in the study region are presented in Fig. 6.3 (see Tables 6.1, 6.2 and 6.3 for crop NPP, C harvest and plant C inputs in each study year, respectively). Of all the crops, the crop-dependent NPP was highest for greenhouse (11.84±0.74 Mg C ha^{-1} yr^{-1}) and following to vegetable (10.12±2.92 Mg C ha^{-1} yr^{-1}), paddy (5.03±0.82 Mg C ha^{-1} yr^{-1}), wheat (4.67±1.69 Mg C ha^{-1} yr^{-1}), fruits (0.93±0.06 Mg C ha^{-1} yr^{-1}), and lowest in buckwheat (0.74±0.08 Mg C ha^{-1} yr^{-1}). Greenhouse had the highest plant C inputs per cropland hectare, followed by vegetable, wheat, maize, soybean and paddy. Onion and potato had relatively low plant C input. Ratios of plant C inputs to NPP varied significantly, depending on crop species (Fig. 6.2), with larger ratios being recorded for buckwheat (58%) and maize (54%) and smaller ratios for onion (10%) and potato (12%). Consequently, 38% of crop NPP was returned to the field at the regional scale.

Table 6. 1 Crop net primary productivity (Mg C ha^{-1} yr^{-1}) data in the Ikushunbetsu watershed from 1959 to 2011.

	1959	1966	1976	1988	1994	2002	2005	2007	2009	2012
Soybean	1.44	0.69	1.81	1.93	2.39	2.11	2.26	2.70	2.22	2.70
Potato					2.64	3.11	3.11	3.42	2.93	2.81
Buckwheat					0.64	0.79	0.79	0.67	0.67	0.85
Vegetable	4.42	5.27	10.00	10.46	10.79	12.03	12.17	12.61	11.06	12.39
Onion	5.23	3.74	4.49	4.01	3.37	4.24	4.07	2.98	2.98	3.99
Maize					2.80	3.11	2.97	2.85	2.85	3.08
Greenhouse					10.79	12.03	12.17	12.61	11.06	12.39
Fruits[a]					0.99	0.81	0.95	0.95	0.95	0.95
Melon[a]					1.63	1.63	1.79	1.87	1.87	1.97
Pumpkin[a]					1.61	1.24	1.19	0.88	0.91	1.04
Wheat	2.70	1.56	4.09	5.33	5.04	5.78	6.02	6.40	3.27	6.48
Grass	6.41	5.07	7.29	8.01	8.21	7.99	8.11	7.91	7.74	7.76
Paddy	3.26	4.04	4.68	5.09	5.47	5.58	5.48	5.59	5.11	5.95
Bush / Fallow [a]	6.85	6.85	6.85	6.85	6.85	6.85	6.85	6.85	6.85	6.85

[a] NPP was estimated from dry weight of total plant, main plant product and by plant product using the linear regression from Osaki (1992).

Table 6. 2 Crop C harvest (Mg C ha^{-1} yr^{-1}) data in the Ikushunbetsu watershed from 1959 to 2011.

	1959	1966	1976	1988	1994	2002	2005	2007	2009	2011
Soybean	0.69	0.33	0.87	0.92	1.15	1.01	1.08	1.29	1.06	1.29
Potato					2.32	2.74	2.74	3.01	2.58	2.48
Buckwheat					0.27	0.33	0.33	0.28	0.28	0.35
Vegetable	2.85	3.40	6.45	6.75	6.96	7.75	7.84	8.13	7.13	7.98
Onion	4.71	3.37	4.05	3.62	3.04	3.82	3.67	2.69	2.69	3.60
Maize					1.29	1.43	1.36	1.31	1.31	1.42
Greenhouse					6.96	7.75	7.84	8.13	7.13	7.98
Fruits[a]					0.62	0.51	0.59	0.59	0.59	0.59
Melon[a]					1.02	1.02	1.12	1.17	1.17	1.23
Pumpkin[a]					0.98	0.76	0.72	0.53	0.55	0.63
Wheat	0.78	0.45	1.18	1.57	1.49	1.71	1.78	1.89	1.31	1.87
Grass	3.42	2.71	3.89	4.28	4.38	4.27	4.33	4.22	4.13	4.15
Paddy	1.34	1.66	1.93	2.09	2.25	2.30	2.26	2.30	2.10	2.45
Bush / Fallow [a]	0.00	0.00	0.00	0.00	0.00	0.00	0.00	0.00	0.00	0.00

[a] C harvest was estimated from dry weight of total plant, main plant product and by plant product using the linear regression from Osaki (1992).

Table 6. 3 Plant C input (Mg C ha^{-1} yr^{-1}) data in the Ikushunbetsu watershed from 1959 to 2012.

	1959	1966	1976	1988	1994	2002	2005	2007	2009	2011
Soybean	0.75	0.36	0.94	1.00	1.25	1.10	1.17	1.41	1.15	1.41
Potato					0.31	0.37	0.37	0.41	0.35	0.34
Buckwheat					0.37	0.46	0.46	0.39	0.39	0.49
Vegetable	1.57	1.87	3.55	3.72	3.84	4.28	4.32	4.48	3.93	4.40
Onion	0.52	0.37	0.44	0.40	0.33	0.42	0.40	0.29	0.29	0.39
Maize					1.51	1.68	1.61	1.54	1.54	1.67
Greenhouse					3.84	4.28	4.32	4.48	3.93	4.40
Fruits[a]					0.37	0.78	0.36	0.36	0.36	0.36
Melon[a]					0.37	0.61	0.67	0.70	0.70	0.74
Pumpkin[a]					0.63	0.61	0.47	0.35	0.36	0.41
Wheat	1.16	0.67	1.76	2.34	2.21	2.54	2.65	2.81	1.95	2.78
Grass	2.99	2.36	3.40	3.73	3.82	3.72	3.78	3.68	3.61	3.62
Paddy	0.56	0.69	0.80	0.87	0.93	0.95	0.93	0.95	0.87	1.01
Bush / Fallow [a]	3.43	3.43	3.43	3.43	3.43	3.43	3.43	3.43	3.43	3.43

[a] C input was estimated from dry weight of total plant, main plant product and by plant product using the linear regression from Osaki (1992).

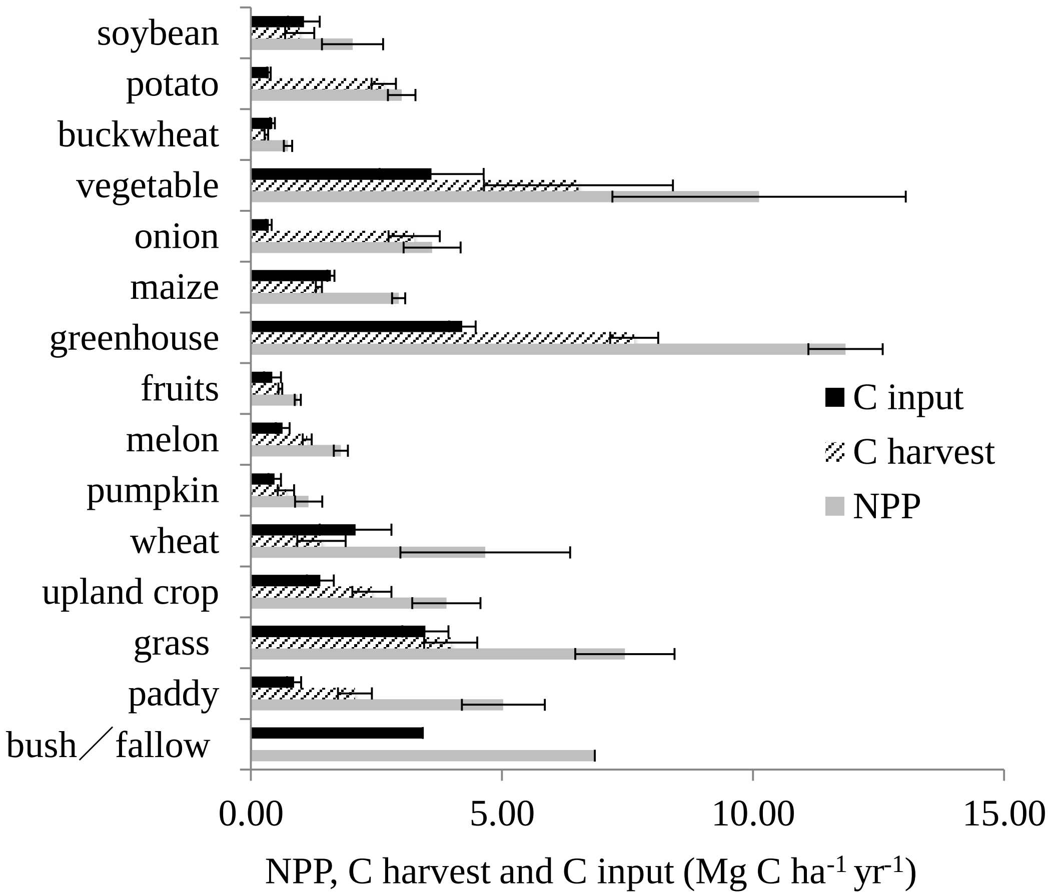

Figure 6. 2 Crop NPP, C harvest and plant C input through the study period. The error bar indicates standard deviation.

Total annual NPP of all land use (upland + paddy + grass) over the analysis period averaged 5.51 ± 1.05 Mg C ha^{-1} yr^{-1}. At regional scale, NPP of all land use over the study period ranged from 4.19 Mg C ha^{-1} yr^{-1} (in 1959) (Fig. 6.6b) to 6.03 Mg C ha^{-1} yr^{-1} (in 2011) (Fig. 6.6g) (Fig. 6.3a), while the plant C inputs over the period ranged from 1.11 Mg C ha^{-1} yr^{-1} in 1959 (Fig. 6.6d) to 2.81 Mg C ha^{-1} yr^{-1} in 2011 (Fig. 6.6i) (Fig. 6.3c). NPP of upland (not included bush/fallow) ranged from 2.85 Mg C ha^{-1} yr^{-1} in 1959 to 4.42 Mg C ha^{-1} yr^{-1} in 2011. NPP of paddy ranged from 3.26 Mg C ha^{-1} yr^{-1} in 1959 to 5.95 Mg C ha^{-1} yr^{-1} in 2011. NPP of grass ranged from 6.41 Mg C ha^{-1} yr^{-1} (in 1959) to 7.76 Mg C ha^{-1} yr^{-1} (in 2011) (Fig. 6.3a). As a result, the annual C harvest from all the field combined increased from 1959 to 2011, by 1.94 Mg C ha^{-1} in all land use, by 0.58 Mg C ha^{-1} in upland (not included bush/fallow), by 0.56 Mg C ha^{-1} in paddy, and by 0.63 Mg C ha^{-1} in grass (Fig. 6.3b). Total annual C input from all the filed combined increased from 1959 to 2011, by 1.85 Mg C ha^{-1} in all land use, by 0.01 Mg C ha^{-1} in upland crop (not included bush/fallow), by 1.58 Mg C ha^{-1} in paddy, by 0.63 Mg C ha^{-1} in grass (Fig. 6.3c). In bush/fallow field, the overall trend was considered as neither increasing nor decreasing over the study period.

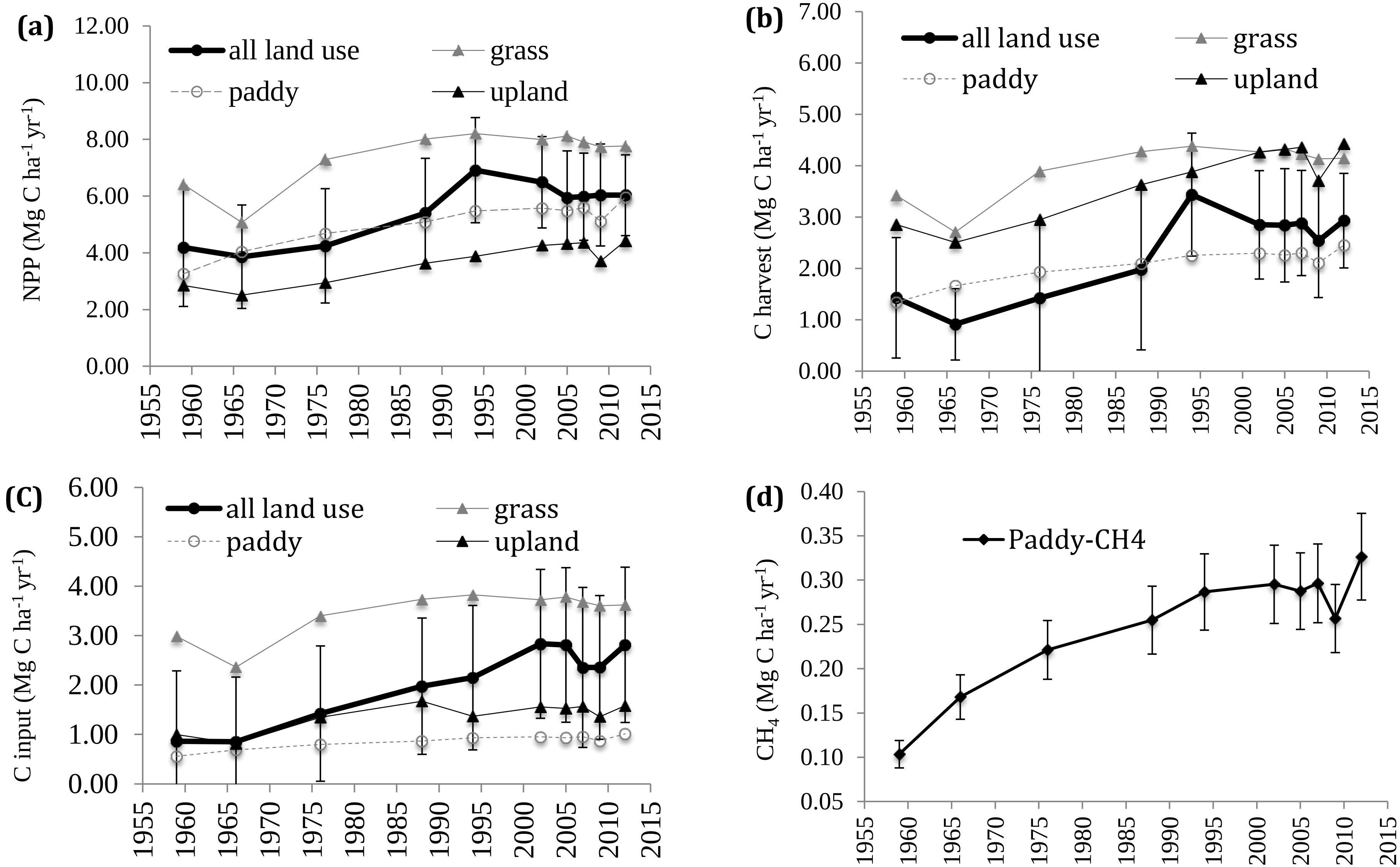

Figure 6. 3 Temporal trends of NPP (a) , C harvest (b), C input (c) during the study period for main land use at the regional scale, and temporal trends of CH_4 emission in paddy (d). The error bar for all filed indicates the range of standard deviation.

6.2.3 Soil heterotrophic respiration and CH_4 emission at regional scale

Heterotrophic respiration (Rh) over the study period of 1959–2011 showed clear seasonality, with high levels in warm year and low levels in cold year (Figs. 6.4a, 6.4b). Rh was estimated at 3.14±0.27 Mg C ha^{-1} yr^{-1} at regional scale, which takes a fraction of 59% (±12%) of the total NPP. The CH_4 emission from the paddy over the analysis period 1959–2011 averaged 0.25±0.07 Mg C ha^{-1} yr^{-1}. CH_4 emission from paddy increased from 0.1 Mg C ha^{-1} yr^{-1} in 1959 to 0.33 Mg C ha^{-1} yr^{-1} in 2011 (Fig. 3d).

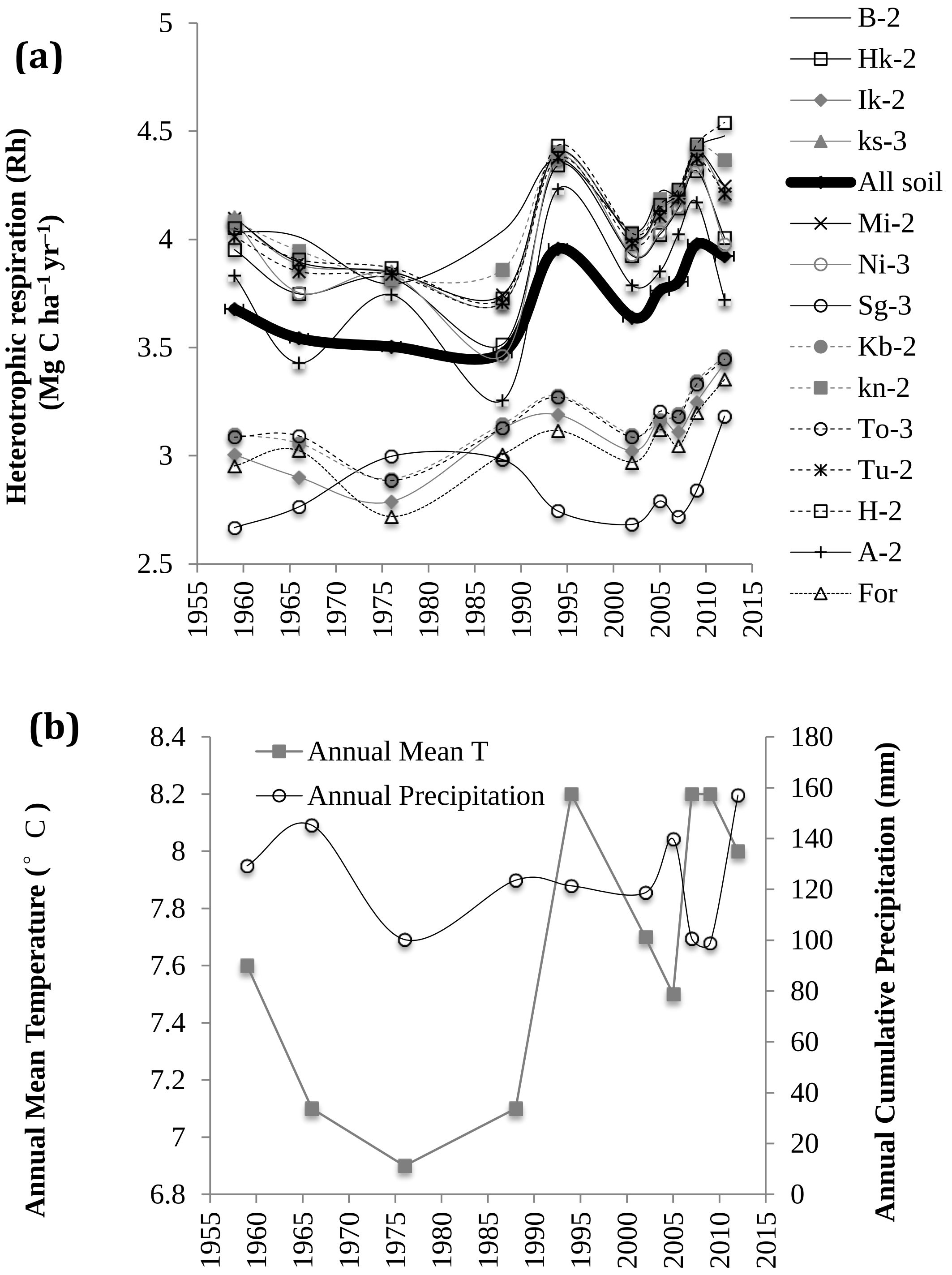

Figure 6. 4 (a) Soil heterotrophic respiration estimated at 15 soil types. Soils of B-2, Hk-2, A-2, H-2 and forest (for) are the sub soil of Grey lowland; Soils of Ik-2, M-3, Sg-3, To-3 and Tu-3 are the sub soil of Brown lowland; Soils of Ks-3, Mi-2 and Kb-2 are the sub soil of Gely lowland; Soils of Ni-3 and Kn-2 are the sub soil of Pseudogleys (Hokkaido Central Agriculture Experiment Station, 1971). (b) Mean annual temperature and mean annual precipitation from 1959 to 2011.

6.2.4 Regional annual net biome productivity

Though the mean NBP in all land use (upland + paddy + grassland) was estimated to –0.32±0.72 Mg C ha^{-1} yr^{-1} through to the period from 1959 to 2011, the time series of NBP in all land use increased over the study period and the change in NBP showed a slowly upward trend, which estimated an average increase of NBP (1.48 Mg C ha^{-1} yr^{-1}) from 1959 to 2011 (Fig. 6.5). Interannual variability of NBP in all land use ranged between –1.42 to 0.48 Mg C ha^{-1} yr^{-1} (Table 6.4). The NBP in 1959 and 2011 in all land use ranged from –1.27±2.53 Mg C ha^{-1} yr^{-1} to 0.52±2.77 Mg C ha^{-1} yr^{-1} (Table 6.6; Fig. 6.5; Figs. 6.6e, 6.6j). NBP of upland (not included bush/fallow) ranged from –1.99 ± 0.53 Mg C ha^{-1} yr^{-1} in 1959 to –2.22±0.57 Mg C ha^{-1} yr^{-1} in 2011 (Table 6.4). NBP of paddy ranged from –0.49 Mg C ha^{-1} yr^{-1} in 1959 to –0.55 Mg C ha^{-1} yr^{-1} in 2011 (Table 6.4). NBP of grass ranged from 1.36 ± 0.84 Mg C ha^{-1} yr^{-1} in 1959 to 1.49±0.86s Mg C ha^{-1} yr^{-1} in 2011 (Table 6.4; Fig. 6.5). The C sequestration efficiency (CE), defined as the ratio of NBP/NPP, ranged from –0.13 to –0.03 for croplands (upland + paddy + fallow), and equal to 0.22±0.04 for grassland.

Table 6. 4 The carbon budget of different land use based on a full carbon flux budget (NBP) from 1959–2011.

Year	Upland	Paddy	Grass	All land use
1959	–1.99 (0.53)	–0.49 (0.68)	1.36 (0.84)	–1.15 (2.84)
1966	–2.29 (0.55)	–0.50 (0.68)	0.68 (0.85)	–1.27 (2.53)
1976	–1.40 (0.54)	–0.52 (0.69)	2.01 (0.85)	–0.87 (2.96)
1988	–1.01 (0.59)	–0.55 (0.70)	2.07 (0.88)	–0.47 (2.93)
1994	–2.29 (0.57)	–0.54 (0.70)	2.02 (0.87)	–1.09 (2.95)
2002	–2.76 (0.56)	–0.54 (0.71)	2.08 (0.86)	0.33 (2.76)
2005	–1.08 (0.55)	–0.54 (0.71)	1.82 (0.85)	0.40 (2.83)
2007	–2.32 (0.58)	–0.54 (0.70)	1.73 (0.88)	0.52 (2.77)
2009	–3.10 (0.60)	–0.53 (0.70)	1.56 (0.89)	0.04 (2.87)
2011	–2.22 (0.57)	–0.55 (0.71)	1.49 (0.86)	0.34 (2.66)

Positive numbers are sinks. Numbers in brackets are total uncertainty.

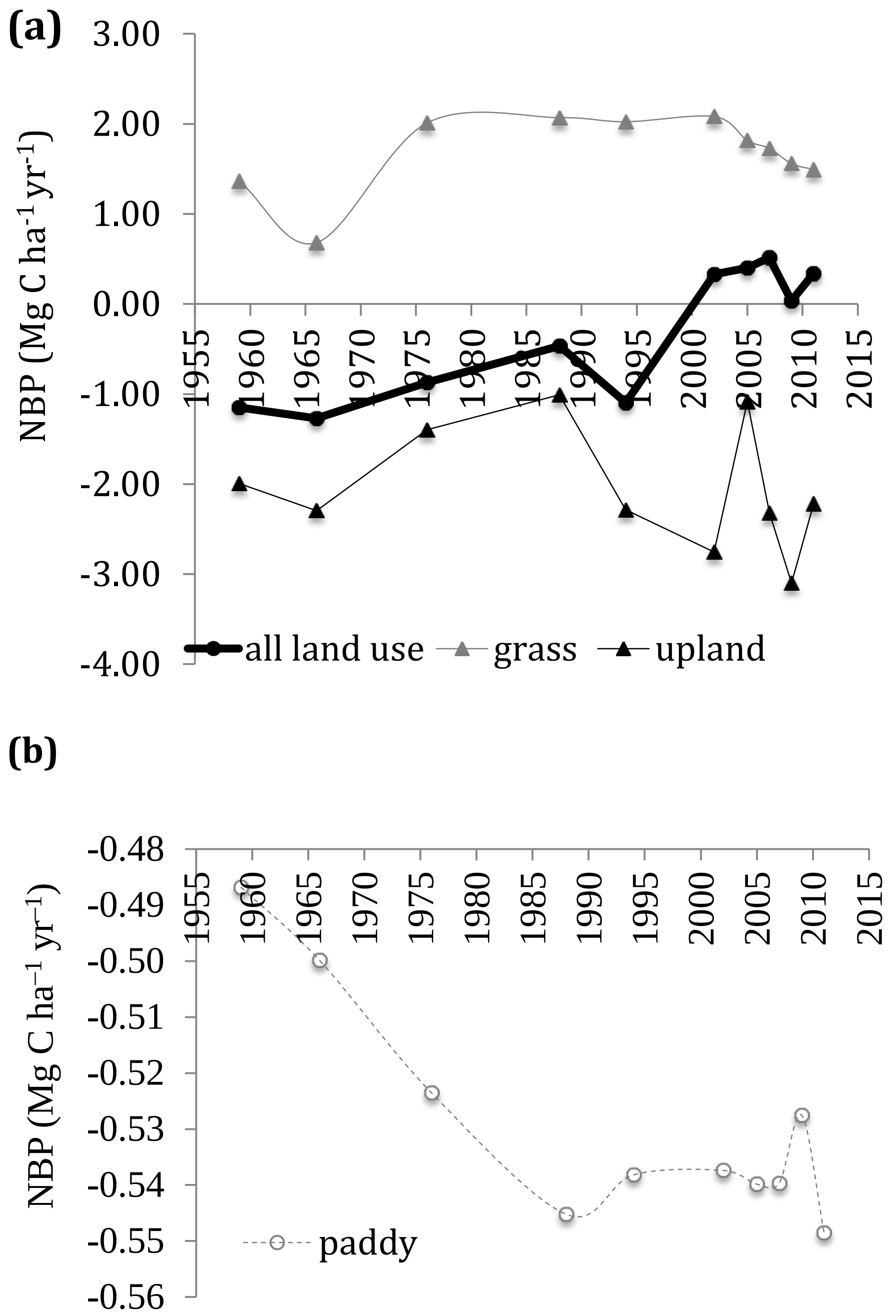

Figure 6. 5 Temporal trends of net biome productivity (NBP) during the study period for (a) all land use, grass and upland, (b) paddy.

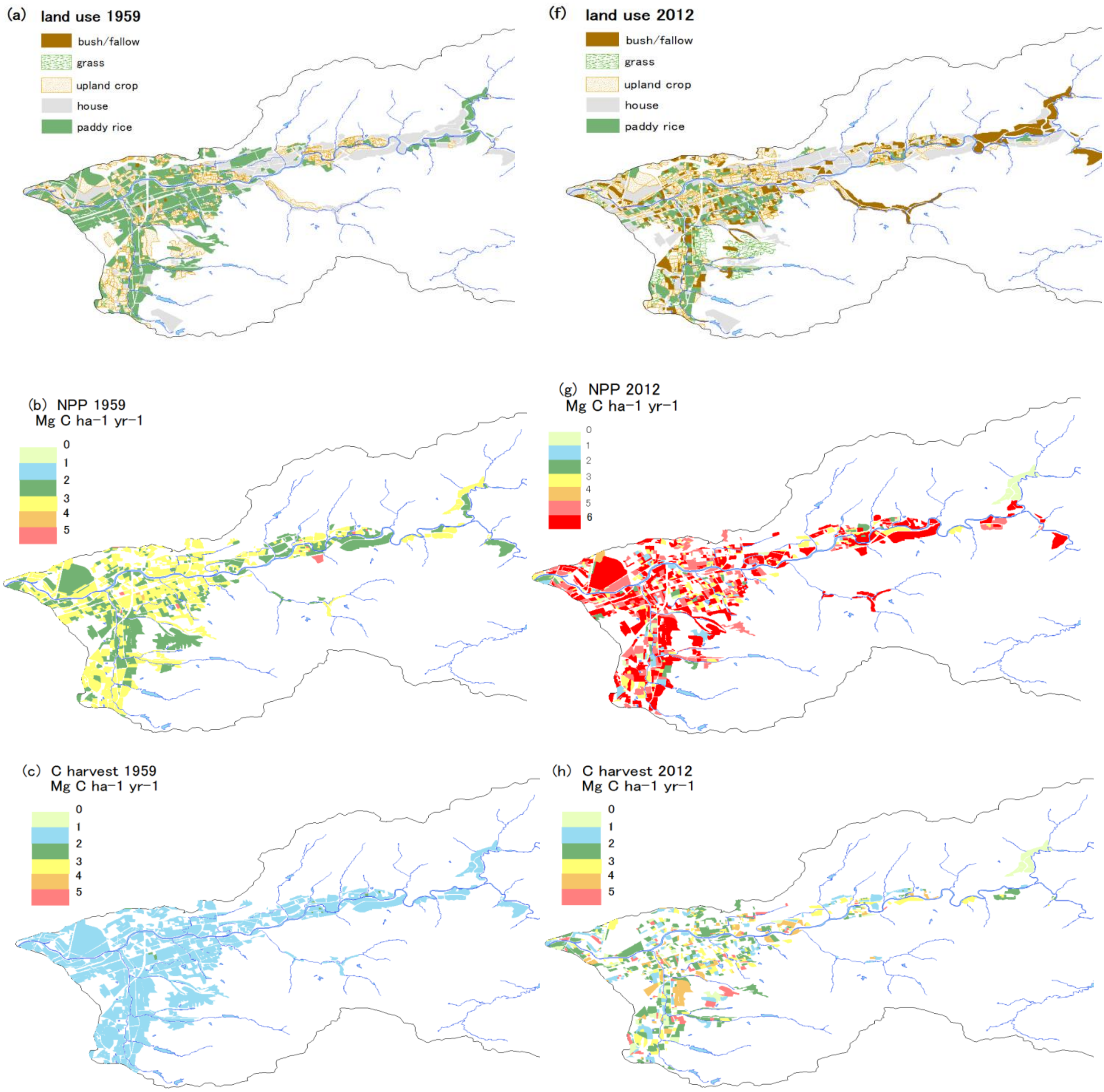
(a) land use 1959
bush/fallow
grass
upland crop
house
paddy rice
(f) land use 2012
bush/fallow
grass
upland crop
house
paddy rice
(b) NPP 1959
Mg C ha−1 yr−1
0
1
2
3
4
5
(g) NPP 2012
Mg C ha−1 yr−1
0
1
2
3
4
5
6
(c) C harvest 1959
Mg C ha−1 yr−1
0
1
2
3
4
5
(h) C harvest 2012
Mg C ha−1 yr−1
0
1
2
3
4
5

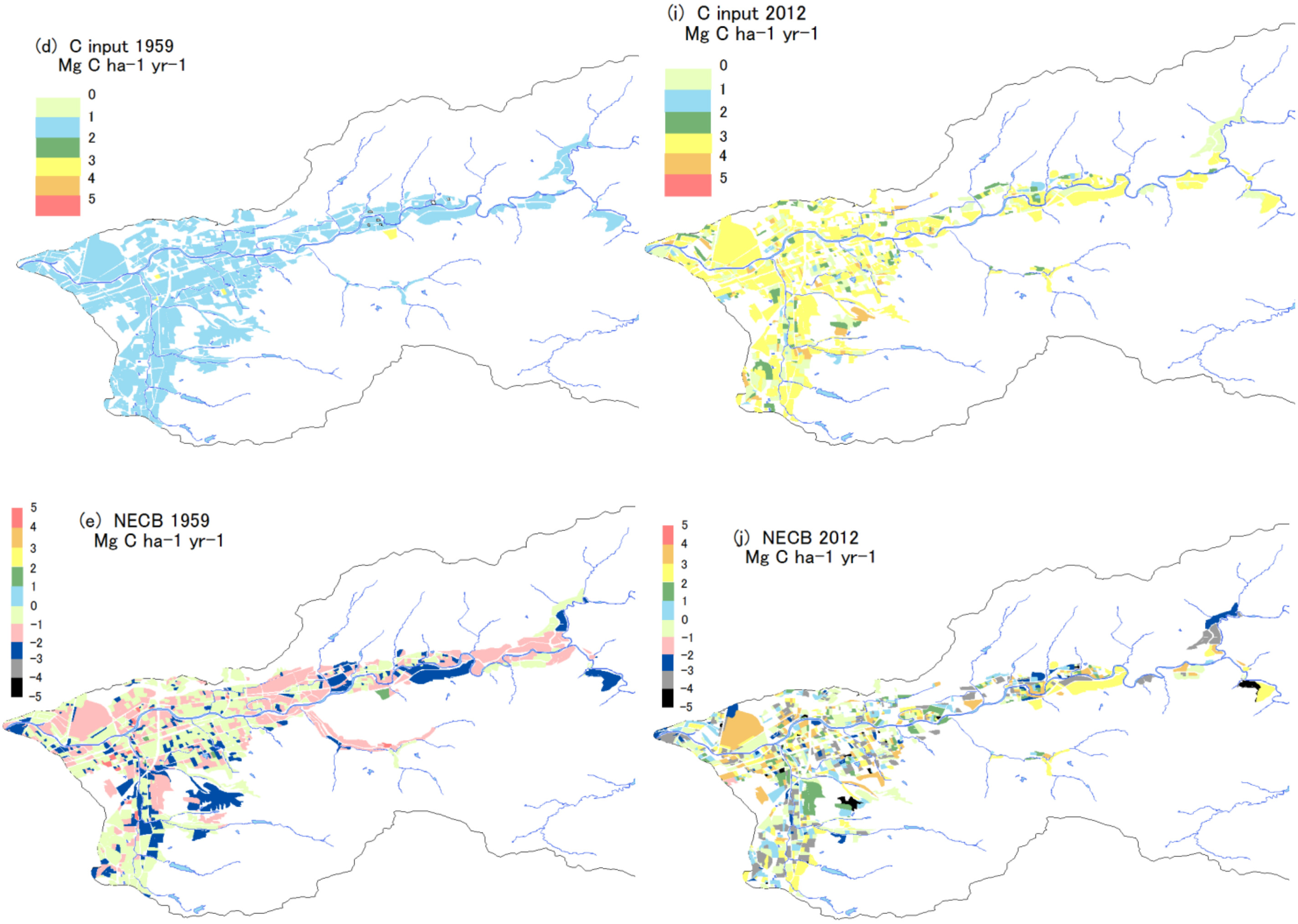

Figure 6. 6 Land use (a,f), NPP (b,g) , C harvest (c,h), C input (d,i), NBP (e,j) at study site in 1959 and 2011.

6.2.5 Temporal variation in net primary production and residue carbon inputs

The Pearson correlation of weather condition with NPP, C harvest, plant C input and NBP was shown in Table 6.5. The NPP for the all land use was positively correlated with annual mean temperature (r=0.74, P<0.05) and was positively correlated with the mean growing season temperature (r=0.48, P<0.05) over the study period (1959–2011). At individual land use level, such a positive correlation with annual mean temperature could be found for upland (r=0.62, P<0.05), paddy (r=0.40, P<0.05), and grass (r=0.46, P<0.05). The observed temporal variation of NPP can be well described by climate relationships in upland, grass and all land use (Table 6.5).

Plant C input varied with changing weather condition over the study period (Table 6.5). Annual plant C input for the all land use was positively correlated with annual mean temperature (r=0.48, P<0.05) and was positively correlated with the mean growing season temperature (r=0.44, P<0.05) over the study period (1959–2011). At individual land use level, such a positive correlation with annual mean temperature could be found for upland (r=0.25, P<0.05), paddy (r=0.40, P<0.05) and grass (r=0.46, P<0.05). The observed temporal variations in plant C input in upland was well described by a quadratic relationship, which incorporated annual total precipitation (Annppt), annual mean temperature (Annt), growing season precipitation (Gppt), squared growing season precipitation (Gppt^2), ratio of precipitation and potential evapotranspiration in growing season (Gratio) in upland. C input = $-1.78 + 0.004 \times \text{Annt} + 0.13 \times \text{Gppt} - 0.001 \times \text{Gppt}^2 - 0.24 \times \text{Gratio}$ (R^2=0.83, P=0.04) for upland (Table 6.6).

Table 6. 5 Pearson correlations of weather condition with net primary productivity (NPP), C harvest, plant C input, net biome productivity (NBP) (*P*<0.05) from 1959–2011.

		Annppt	Annt	Gppt	Gtmean	Annratio	Gratio
Upland	NPP	–0.23	0.62	–0.19	0.31	–0.18	–0.29
	Charvest	–0.20	0.80	–0.02	0.36	–0.16	0.01
	Cinput	–0.19	0.25	–0.34	0.14	–0.28	–0.64
	NBP	0.25	–0.69	–0.04	–0.29	0.30	–0.08
Paddy	NPP/Charvest/Cinput/NBP	–0.13	0.40	–0.09	0.31	–0.03	–0.19
Grass	NPP/Charvest/Cinput	–0.31	0.46	–0.53	0.31	–0.25	–0.40
	NBP	–0.49	0.10	–0.73	0.09	–0.12	–0.46
All land use	NPP	–0.11	0.74	–0.32	0.48	–0.07	0.04
	Charvest	–0.07	0.52	–0.28	0.42	0.06	0.03
	Cinput	0.11	0.48	–0.12	0.44	0.02	–0.21
	NBP	0.21	0.35	0.24	–0.12	–0.23	–0.25

ppt: precipitation; t: temperature, ratio: ratio of precipitation and potential evapotranspiration. “Ann” stands for annual mean value; “G” stands for growing season.

Table 6. 6 The relationship of NPP, C harvest, C input and NBP with climate data in different land use from 1959–2011.

Land use	Equation	R^2	*P*
Upland	$NPP = -3.02 + 0.88 \times Annt$	0.39	0.05
	$Charvest = -7.39 - 0.001 \times Annppt + 1.29 \times Annt + 0.0004 \times Gppt^2 - 0.383 \times Gratio$	0.82	0.04
	$Cinput = -1.78 + 0.04 \times Annt + 0.13 \times Gppt - 0.001 \times Gppt^2 - 0.24 \times Gratio$	0.83	0.04
Grass	$NPP = 2.70 - 0.18 \times Annt - 0.06 \times Gppt + 0.0005 \times Gppt^2 + 0.002 \times Gtmean^2 - 0.07 \times Gratio$	0.92	0.02
	$NBP = 3.01 - 0.28 \times Annt - 0.0004 \times Gppt^2 + 0.006 \times Gtmean^2$	0.72	0.04
All land use	$NPP = -6.43 + 1.56 \times Annt$	0.54	0.02
	$NBP = 0.87 + 0.22 \times Annt - 0.07 \times Gppt + 0.001 \times Gppt^2 - 0.21 \times Gratio$	0.75	0.09

ppt: precipitation; t: temperature, ratio: ratio of precipitation and potential evapotranspiration. “Ann” stands for annual mean value; “G” stands for growing season.

6.2.6 Method comparison

C budget for upland, paddy, grass from 2005–2011 based on NBP method was listed in Table 6.7 together with the results from the repeated soil inventory. For individual fields, both methods NBP and soil inventory indicate a decrease of soil C from 2005–2011, however, a higher C loss measured by soil inventory and a much smaller C decline for NBP. Soil inventory showed that the higher C loss (–3.21±2.51 Mg C ha^{-1} yr^{-1} $layer^{-1}$) in 3rd layer than in 1st and 2nd layer in upland. Though in paddy, soil acts as C sink in 1st layer, the higher C loss in 2nd layer cause the soil to be C source (–0.38±2.56 Mg C ha^{-1} yr^{-1} layer^{-1}) in 30cm soil depth. In grass, the higher C loss was found (–0.95±6.43 Mg C ha^{-1} yr^{-1} layer^{-1}) by means of soil inventory than –0.32±1.21 Mg C ha^{-1} yr^{-1} layer^{-1}) by means of NBP method.

Table 6. 7 Six year (2005–2011) carbon budget of different land use based on a full carbon flux budget (NBP) and repeated soil carbon inventories.

Land use	NBP Mg C ha^{-1} yr^{-1}	Soil inventory Mg C ha^{-1} yr^{-1} layer^{-1}			
		30cm (1st ~ 3nd layer)	1st layer	2nd layer	3rd layer
Upland	–1.13 (0.79)	–1.55 (3.76)	–0.34 (2.24)	–0.62 (2.17)	–3.21(2.51)
Paddy	–0.01(0.95)	–0.38 (2.56)	0.14 (1.56)	–0.73 (2.79)	
Grass	–0.32 (1.21)	–0.95 (6.43)	–1.21 (3.14)	–0.93 (5.98)	
Paddy-upland		–1.05 (8.24)	0.17 (4.69)	–2.34 (4.69)	

Positive numbers are sinks. Numbers in brackets are total uncertainty. "paddy-upland" represented land use change from paddy to upland.

6.3 Discussion

6.3.1 Influence of residue management on net biome productivity

Over the whole study region during 1988–2011, mean cropland NPP (±SD) was 5.51±1.05 Mg C ha^{-1} yr^{-1}. Compared to NPP for other regions, the NPP was 6.66 Mg C ha^{-1} yr^{-1} for Tokachi region of Hokkaido over the period of 1971–2010 (Koga et al., 2011), 5.5 Mg C ha^{-1} yr^{-1}, for the European cropland (Ciais et al., 2010) and 3.5–4.2 Mg C ha^{-1} yr^{-1} for Canadian cereal-based cropland (Bolinder et al., 2007). The average amount of C input (±SD) at regional scale in this study area over the period of 1959–2011 was 2.04±0.80 Mg C ha^{-1} yr^{-1}, and this plant C input represented 37% of the NPP. This result was close to the result in arable farmlands of northern Japan estimated by Koga et al. (2011), which the regional annual plant C input was 2.52±0.32 Mg C ha^{-1} yr^{-1} and the C input represented 38% of the NPP.

Crop production increased markedly between 1959 and 2011, which augmented the amount of residue and root input to the soil (Figs. 6.3a; 6.3c). Under field conditions, merely

15–50% of the C input will remain in soil un-decomposed after one year (Sleutel et al., 2006). The average amount of C input (±SD) in upland and paddy in this study over the period of 1959–2011 was 1.38±0.27 Mg C ha^{-1} yr^{-1} and 0.86±0.14 Mg C ha^{-1} yr^{-1}. Even though the increasing C input to the soil over the years, NBP in upland and paddy showed decreasing trend from 1959–2011, especially for upland, because the C input in Ikushunbetsu watershed was far more smaller than the value of Japanese C input to mention soil C level metioned by Yokozawa et al. (2010). Our study demonstrated that C budget by NBP decreased in upland and paddy in central Hokkaido under the recent C input scenario. Yokozawa et al. (2010) used Roth C to simulate soil C stocks in Japanese upland and paddy at a national scale, showed that the required C input to upland and paddy are 5.06–5.66 Mg C ha^{-1} yr^{-1} and 2.76 Mg C ha^{-1} yr^{-1}, respectively, to maintain the soil C level in 1990. This illustrates that crop residues play a crucial role in maintaining soil C stocks in croplands and that the removal of residues or smaller return of C to the soil has adverse effects on soil C storage and the mitigation of GHG emissions from agricultural lands (Zhang et al., 2006; Koga et al., 2011).

The C sequestration efficiency (CE) of croplands (upland + paddy + fallow), defined as the ratio of NBP/NPP, ranged from –0.13 to –0.03. This CE value is low compared to the values of European cropland, ranged from –0.03 to 0.01 (Ciais et al., 2010). The grasslands CE equal to 0.22 (±0.04), which is higher than the grasslands CE in European (0.13) (Ciais et al., 2010). The smaller CE values in croplands reflect a smaller return of C to the soil, coupled with an accelerated composition of soil organic matter due to plowing and tillage (e.g. destruction of soil micro aggregates and oxygenation). Another reason is that our estimates do not include manure additions that are accounted for in the cropland inventory estimates. At face value, improved cropland management can greatly increase cropland soil C sequestration (Smith et al., 2007a). Smith et al. (2005) suggested that croplands could become a net C sink under improved technology, but the uncertainty (due to climate projections and interactions between decomposition, NPP and technology) was also large, with a 9% uncertainty due to forecast changes in technology alone. The major contribution of croplands to longer term sequestration of C, and hence mitigation of the greenhouse effect, is likely to be in soil C accumulation, especially in “no-till” agriculture where the land is not ploughed (Prince et al., 2001).

6.3.2 Influence of climate condition on net biome productivity

Regional patterns in crop production in agricultural ecosystems are driven by differences in the productivity potential of different crop species, which are largely governed by climate, but modified by management (i.e. irrigation). Temporal trends in production are influenced by developing technology (i.e. crop genetics, fertilization) and changes in management and agricultural policies, and by long-term trends in climate and CO_2 concentrations. In longer trends, the interannual variability of production, largely driven by weather variability and climate cycles, and also vary spatially across the regional scale related to differences in soil quality, moisture and nutrient availability that may be directly or indirectly related to climatic differences (Lokupitiya et al., 2012).

To simulate both spatial and temporal changes in ecosystem C balance at a regional scale, detailed information regarding C inputs from crop residues, green manure and composted manure is necessary. However, accurate measurements or simulations of annual plant C inputs (part of crop NPP) to croplands are difficult due to the unpredictability of a number of regional-specific factors such as crop species, cultivars and field management practices, as well as variable micrometeorological and soil conditions. The temporal variability of cropland NPP and pant C input is determined by fluctuating climate conditions (Ciais et al., 2005; Lokupitiya et al., 2012). According to our study, yields and plant C inputs showed an increase trend for most crops over the 1959–2005. Our study revealed that plant C inputs could be well predicted by a quadratic relationship. Plant C inputs in this study tended to be positively proportional to the annual mean temperature (Annt) and growing season temperature (Gtmean) (Table 6.5). Increasing temperature may increase NPP where it can increase the length of the seasonal and daily growing cycles, but it may decrease NPP in water-stressed ecosystems as it increases water loss (Gómez et al., 2006). Lokupitiya et al. (2012) found a negative relation over the 16-year period in US croplands, for instance, a 1°C increase in the growing season temperature (and a decrease in precipitation of 80 mm compared to the previous year), a decrease of 0.76 Mg ha^{-1} in plant C input rate was observed. Reduction in productivity in region with increases in growing season temperature, due to the higher temperature and drought occurred in North Central region, US in 1993. Fungal epidemics in corn, soybean and alfalfa caused by high moisture, and outbreak of soybean sudden death syndrome in the US in 1993, may have led to the low productivity and low plant C inputs observed.

In this study, we estimated trends in C budget by NBP at regional scale based on residue inputs and climate impacts on Rh modeling (Chapter 4). Our study revealed that NBP could be well predicted by a quadratic relationship based on climate condition in grass and all land use (Table 6.4), however, this relationship cannot be found in upland and paddy. Much more complicated C budget was in managed upland and paddy than permanent grass, because plowing and tillage intensity impacts on Rh, crop species change within upland, smaller return of C to the soil might have the major impact on C budget.

6.3.3 Influence of land use change on net biome productivity

The land area of upland and paddy was found to decrease from 1956 to 2011, however, the yield and plant C input in all land use showed an overall increase (Fig. 6.3c). The upland and paddy are the main land use contributing the increase of plant C input at the regional scale. The long-term trend of increasing yields for most major crops such as soybean, vegetable, wheat and paddy are largely attributed to an array of technology and management developments (i.e., crop genetics, fertilization, plant breeding and pesticide use, etc.). The declined in paddy area has been encouraged by the set aside policy of the Japanese government (Ministry of Agriculture, Forestry and Fisher, 2006). The decline in onion area might be due to the low market price of onion from 2002. The fallow land area increased from 1989 due to the closure of mine activity in 1989 (Mikasa City, 1994) and agricultural activity in this area (Kimura et al., 2004).

The upland in this study showed decreased NBP over the period of 1959–2011. In Japanese upland cropland, Koizumi (2001) reported that the amount of C loss from the soil was within 1.58–3.14 Mg C ha^{-1} yr^{-1} in fields under upland crop cultivation. Another field experiments in upland under wheat, onion and soybean cultivation in the northern part of Japan showed significant loss of 1.47–4.10 Mg C ha^{-1} yr^{-1} from the soil (Hu et al., 2004; Mu et al., 2006). The NBP in upland declined from 1988 was caused by the increased wheat cultivation from 79 ha in 1959 to 188 ha in 2012. However, there is large uncertainty in this estimate because the historical land use changes are poorly quantified in terms of both spatial and temporal before 1994 in our study. Generally, the range of estimated NBP shown in this study is similar to those literatures in cropland (Koizumi, 2001). Other previous studies showed quite different results, with NBP near zero or with significant C accumulation into the soil, however, these results were only found in no-tillage cultivation (Hollinger et al., 2005; Nouchi and Yonemura, 2005).

The paddy in this study showed decreased NBP over the period of 1959–2011. We ignored the low CH_4 emission from the upland aerobic soils. Methanogenesis is restricted to completely anaerobic soil conditions as occur in paddy when the soils are flooded. C input in paddy increased over the study period along with increasing paddy rice yield, however, the increased C input leads to higher CH_4 emission loss from paddy field. These CH_4 emissions were estimated at 1.28±0.27 Mg C ha^{-1} yr^{-1} over the study period. Paddy was not a C source in fallow season, due to non harvest, retention of crop residues, and the fact that biomass incorporated into the soil was not completely decomposed during the season. Our estimation was based the over one year including fallow season, therefore, the paddy showed a C source during study period. The land area of paddy declined from 1254 ha in 1959 to 430 ha in 2012, which land use of paddy changed to upland, grassland and bush/fallow (Figs. 6.6a; 6.6f). Though land use change from paddy cultivation to upland cultivation might cause significant loss of C from cropland soil; 1.05 Mg C ha^{-1} yr^{-1} C loss from 2005–2011 in this study (Table 6.7). In the case of increased agricultural abandonment (fallow/bush) from 1988, C pools slowly start to build up.

In our study, we find a tendency for a C sink in grassland. Our study indicated that cropland to grassland conversion sequester C from 2002. The NBP in all land use across the whole region showed a slowly increase. Though upland and paddy showed decreased NBP over the period of 1959–2011, the increased land use of grassland and bush/fallow contributed to less C loss from field, which lead to the increased NBP at regional scale.

6.3.4 Comparison of repeated soil inventory and net biome productivity method

In this study, for the same period and in same land use, the soil inventory method showed a tendency towards higher C loss than NBP method (Table 6.7). Hardly any direct comparisons of the NBP approach and repeated soil inventories are reported in cropland in the literature. One study comparing NBP and soil C inventories over a 3 year period for maize-soybean rotations found similar C budgets between methods with non significant changes in soil inventories and no or small changes in NBP, however, no indication for the uncertainty in NBP was provide and thus a direct quantitative evaluation of methods proved difficult. Leifeld et al. (2011) made a comparison of soil inventory and NBP to detect soil C stock after conversion from cropland to grasslands, and showed that the soil inventory method showed a tendency towards higher C loss / smaller C gain than NBP method. Though grassland was calculated as a C sink from 1959–2011 by NBP method in our study site, both methods showed that C loss occurs in grassland from 2005–2011. Ciais et al. (2010) reported that European grasslands to be a C sink by means of NBP. However, the long-term grass use does not go along with a change in soil C by means of soil inventory (Hopkins et al., 2009). Together, these data tentatively indicate that an underestimation measured by means of NBP or an overestimation by means of repeated C inventories in this study cannot be excluded.

6.3.5 Uncertainty

The capability of the two methods to detect changes in soil C stocks is limited by their total uncertainty resulting from various error sources. The temporal uncertainty of NBP in all land use at regional scale was estimated to be 0.72 Mg C ha^{-1} yr^{-1} described by standard deviation value as the inter-annual variation between 1959 and 2011. Another uncertainty result from systematic errors in individual land use was described in Table 6.4. The NBP approach uncertainty resulting from temporally random-like errors is generally not very problematic, because of the large number of measurements during a multiyear experiment. Instead, the NBP method encounters a number of sources for systematic errors, including limited field size, field heterogeneity, and measurement limitations, such as imperfect quantification/correction of high-frequency damping and of (correlated) density fluctuations. Thus, it is important that they are accounted for in the NBP uncertainty estimation (Leifeld et al., 2011). Random-like uncertainty that strongly depend on the number of distributed samples and the heterogeneity of the investigated field dominate the uncertainty of the soil inventory approach.

Estimates of NBP in cropland remain uncertain and vary strongly in the literature (Bondeau et al., 2007). Bondeau et al. (2007) indicated that the larger uncertainties for NBP than for net ecosystem productivity (NEP=NPP–Rh), which were mostly related to uncertainties in C removal by harvest and in C inputs or organic fertilization. The highest uncertainties are associated with the estimates o NBP. This is presumably due to the fact that many of the components that contribute to the cropland C balance are site-specific, reflecting the impact of geographic factors, such as soil type, climate, or the types of crops/cropping practice on the total C budget. This is important as differences among sites in the contribution of the different components to the overall budget result in a high level of variation in NBP at regional scale (Osborne et al., 2010). Our uncertainty ranges calculated for annual NBP are larger than those published in other grassland studies (Rogiers et al., 2008) and cropland studies (Ciais et al., 2010). Yet, many authors even presented and interpreted their C budget results without indicating any uncertainty (Lloyd, 2006).

6.4 Conclusion

Cropland NPP and residue C input rate over the study period showed significant interannual variability, depending on the changes in crop production and weather variability. Variation in plant C input can be predicted by climate conditions. For the whole region, overall NBP for all land use was slightly increased 1959 to 2011. Though upland and paddy showed decreased NBP over the period of 1959–2011, in the case of increased agricultural abandonment (fallow/bush) and grassland from 1988, the regional C pools slowly start to build up. The combination of allometric relationship-based estimation of plant C inputs and Rh simulation modeling used in the present study allows us to simulate C balance in an agro-ecosystem where various crops are grown under different environmental (climate and soil) conditions across large scale.

None of the agro-ecosystem studies published used NBP and soil inventories combination. Our study provides this comparison in upland, paddy and grassland, and indicates that C loss occurs in each individual land use from 2005–2011. However, differences and large uncertainties in both methods stress the need for more direct comparisons to evaluate whether the observed difference in the outcome of the two approaches reflects a general methodological bias, and the uncertainty analysis would have important implications for regional C budgets.

7. General Discussion

7.1 Achievements of this study

Whilst there are a growing number of models for estimating soil GHG emission, the final choice of model is ultimately dependent on both the specific question being asked by the user and the availability of sufficiently detailed input data. For example, to develop sub-regional mitigation strategies based on C and N management would normally require high resolution of soil, climate and management data and a fully functional mechanistic or advanced empirical soil-plant simulation approach. In contract, a regional or national emissions inventory may only require simple regression approaches with coarse resolution soil and climate data. However, the national-scale study indicates that integrating process-based models with spatial databases can form a powerful tool to assess the effectiveness of GHG mitigation strategies at large scales. Quantifying soil GHG emissions is a scientific challenge that requires capacity to extend the understanding at a microbial or soil chemical scale to a regional or global scale. Process-based theory modeling, spatial data acquisition and computing techniques in this study have provided potentials to quantify soil GHG emission across the scales in space and time.

One of the major purposes for developing process-based models is to extend our understanding gained at specific sites to regional, national or global scales. In fact, policy decisions can only be made based on their effectiveness at regional or national scales. When a process-based model is applied to a regional scale, an issue of uncertainty will arise even when the model may have been well calibrated and validated at a site scale. The uncertainty mainly results from spatial heterogeneity of the input parameters used for the upscaling. For applying this type of model to a region, the region is routinely divided into many grid cells or polygons, with an assumption that each grid cell is uniform in all its properties. This assumption is against the fact that some of the input parameters, especially soil properties, usually vary even within small scales, such as a county or a farm. Averaging the variations of the input data may not resolve the problem because the correlation between the modeled output (e.g. GHG flux or other concerned items) and the drivers is non-linear. There are a number of measures to cope with this challenge. A relatively approach such as, the Most Sensitive Factor (MSF) method (Li et al., 2004), Monte Carlo method (Li et al., 2004) are widely used, and the method used in this study Bayesian Calibration are becoming popular. Bayesian method is clearly not the only way to address uncertainty; it stands out as an approach that can accommodate complex systems in a fully consistent framework. Compared to Bayesian calibration, the hierarchical approach would be beneficial to identify "hyper parameters", which may explain spatial variability. The advantage of hierarchical methods come as complexity increase (Clark, 2005), therefore it would be beneficial to apply HB calibration across different soils globally to deal with parameters' variability based on soil classification.

The magnitude of CO_2, N_2O and NO fluxes from arable land has been successfully simulated on a daily time-step using the CO_2-HB and N-HB models. Although the small number of studied soils and seasonal patterns limits the application of the model to other fields, the results obtained are sufficient to establish a reliable methodology and provide conclusions that may be generalizable to other soils and climate. This study proposed a method to predict the influence of soil texture on the effects of parameters on CO_2, N_2O and NO flux, and soil texture could thus be regarded as an upscaling factor for future research on regional extrapolation. We sought to calibrate the model parameters on different sites in order to minimize the uncertainty and to find the parameter values that would be universally applicable. Although the studied soil types in this study are limited, the results of our calibration could be suitable for simulating N_2O and NO fluxes in a new site where no measured data are available.

Our uncertainty ranges calculated for annual NBP (Table 6.4) are larger than those published in other grassland studies (e.g., Rogiers et al., 2008) and cropland studies (e.g., Ciais et al., 2010). Yet, many authors even presented and interpreted their C budget results without indicating any uncertainty (e.g., Lloyd, 2006; Allard et al., 2007). The NBP in all land use across the whole region showed a slowly increase. Though upland field and paddy field showed decreased NBP over the period of 1959–2012, in the case of increased agricultural abandonment (fallow/bush) and grassland from 1988, the regional C pools slowly start to build up. The combination of allometric relationship-based estimation of plant C inputs and CO_2-HB modeling used in the present study allows us to simulate C balance in an agro-ecosystem where various crops are grown under different environmental (climate and soil) conditions. None of the agro-ecosystem studies published used NBP and soil inventories combination. Our study provides this comparison in upland, paddy and grassland, and indicates that C loss occurs in each individual land use from 2005–2011. However, the soil inventory showed a tendency towards higher C loss than NBP. Thus either method may be suitable for tracking absolute changes in soil C unless with indication of uncertainty analysis, but both give similar answers respect to relative changes.

7.2 Suitability and benefits of Hierarchical Bayesian calibration

In recent years, hierarchical method has been successfully applied in different fields (Li et al., 2015; Ganesan et al., 2014; Riccio et al., 2006; Cressie et al., 2009). Under the hierarchical model, each site is unique but shares some commonality of behavior with other sites. Hierarchical modeling is the compromise between entirely site-specific and globally common parameter estimates (Malve and Qian, 2006). If the data do not demonstrate substantial inter-site variation, then the parameters of hierarchical structure will be closely identical to the global cross-site parameter.

Hierarchical method is clearly not the only way to address uncertainty; it stands out as an approach that can accommodate complex systems in a fully consistent framework. The hierarchical method solves for a larger number of parameters, including a small additional computational cost. Ganesan et al. (2014) indicated that based on traditional computational methods, as the size of the observation and/or parameter grows, the cost of computing will be approximately n^3. Our application in N-HB model involves 19 parameters, which 15 parameters were site-specific. Our data including total 15 different experimental sites and 26 different site/treatment combinations cross 9 years. In this study, the computational burden was released by HB calibration. The advantage of hierarchical methods come as complexity increase (Clark, 2005), therefore it would be beneficial to apply HB calibration across different soils globally to deal with parameters' variability based on soil classification.

7.3 Model application

The CO_2-HB model established in Chapter 4 requires only a few inputs (soil temperature, soil water texture, soil texture), they can be easily applied on a range of scales and incorporated into other models, such as shown in the establishment of N-HB model in Chapter 5. The CO_2-HB model was not designed for tracing detailed processes. Compared to the SG model constructed by Hashimoto et al. (2011), the CO_2-HB model not only has the advantage of being simple but also reveals that soil texture should be regarded as a possible scaling factor when upscaling the model from the site to the regional scale.

The N-HB model shown in Chapter 5 is designed based on process-based theory to simulate soil N gaseous emissions from agriculture soils. The main advantages of using the N-HB model in estimating cropland N_2O and NO fluxes arise as follows: (i) flexibility over the scale range. N-HB model was validated to performance well in predicting N_2O and NO flux at plot scale. The N-HB model shares the same N-cycle theory with other process-based models (Gabrielle et al., 2006a), NEMIS (Hénault et al., 2005), CERES-EGC (Gabrielle et al., 2006a) and ECOSSE model (Bell et al., 2012) and therefore is easily incorporation into other models as a sub-model. The N-HB model follows the alternative approach, using only the measurements that are available at large scale to drive the model at the range of scales. When attempting to stimulate emissions for a large scale, detailed information on plant/ soil input/ characteristics is not available. As such simulation at site level using the N-HB do not require this information, enabling the same model structure/process to be used at the large scale. This means that evaluations of the N-HB model using field scale measurements can be used directly to determine the uncertainty in simulation at larger scale. (ii) parameter variability. The N-HB model offers a critical guidance for parameterization. Generally, the parameters with less variability would be regarded as the global parameters and are extremely useful for spatial extrapolation, however, the parameters with the large variability need to be parameterized on site-specific basis. The simple linear relationship of calibrated parameters and soils provide a pre-requisite for simulation over space. Parameters of the NO module could be considered constant for model extrapolation to regional scale. The calibrated parameters derived from soil-specific calibration could be served as default values for the N_2O module extrapolation for similar soil types. Otherwise, the mean value of posterior distribution of calibration parameters could be served as global-parameter for new sites or soils.

7.4 Shortages & perspective

Although, both CO_2-HB and N-HB models showed several parameters significantly related to soil texture, to enhance the reliability and applicability of the CO_2-HB and N-HB models up-scaled to a larger scale and for similar soils, future studies should evaluate data across more soils types and seasonal patterns. It is difficult to apply the liner relation to other soils due to the limited breadth of input soil textures, however, it agrees with other models' result that the soil or landscape characteristics could control these parameters. Therefore, it will be interesting to apply HB calibration across different soils and establish a database of parameters based on soil classification.

Agriculture soils are so diverse in terms of crops grown, rotation, management, soil types, and climatic conditions that it is not possible to directly upscale results from individual cropland sites to the large scale, even with an extensive network of sites. Instead, the data are most valuable to calibrate and parameterize or validate ecosystem models, which are then combined with detailed spatial datasets, to allow a more process-based understanding at the plot scale to be up-scaled to the continent's total agriculture area. Through this combination of detailed measurement, improved understanding, and model development, we will be able to better estimate and project agricultural GHG fluxes, as well as advance our understanding of the factors controlling GHG fluxes in agriculture.

8. Summary

The carbon (C) balance in terrestrial ecosystems has large implications on the variation in atmospheric carbon dioxide (CO_2) emission. Soils are the main source of nitrous oxide (N_2O) emission and nitrogen monoxide (NO) emissions via the microbial processes of nitrification and denitrification. Modeling is an effective supplementary tool to estimate soil gas fluxes that allows the extrapolation of the results from the site scale to the large scale. Hierarchical Bayesian (HB) theory is useful tools for modeling multifaceted, nonlinear phenomena such as those encountered in ecology, and potentially used to reduce the uncertainty of estimated parameters.

The first goal of this study was to modeling CO_2, N_2O and NO flux at Ikushunbetsu River watershed, central Hokkaido, Japan by using HB theory. Secondly, the spatial and temporal patterns of net biome productivity (NBP) impacted by land management, climate condition and land use were estimated during the last four decades, and the C stocks change from 2005 to 2011 was compared with soil inventory method.

1. Modeling soil CO_2 flux from cropland (CO_2-HB model)

The CO_2-HB model was developed to simulate soil CO_2 flux derived from heterotrophic respiration (Rh) based on soil temperature (T), water-filled pore space (WFPS) and soil texture using HB theory. The simulation-observation fit of the CO_2 flux model was $R^2 = 0.64$ ($P < 0.001$). More than 90% of the observed daily data were within the 95% confidence interval. The CO_2-HB model calibration revealed differing sensitivity of CO_2 flux to T and WFPS in different soil texture classes. The CO_2-HB model provided a method for predicting how the effects of soil temperature and moisture on CO_2 flux change with texture, and soil texture could be regarded as an up-scaling factor for model extrapolation.

2. Modeling soil N_2O and NO flux from cropland (N-HB model)

The N-HB model was developed based on the nitrogen transformation process theory using HB method. Simulation of N_2O and NO fluxes showed appropriate correlation corresponding to observations on a daily time-step, with R^2 value of 0.35 in N_2O simulation and 0.51 in NO simulation. The main advantages of using N-HB model in estimating cropland N_2O and NO fluxes arise as follows: (i) flexibility over the scale range. The N-HB was validated to performance well in predicting N_2O and NO flux at plot scale, and it is easily incorporation into other models as a sub-model, which demonstrate its ability to adequately simulate soil N_2O flux at large scale. (ii) parameter variability. The N-HB model offers a critical guidance for parameterization. Parameters of the NO module could be considered constant for model extrapolation. The calibrated parameters derived from soil-specific calibration could be served as default values for the N_2O module extrapolation for similar soil types. Otherwise, the mean value of the calibration parameters could be served as global-parameter for similar soils.

3. NBP at regional scale during the last four decades

The complete crop-level yields, the CO_2-HB model and Geographic Information System (GIS) land use data were used to estimate the spatio-temporal changes of net primary productivity (NPP), plant C inputs, and NBP from 1959–2011. For the whole region (2193 ha), overall annual plant C inputs to the soil representing 37% of the whole region NPP. Plant C inputs in upland field (without bush/fallow) could be predicted by climate conditions. Overall NBP for all land use increased from –1.15 Mg C ha^{-1} yr^{-1} in 1959 to 0.34 Mg C ha^{-1} yr^{-1} in 2011. Though upland and paddy showed decreased NBP over the period of 1959–2011, in the case of increased agricultural abandonment (fallow/bush) and grassland from 1988, the regional C pools slowly start to build up. The comparison of soil inventory and NBP method in upland, paddy and grassland indicates that C loss occurs in each individual land use from 2005–2011, however, the soil inventory showed a tendency towards higher C loss than NBP.

9. References

Abdalla M, Jones M, Yeluripati J, Smith P, Burke J, Williams M 2010: Testing daycent and dndc model simulations of N_2O fluxes and assessing the impacts of climate change on the gas flux and biomass production from a humid pasture. Atmos. Environ., 44, 2961-2970.

Agarwal DK, Silander JA, Gelfand AE, Dewar RE, Mickelson JG 2005: Tropical deforestation in madagascar: analysis using hierarchical, spatially explicit, bayesian regression models. Ecol. Model., 185, 105-131.

Akaike H 1987: Factor analysis and AIC. Psychometrika, 52, 317-332.

Alexander, Martin 1977: Introduction to soil microbiology, pp. 251-271.No. Ed. 2. John Wiley & Sons.

Allard V, Soussana JF, Falcimagne R, Berbigier R, Bonnefond J, Ceschia E, D'hour P, Hénault C, Laville P, Martin C 2007: The role of grazing management for the net biome productivity and greenhouse gas budget (CO_2, N_2O and CH_4) of semi-natural grassland. Agric. Ecosyst. Environ., 121, 47-58.

AO/IFA 2001: Global estimates of gaseous emissions of NH_3, NO and N_2O from agricultural land. Food and Agriculture Organization of the United Nations (FAO)/ International Fertilizer Industry Association (IFA), pp. 106. Rome. http://www.fertilizer.org/ifa

Beck MB 1987: Water quality modeling: A review of the analysis of uncertainty. Water Resour. Res., 23, 1393-1442.

Beheydt D, Boeckx P, Sleutel S, Li C, Van C 2007: Validation of dndc for 22 long-term N_2O field emission measurements. Atmos. Environ., 41, 6196-6211.

Bell M, Jones E, Smith J, Smith P, Yeluripati J, Augustin J, Juszczak R, Olejnik J, Sommer M 2012: Simulation of soil nitrogen, nitrous oxide emissions and mitigation scenarios at

3 European cropland sites using the ECOSSE model. Nutr. Cycl. Agroecosyst., 92, 161-181.

Bolinder M, Janzen H, Gregorich E, Angers D, Vandenbygaart A 2007: An approach for estimating net primary productivity and annual carbon inputs to soil for common agricultural crops in canada. Agric. Ecosyst. Environ., 118, 29-42.

Bond-lamberty B, Thomson A 2010: Temperature-associated increases in the global soil respiration record. Nature, 464, 579-582.

Bondeau A, Smith PC, Zaehle S, Schaphoff S, Lucht W, Cramer W, Gerten D, Lotze-campen H, Müller C, Reichstein M, Smith B 2007: Modelling the role of agriculture for the 20th century global terrestrial carbon balance. Glob. Change Biol., 13, 679-706.

Borsuk ME, Higdon D, Stow CA, Reckhow KH 2001: A bayesian hierarchical model to predict benthic oxygen demand from organic matter loading in estuaries and coastal zones. Ecol. Model., 143, 165-181.

Bosatta E, Agren GI 1999: Soil organic matter quality interpreted thermodynamically. Soil Biol. Biochem., 31, 1889-1891.

Bouwman A, Boumans L, Batjes N 2002: Modeling global annual N_2O and NO emissions from fertilized fields. Glob. Biogeochem. Cycles, 16, 1-9.

Bradbury N, Whitmore A, Hart P, Jenkinson D 1993: Modelling the fate of nitrogen in crop and soil in the years following application of 15 N-labelled fertilizer to winter wheat. J. Agr. Sci., 121, 363-379.

Buchmann N, Schulze ED 1999: Net CO_2 and H_2O fluxes of terrestrial ecosystems. Glob. Biogeochem. Cycles, 13, 751-760.

Butterbach-bahl K, Kesik M, Miehle P, Papen H, Li C 2004: Quantifying the regional source strength of N-trace gases across agricultural and forest ecosystems with process based models. Plant Soil, 260, 311-329.

Buyanovsky G, Brown J, Wagner G 1996: Sanborn field: Effect of 100 years of cropping on soil parameters influencing productivity. In: Soil organic matter in temperate agroecosystems: long-term experiments in North America, pp. 215-220. CRC Press.

Cable JM, Ogle K, Tyler AP, Pavao-zuckerman MA, Huxman TE 2009: Woody plant encroachment impacts on soil carbon and microbial processes: results from a hierarchical bayesian analysis of soil incubation data. Plant Soil, 320, 153-167.

Campbell C, Mcconkey B, Zentner R, Dyck F, Selles F, Curtin D 1995: Carbon sequestration in a brown chernozem as affected by tillage and rotation. Can. J. Soil Sci., 75, 449-458.

Chapin iii FS, Woodwell GM, Randerson JT, Rastetter EB, Lovett GM, Baldocchi DD, Clark DA, Harmon ME, Schimel DS, Valentini R 2006: Reconciling carbon-cycle concepts, terminology, and methods. Ecosystems, 9, 1041-1050.

Chatskikh D, Olesen JE 2007: Soil tillage enhanced CO_2 and N_2O emissions from loamy sand soil under spring barley. Soil Till. Res., 97, 5-18.

Chatskikh D, Olesen JE, Berntsen J, Regina K, Yamulki S 2005: Simulation of effects of soils, climate and management on N_2O emission from grasslands. Biogeochemistry, 76, 395-419.

Chatskikh D, Olesen JE, Hansen EM, Elsgaard L. Petersen BM 2008: Effects of reduced tillage on net greenhouse gas fluxes from loamy sand soil under winter crops in denmark. Agric. Ecosyst. Environ., 128, 117-126.

Chen D, Li Y, Edis R, White R 2005: A GIS based water and nitrogen management model (WNMM) and agricultural decision support tool (ADST) for irrigated wheat and maize in north china plain. Proceedings of the 3rd international nitrogen conference. Science Press USA Inc. 899-908.

Chen D, Li Y, Grace P, Mosier AR 2008: N_2O emissions from agricultural lands: a synthesis of simulation approaches. Plant Soil, 309, 169-189.

Chevallier T, Blanchart E, Albrecht A, Feller C 2004: The physical protection of soil organic carbon in aggregates: A mechanism of carbon storage in a vertisol under pasture and market gardening (Martinique, West Indies). Agric. Ecosyst. Environ., 103, 375-387.

Ciais P, Reichstein M, Viovy N, Granier A, Ogée J, Allard V, Aubinet M, Buchmann N, Bernhofer C, Carrara A 2005: Europe-wide reduction in primary productivity caused by the heat and drought in 2003. Nature, 437, 529-533.

Ciais P, Soussana J, Vuichard N, Luyssaert S, Don A, Janssens I, Piao S, Dechow R, Lathière J, Maignan F 2010: The greenhouse gas balance of european grasslands. Biogeosci. Discuss., 7, 5997-6050.

Clark JS 2003: Uncertainty and variability in demography and population growth: a hierarchical approach. Ecology, 84, 1370-1381.

Clark JS 2005: Why environmental scientists are becoming bayesians. Ecol. Lett., 8, 2-14.

Cole C, Duxbury J, Freney J, Heinemeyer O, Minami K, Mosier A, Paustian K, Rosenberg N, Sampson N, Sauerbeck D 1997: Global estimates of potential mitigation of greenhouse gas emissions by agriculture. Nutr. Cycl. Agroecosys., 49, 221-228.

Cressie N, Calder CA, Clark JS, Hoef JMV, Wikle CK 2009: Accounting for uncertainty in ecological analysis: the strengths and limitations of hierarchical statistical modeling. Ecol. Appl., 19, 553-570.

Darmody R, Peck T 1996: Soil organic carbon changes through time at the university of illinois morrow plots. Soil organic matter in temperate agroecosystems: long-term experiments in North America. Soil organic carbon changes through time at the university of illinois morrow plots, pp. 161-169. CRC Press.

Davidson E, Belk E, Boone RD 1998: Soil water content and temperature as independent or confounded factors controlling soil respiration in a temperate mixed hardwood forest. Glob. Change Biol., 4, 217-227.

Davidson EA, Janssens IA, Luo Y 2006: On the variability of respiration in terrestrial ecosystems: moving beyond Q10. Glob. Change Biol., 12, 154-164.

Davidson EA, Rogers J, Whitman W 1991: Fluxes of Nitrous Oxide and Nitric Oxide from terrestrial ecosystems. In: Microbial production and consumption of greenhouse gases: Methane, Nitrogen Oxides, and halomethanes, pp. 219-235. CRC Press.

Davidson EA, Verchot LV, Cattânio, JH, Ackerman IL, Carvalho J 2000: Effects of soil water content on soil respiration in forests and cattle pastures of eastern amazonia. Biogeochemistry, 48, 53-69.

De K, Can L 1996: Denitrification in grassland soils in the netherlands in relation to irrigation, N-application rate, soil water content and soil temperature. Soil Biol. Biochem., 28, 231-237.

Del Galdo, Six J, Peressotti A, Francesca C 2003: Assessing the impact of land -use change on soil C sequestration in agricultural soils by means of organic matter fractionation and stable C isotopes. Glob. Change Biol., 9, 1204-1213.

Del Grosso, Mosier A, Parton W, Ojima D 2005: Daycent model analysis of past and contemporary soil N_2O and net greenhouse gas flux for major crops in the USA. Soil Till. Res., 83, 9-24.

Del Grosso, Ogle S, Parton W, Breidt F 2010: Estimating uncertainty in N_2O emissions from us cropland soils. Global biogeochemical cycles, 24. DOI: 10.1029/2009GB003544.

Del grosso, Parton W, Mosier A, Ojima D, Kulmala A, Phongpan S 2000: General model for N_2O and N_2 gas emissions from soils due to dentrification. Glob. Biogeochem. Cycles, 14, 1045-1060.

Desjardins R, Pattey E, Smith W, Worth D, Grant B, Srinivasan R, Macpherson J, Mauder M 2010: Multiscale estimates of N_2O emissions from agricultural lands. Agr. Forest Meteorol., 150, 817-824.

Dixon J 1999: An evaluation of unsaturated flow models in an arid climate. PhD thesis. US Department of Energy.

Doran J 1987: Microbial biomass and mineralizable nitrogen distributions in no-tillage and plowed soils. Biol. Fert. Soils, 5, 68-75.

Douglas L, Tedrow J 1959: Organic matter decomposition rates in arctic soils. Soil Sci., 88, 305.

Dregne H 1982: Historical perspective of accelerated erosion and effect on world civilization.

Determinants of soil loss tolerance, 45, 1-14.

Drewnik M 2006: The effect of environmental conditions on the decomposition rate of cellulose in mountain soils. Geoderma, 132, 116-130.

Engel T, Priesack E 1993: Expert-N-A building block system of nitrogen models as resource for advice, research, water management and policy. In: Integrated soil and sediment research: a basis for proper protection, pp. 503-510. Springer.

Follett RF, Stewart CE, Pruessner EG 2015: Great plains climate and land-use effects on soil organic carbon. Soil Sci. Soc. Am J., 79, 261-271.

Frolking S, Mosier A, Ojima D, Li C, Parton W, Potter C, Priesack E, Stenger R, Haberbosch C, Dörsch P 1998: Comparison of N_2O emissions from soils at three temperate agricultural sites: Simulations of year-round measurements by four models. Nutr. Cycl. Agroecosys., 52, 77-105.

Gabrielle B 2006: Sensitivity and uncertainty analysis of a static denitrification model. In: Working with dynamic crop models, pp. 359-366. Elsevier.

Gabrielle B, Laville P, Duval O, Nicoullaud B, Germon JC, Hénault C 2006a: Process -based modeling of Nitrous Oxide emissions from wheat -cropped soils at the subregional scale. Glob. Biogeochem. Cycles, 4. DOI: 10.1029/2006GB002686

Gabrielle B, Laville P, Hénault C, Nicoullaud B, Germon JC 2006b: Simulation of nitrous oxide emissions from wheat-cropped soils using ceres. Nutr. Cycl. Agroecosys., 74, 133-146.

Gallagher M, Doherty J 2007: Parameter estimation and uncertainty analysis for a watershed model. Environ. Modell. Softw., 22, 1000-1020.

Ganesan A, Rigby M, Zammit-mangion A, Manning A, Prinn R, Fraser P, Harth C, Kim KR, Krummel PS 2014: Characterization of uncertainties in atmospheric trace gas inversions using hierarchical bayesian methods. Atmos. Chem. Phys., 14, 3855-3864.

Gelman A, Rubin DB 1992: Inference from iterative simulation using multiple sequences. Statistical science, 457-472.

Gervois S, Ciais P, De Noblet -ducoudré, Brisson N, Vuichard N 2008: Carbon and water balance of european croplands throughout the 20th century. Glob. Biogeochem. Cycles, 22. doi:10.1029/2007GB003018.

Gilmour J 1984: The effects of soil properties on nitrification and nitrification inhibition. Soil Sci. Soc. Am. J., 48, 1262-1266.

Gioli B, Miglietta F, De Martino, Hutjes R, Dolman A, Lindroth A, Lloyd J, Sanz M, Valentini R, Dumas E 2004: Comparison between tower and aircraft-based eddy correlation fluxes in five regions of europe. Agric. For. Meteorol., 127, 1-16.

Gómez DR, Watterson JD, Americano BB, Ha C, Marland G, Matsika E, Namayanga LN, Osman-elasha B, Saka J, Treanton K 2006: IPCC guidelines for national greenhouse gas inventories. Institute for global environmental strategies, kamiyamaguchi hayama, Japan. http://www.ipcc-tfi.iges.or.jp/meeting/pdfiles/Washington_Report.pdf.

Grace P, Gage S, Colunga-garcia M, Robertson G, Safir G 2005: Maximizing net carbon sequestration in agroecosystems of the north central region. Third USDA symposium greenhouse gases & carbon sequestration in agriculture and forestry.

Groffman PM, Tiedje JM 1991: Relationships between denitrification, CO_2 production and air-filled porosity in soils of different texture and drainage. Soil Biol. Biochem., 23, 299-302.

Haines A 2003: Climate change 2001: The scientific basis. Contribution of working group 1 to the third assessment report of the intergovernmental panel on climate change. International Journal of Epidemiology, 32, 321-321.

Hargreaves K, Skiba U, Fowler D, Arah J, Wienhold F, Klemedtsson L, Galle B 1994: Measurement of nitrous oxide emission from fertilized grassland using micrometeorological techniques. J. Geophys. Res-OC Atm., 99, 16569-16574.

Hashimoto S 2005: Q10 values of soil respiration in japanese forests. J. For. Res., 10, 409-413.

Hashimoto S, Morishita T, Sakata T, Ishizuka S, Kaneko S, Takahashi M 2011: Simple models for soil CO_2, CH_4, and N_2O fluxes calibrated using a bayesian approach and multi-site data. Ecol. Model., 222, 1283-1292.

Hassink J 1993: Relationship between the amount and the activity of the microbial biomass in dutch grassland soils: comparison of the fumigation-incubation method and the substrate-induced respiration method. Soil Biol. Biochem., 25, 533-538.

Hayakawa C, Funakawa S, Fujii K, Kadono A, Kosaki T 2014: Effects of climatic and soil properties on cellulose decomposition rates in temperate and tropical forests. Biol. Fert. Soils, 50, 633-643.

Heinen M 2006: Application of a widely used denitrification model to dutch data sets. Geoderma, 133, 464-473.

Hénault C, Bizouard F, Laville P, Gabrielle B, Nicoullaud B, Germon J, Cellier P 2005: Predicting in situ soil N_2O emission using NOE algorithm and soil database. Glob. Change Biol., 11, 115-127.

Hénault C, Germon JC 2000: NEMIS, a predictive model of denitrification on the field scale. Eur. J. Soil Sci., 51, 257-270.

Hokkaido Central Agricultural Experiment Station 1971. Results of the basic survey on soil fertility, pp. 1-109. Ed. Mori T. et al. Hokkaido (in Japanese).

Hollinger SE, Bernacchi CJ, Meyers TP 2005: Carbon budget of mature no-till ecosystem in north central region of the united states. Agric. For. Meteorol., 130, 59-69.

Hopkins D, Waite I, Mcnicol J, Poulton P, Macdonald A, O'donnell A 2009: Soil organic carbon contents in long -term experimental grassland plots in the UK (palace leas and park grass) have not changed consistently in recent decades. Glob. Change Biol., 15, 1739-1754.

Howard D, Howard P 1993: Relationships between CO_2 evolution, moisture content and temperature for a range of soil types. Soil Biol. Biochem., 25, 1537-1537.

Hu R, Hatano R, Kusa K, Sawamoto T 2004: Soil respiration and net ecosystem production in an onion field in central Hokkaido, Japan. Soil Sci. Plant Nutr., 50, 27-33.

Janzen H 2004: Carbon cycling in earth systems-a soil science perspective. Agric. Ecosyst. Environ., 104, 399-417.

Janzen H, Campbell C, Gregorich E, Ellert B 1997: Soil carbon dynamics in canadian agroecosystems. Soil Processes and the Carbon Cycle, 57-80.

Jenkinson DS, Adams D, Wild A 1991: Model estimates of CO_2 emissions from soil in response to global warming. Nature, 351, 304-306.

Jensen M, Burman R, Allen R 1990: Evaporation and irrigation water requirements. In: Manuals of Practice. Practices No. 70, pp. 360. American society of civil engineers, New York, NY.

Jia J, Ma Y, Xiong Z 2012: Net ecosystem carbon budget, net global warming potential and greenhouse gas intensity in intensive vegetable ecosystems in China. Agric. Ecosyst. Environ., 150, 27-37.

Johnsson H, Klemedtsson L, Nilsson å., Svensson HB 1991: Simulation of field scale denitrification losses from soils under grass ley and barley. Plant Soil, 138, 287-302.

Jones RJ, Hiederer R, Rusco E, Montanarella L 2005: Estimating organic carbon in the soils of Europe for policy support. Eur. J. Soil Sci., 56, 655-671.

Kätterer T, Reichstein M, Andrén O, Lomander A 1998: Temperature dependence of organic matter decomposition: A critical review using literature data analyzed with different models. Biol. Fert. Soils, 27, 258-262.

Kim C, An HC, Byun JK 2010: Cellulose decomposition rates in clear -cut and uncut red pine (pinus densiflora S. et Z.) Stands. For. Sci. Technol., 6, 29-34.

Kimura S, Liang L, Hatano R 2004: Influence of long-term changes in nitrogen flows on the environment: A case study of a city in Hokkaido, Japan. Nutr. Cycl. Agroecosyst., 70, 271-282.

Kimura SD, Toma Y, Mu Z, Yamada H, Hatano R 2010: Eco-balance analysis of land use combinations to minimize environmental impacts and maximize farm income in northern japan. Sustainability Sci., 5, 19-27.

Kirschbaum MU 1995: The temperature dependence of soil organic matter decomposition, and the effect of global warming on soil organic C storage. Soil Biol. Biochem., 27, 753-760.

Koga N, Smith P, Yeluripati J, Shirato Y, Kimura SD, Nemoto M 2011: Estimating net primary production and annual plant carbon inputs, and modelling future changes in soil carbon stocks in arable farmlands of northern Japan. Agric. Ecosyst. Environ., 144, 51-60.

Koizumi H 2001: Carbon cycling in croplands. In: Structure and function in agroecosystem design and management, pp. 207-226. CRC Press.

Kraft NJ, Metz MR, Condit RS, Chave J 2010: The relationship between wood density and mortality in a global tropical forest data set. New Phytol., 188, 1124-1136.

Kusa K, Sawamoto T, Hatano R 2002: Nitrous oxide emissions for 6 years from a gray lowland soil cultivated with onions in Hokkaido, Japan. Nutr. Cycl. Agroecosyst., 63, 239-247.

Langeveld C, Leffelaar P 1996: Approaches in field scale modelling of nitrous oxide emission from grassland soils. Research theme: Nitrogen transformations in soil, 153-156.

Lehuger S, Gabrielle B, Van O, Makowski D, Germon JC, Morvan T, Hénault C 2009: Bayesian calibration of the nitrous oxide emission module of an agro-ecosystem model. Agrc. Ecosyst. Environ., 133, 208-222.

Leifeld J, Ammann C, Neftel A, Fuhrer J 2011: A comparison of repeated soil inventory and carbon flux budget to detect soil carbon stock changes after conversion from cropland to grasslands. Glob. Change Biol., 17, 3366-3375.

Lenton TM, Huntingford C 2003: Global terrestrial carbon storage and uncertainties in its temperature sensitivity examined with a simple model. Glob. Change Biol., 9, 1333-1352.

Li C 2000: Modeling trace gas emissions from agricultural ecosystems. Nutr. Cycl.

Agroecosyst., 58, 259-276.

Li C 2007: User's guide for the dndc model (ver 9.1). Institute for the study of earth, oceans, and space. University of New Hampshire, Durham, NH.

Li C, Frolking S, Frolking TA 1992: A model of nitrous oxide evolution from soil driven by rainfall events: 1. model structure and sensitivity. J. Geophys. Res., 97, 9759-9776.

Li C, Mosier A, Wassmann R, Cai Z, Zheng X, Huang Y, Tsuruta H, Boonjawat J, Lantin R 2004: Modeling greenhouse gas emissions from rice -based production systems: sensitivity and upscaling. Glob. Biogeochem. Cycles, 18. DOI: 10.1029/2003GB002045

Li X, Ishikura K, Wang C, Yeluripati J, Hatano R 2015: Hierarchical bayesian models for soil CO_2 flux using soil texture: a case study in central hokkaido, Japan. Soil Sci. Plant Nutr., 61, 116-132.

Li Y, Chen D, Zhang Y, Edis R, Ding H 2005: Comparison of three modeling approaches for simulating denitrification and nitrous oxide emissions from loam -textured arable soils. Glob. Biogeochem. cycles, 19. DOI: 10.1029/2004GB002392

Li Y, White R, Chen D, Zhang J, Li B, Zhang Y, Huang Y, Edis R 2007: A spatially referenced water and nitrogen management model (WNMM) for (Irrigated) intensive cropping systems in the north china plain. Ecol. Model., 203, 395-423.

Linn D, Doran J 1984: Effect of water-filled pore space on carbon dioxide and nitrous oxide production in tilled and nontilled soils. Soil Sci. Soc. America J., 48, 1267-1272.

Lloyd C 2006: Annual carbon balance of a managed wetland meadow in the somerset levels, UK. Agr. Forest Meteorol., 138, 168-179.

Lokupitiya E, Paustian K 2006: Agricultural soil greenhouse gas emissions. J. Environ. Qual., 35, 1413-1427.

Lokupitiya E, Paustian K, Easter M, Williams S, Andrén O, Kätterer T 2012: Carbon balances in us croplands during the last two decades of the twentieth century. Biogeochemistry, 107, 207-225.

Lu D, Ye M, Hill MC 2012: Analysis of regression confidence intervals and bayesian credible intervals for uncertainty quantification. Water resources research, 48, W09521, DOI:10.1029/2011WR011289.

Lyon D, Monz C, Brown R, Metherell A 1996: Soil organic matter changes over two decades of winter wheat-fallow cropping in western nebraska. Soil organic matter in temperate agroecosystems: long-term experiments in north America, pp. 343-351. CRC Press.

Ma L, Shaffer M 2001: A review of carbon and nitrogen processes in nine us soil nitrogen dynamics models. Modeling carbon and nitrogen dynamics for soil management, pp. 55-103. Lewis Publication.

Maag M, Vinther FP 1996: Nitrous oxide emission by nitrification and denitrification in different soil types and at different soil moisture contents and temperatures. Appl. Soil Ecol., 4, 5-14.

Maag M, Vinther FP 1999: Effect of temperature and water on gaseous emissions from soils treated with animal slurry. Soil Sci. Soc. Am. J., 63, 858-865.

Makowski D, Hillier J, Wallach D, Andrieu B, Jeuffroy M 2006: Parameter estimation for crop models. Agron. J., 4, 757-766.

Malhi S, Mcgill W 1982: Nitrification in three alberta soils: effect of temperature, moisture and substrate concentration. Soil Biol. Biochem., 14, 393-399.

Malve O, Qian SS 2006: Estimating nutrients and chlorophyll a relationships in finnish lakes. Environ. Sci. Technol., 40, 7848-7853.

Matsumoto N 2000: Development of estimation method and evaluation of nitrogen flow in regional areas. Nogyo kankyo gijutsu kenkyusho hokoku bulletin of the national institute of agro-environmental sciences, 18, 81-152.

McCuen RH 2003: Sensitivity Analysis. In: Modeling Hydrologic Change: Statistical Methods, pp. 333-363. Lewis Publishers.

Mcgechan M, Lewis D, Wu L, Mctaggart L 2001: Modeling the effects of manure and fertilizer management options on soil carbon and nitrogen processes. In: Modeling carbon and nitrogen dynamics for soil management, pp. 427-458. CRC Press.

Mcgill W, Cole C 1981: Comparative aspects of cycling of organic C, N, S and P through soil organic matter. Geoderma, 26, 267-286.

Melillo JM, Aber JD, Linkins AE, Ricca A, Fry B, Nadelhoffer KJ 1989: Carbon and Nitrogen dynamics along the decay continuum: plant litter to soil organic matter. In Ecology of Arable Land-Perspectives and Challenges, pp. 53-62. Springer.

Miglietta F, Gioli B, Hutjes R, Reichstein M 2007: Net regional ecosystem CO_2 exchange from airborne and ground-based eddy covariance, land -use maps and weather observations. Glob. Change Biol., 13, 548-560.

Miller FP, Rasmussen WD, Meyer LD 1985: Historical perspective of soil erosion in the united states. In: Soil erosion and crop productivity, pp. 23-48. Madison, Wisconsion.

Mitchell TD, Carter TR, Jones PD, Hulme M, New M 2004: A comprehensive set of high-resolution grids of monthly climate for europe and the globe: the observed record (1901–2000) and 16 scenarios (2001–2100). Tyndall centre for climate change research working paper, 55, 25.

Monger H, Martinez-rios J 2000: Inorganic carbon sequestration in grazing lands. The potential of us grazing lands to sequester carbon and mitigate the greenhouse effect, pp. 87-118. Lewis Publisher.

Monod H, Naud C, Makowski D 2006: Uncertainty and sensitivity analysis for crop models. Working with dynamic crop models: evaluation, analysis, parameterization, and applications, 4, 55-100.

Mortland M 1970: Clay-organic complexes and interactions. Adv. Agron, 22, 117.

Mosier A, Duxbury J, Freney J, Heinemeyer O, Minami K, Johnson D 1998: Mitigating agricultural emissions of methane. Climatic Change, 40, 39-80.

Mosier A, Parton A, Hutchinson G 1983: Modelling nitrous oxide evolution from cropped and native soils. Ecol. Bull., 35, 229-241.

Mosier A, Parton WJ 1985: Denitrification in a shortgrass prairie: a modeling approach, pp.

441-452. Van Nostrand Reinhold Co., NY.

Mu Z, Kimura SD, Hatano R 2006: Estimation of global warming potential from upland cropping systems in central Hokkaido, Japan. Soil Sci. Plant Nutr., 52, 371-377.

Mu Z, Kimura SD, Toma Y, Hatano R 2008a: Evaluation of the soil carbon budget under different upland cropping systems in central Hokkaido, Japan. Soil Sci. Plant Nutr., 54, 650-661.

Mu Z, Kimura SD, Toma Y, Hatano R 2008b: Nitrous oxide fluxes from upland soils in central Hokkaido, Japan. J. Environ. Sci., 20, 1312-1322.

Nakane K, Kohno T, Horikoshi T, Nakatsubo T 1997: Soil carbon cycling at a black spruce (picea mariana) forest stand in saskatchewan, Canada. J. Geophys. Res-OC Atm (1984–2012), 102, 28785-28793.

Naser HM, Nagata O, Tamura S, Hatano R 2007: Methane emissions from five paddy fields with different amounts of rice straw application in central Hokkaido, Japan. Soil Sci. Plant Nutr., 53, 95-101.

Nobre A, Harriss R 2000: Saving the rainforest with sustainable enterprises in degraded lands: the amazonian phoenix project. Proceeding of Working Forests in the Tropics Conference, Gainesville, FL, USA.

Nouchi I, Yonemura S 2005: CO_2, CH_4 and N_2O fluxes from soybean and barley double-cropping in relation to tillage in Japan. Phyton, 45, 327-338.

Oenema O, Wrage N, Velthof GL, Van Groenigen JW, Dolfing J, Kuikman PJ 2005: Trends in global nitrous oxide emissions from animal production systems. Nutr. Cycl. Agroecosyst., 72, 51-65.

Ogawa K 1988: Biomass production and the amounts of absorbed inorganic elements by crops in arable lands in Hokkaido, and its evaluation. Research bulletin of Hokkaido national agricultural experiment station, 149, 57-91.

Ogle SM, Breidt FJ, Easter M, Williams S, Paustian K 2007: An empirically based approach for estimating uncertainty associated with modelling carbon sequestration in soils.

Ecol. Model., 205, 453-463.

Ogle SM, Breidt FJ, Paustian K 2005: Agricultural management impacts on soil organic carbon storage under moist and dry climatic conditions of temperate and tropical regions. Biogeochemistry, 72, 87-121.

Osborne B, Saunders M, Walmsley D, Jones M, Smith P 2010: Key questions and uncertainties associated with the assessment of the cropland greenhouse gas balance. Agric. Ecosyst. Environ., 139, 293-301.

Parton W, Holland E, Del Grosso, Hartman M, Martin R, Mosier A, Ojima D, Schimel D 2001: Generalized model for NO_x and N_2O emissions from soils. J. Geophys. Res-OC Atm. (1984–2012), 106, 17403-17419.

Parton W, Mosier A, Ojima D, Valentine D, Schimel D, Weier K, Kulmala AE 1996: Generalized model for N_2 and N_2O production from nitrification and denitrification. Global Biogeochem. Cycles, 10, 401-412.

Parton W, Mosier A, Schimel D 1988a: Rates and pathways of nitrous oxide production in a shortgrass steppe. Biogeochemistry, 6, 45-58.

Parton W, Gutmann MP, Williams SA, Easter M, Ojima D. 2005: Ecological impact of historical land-use patterns in the great plains: a methodological assessment. Ecol. Appl., 15, 1915-1928.

Parton W, Stewart JW, Cole CV 1988b: Dynamics of C, N, P and S in grassland soils: a model. Biogeochemistry, 5, 109-131.

Patrick LD, Ogle K, Tissue DT 2009: A hierarchical bayesian approach for estimation of photosynthetic parameters of C_3 plants. Plant Cell Environ., 32, 1695-1709.

Paustian K, Babcock B, Hatfield J, Lal R, Mccarl B, Mclaughlin S, Mosier A, Rice C, Robertson G, Rosenberg N 2004: Agricultural mitigation of greenhouse gases: science and policy options. Cast (council on agricultural science and technology) report, 141.

Peoples M, Freney J, Mosier A, Bacon P 1995: Minimizing gaseous losses of nitrogen. In: Nitrogen fertilization in the environment, pp. 565-602. CRC Press.

Peterson G, Westfall D 1996: Management of dryland agroecosystems in the central great plains of colorado. In: Soil organic matter in temperate agroecosystems, pp. 371-380. Lewis Publishers.

Ping C, Michaelson G, Day X, Candler R 2001: Characterization of soil organic matter. In: Assessment methods for soil carbon, pp. 273-283. CRC Press.

Plummer M 2003: Jags: A program for analysis of bayesian graphical models using gibbs sampling. Proceedings of the 3rd international workshop on distributed statistical computing. Technische Universit at Wien, 124, 125.

Potter C, Davidson E, Verchot L 1996: Estimation of global biogeochemical controls and seasonality in soil methane consumption. Chemosphere, 32, 2219-2246.

Povirk K, Welker J, Vance G 2000: Carbon sequestration in arctic and alpine tundra and mountain meadow ecosystems. In: The potential of us grazing lands to sequester carbon and mitigate the greenhouse effect, pp. 189-228. Lewis publishers.

Prince SD, Haskett J, Steininger M, Strand H, Wright R 2001: Net primary production of us midwest croplands from agricultural harvest yield data. Ecol. Appl., 11, 1194-1205.

Raich JW, Potter CS 1995: Global patterns of carbon dioxide emissions from soils. Glob. Biogeochem. Cycles, 9, 23-36.

Reeder JD, Franks CD, Milchunas DG 2001: Root biomass and microbial processes. In: The potential of US grazing lands to sequester carbon and mitigate the greenhouse effect, pp. 139-166. Lewis Publishers.

Reicosky D, Kemper W, Langdale G, Douglas C, Rasmussen P 1995: soil organic matter changes resulting from tillage and biomass production. J. Soil Water Conserv., 50, 253-261.

Reth S, Hentschel K, Drösler M, Falge E 2005: Dennit-experimental analysis and modelling of soil N_2O efflux in response on changes of soil water content, soil temperature, soil ph, nutrient availability and the time after rain event. Plant Soil, 272, 349-363.

Riccio A, Barone G, Chianese E, Giunta G 2006: A hierarchical bayesian approach to the spatio-temporal modeling of air quality data. Atmos. Environ., 40, 554-566.

Richter JR 2014: Long-term soil experiments: A key to managing earth's rapidly changing critical zones. Agu fall meeting abstracts. http://adsabs.harvard.edu/abs/2014AGUFM.H12D..05R (September 2014).

Riley W, Matson P 2000: Nloss: A mechanistic model of denitrified N_2O and N_2 evolution from soil. Soil Sci., 165, 237-249.

Römkens M, Nelson D, Mannering J 1973: Nitrogen and phosphorus composition of surface runoff as affected by tillage method. Journal Environ. Qual., 2, 292-295.

Rounsevell M, Reginster I, Araújo MB, Carter T, Dendoncker N, Ewert F, House J, Kankaanpää S, Leemans R, Metzger M 2006: A coherent set of future land use change scenarios for europe. Agric. Ecosyst Environ., 114, 57-68.

Rovira A 1953: Use of the warburg apparatus in soil metabolism studies. Nature, 172, 29-30.

Sabey B, Frederick L, Bartholomew W 1959: The formation of nitrate from ammonium nitrogen in soils: iii influence of temperature and initial population of nitrifying organisms on the maximum rate and delay period. Soil Sci. Soc. Am. J., 23, 462-465.

Saxton KE, Rawls WJ, 2006: Soil water characteristic estimates by texture and organic matter for hydrologic solutions. Soil Sci. Soc. Am. J., 70, 1569-1578.

Scheibehenne B, Pachur T 2015: Using bayesian hierarchical parameter estimation to assess the generalizability of cognitive models of choice. Psychonomic Bull. & Rev., 22, 391-407.

Schulze E, Heimann M 1998: Carbon and water exchange of terrestrial systems. Asian Change in the Context of Global Change, 3, 145-161.

Sexstone A, Parkin T, Tiedje J 1988: Denitrification response to soil wetting in aggregated and unaggregated soil. Soil Biol. Biochem., 20, 767-769.

Shaffer M, Wylie B, Follett R, Bartling P 1994: Using climate/weather data with the nleap model to manage soil nitrogen. Agric. For. Meteorol., 69, 111-123.

Shaffer M, Wylie B, Hall M 1995: Identification and mitigation of nitrate leaching hot spots using NLEAP-GIS technology. J. Contam. Hydrol., 20, 253-263.

Singh J, Gupta S 1977: Plant decomposition and soil respiration in terrestrial ecosystems. Bot. Rev., 43, 449-528.

Six J, Carpentier A, Van Kessel, Merckx R, Harris D, Horwath WR, Lüscher A 2001: Impact of elevated CO_2 on soil organic matter dynamics as related to changes in aggregate turnover and residue quality. Plant Soil, 234, 27-36.

Skopp J, Jawson M, Doran J 1990: Steady-state aerobic microbial activity as a function of soil water content. Soil Sci. Soc. Am. J., 54, 1619-1625.

Smith C, Freney J, Bond WJ 1996: Ammonia volatilisation from soil irrigated with urban sewage effluent. Soil Res., 34, 789-802.

Smith J, Gottschalk P, Bellarby J, Chapman S, Lilly A, Towers W, Bell J, Coleman K, Nayak D, Richards M 2010: Estimating changes in national soil carbon stocks using ECOSSE-a new model that includes upland organic soils. Part i. Model description and uncertainty in national scale simulations of scotland. Climate Res., 45, 179-192.

Smith J, Gottschalk P, Bellarby J, Richards M, Nayak D, Coleman K 2010c：Model to estimate carbon in organic soils-sequestration and emissions (ECOSSE) user-manual, pp. 1-76. University of Aberdeen Press, UK.

Smith J, Smith P, Monaghan R, Macdonald A 2002: When is a measured soil organic matter fraction equivalent to a model pool. Eur. J. Soil Sci., 53, 405-416.

Smith J, Smith P, Wattenbach M, Zaehle S, Hiederer R, Jones RJ, Montanarella L, Rounsevell MD, Reginster I, Ewert F 2005: Projected changes in mineral soil carbon of European croplands and grasslands, 1990–2080. Glob. Change Biol., 11, 2141-2152.

Smith K, Ball T, Conen F, Dobbie K, Massheder J, Rey A 2003: Exchange of greenhouse gases between soil and atmosphere: interactions of soil physical factors and biological processes. Eur. J. Soil Sci., 54, 779-791.

Smith K, Conen F 2004: Impacts of land management on fluxes of trace greenhouse gases. Soil Use Manage., 20, 255-263.

Smith K, Thomson P, Clayton H, Mctaggart I, Conen F 1998: Effects of temperature, water content and nitrogen fertilisation on emissions of nitrous oxide by soils. Atmos. Environ., 32, 3301-3309.

Smith P, Field C, Raupach M 2004: Engineered biological sinks on land. The global carbon cycle: integrating humans, climate and the natural world, 479-491.

Smith P, Martino D, Cai Z, Gwary D, Janzen H, Kumar P, Mccarl B, O'mara F, Rice c, Scholes B 2007a: Greenhouse gas mitigation in agriculture philosophical transactions of the royal society (b). DOI: 10.1098/rstb.2007.2184

Smith P, Martino D, Cai Z, Gwary D, Janzen H, Kumar P, Mccarl B, Ogle S, O'mara F, Rice C 2007b: Policy and technological constraints to implementation of greenhouse gas mitigation options in agriculture. Agric. Ecosyst. Environ., 118, 6-28.

Smith P, Smith J, Powlson D, Mcgill W, Arah J, Chertov O, Coleman K, Franko U, Frolking S, Jenkinson D 1997: A comparison of the performance of nine soil organic matter models using datasets from seven long-term experiments. Geoderma, 81, 153-225.

Sobecki T, Moffitt D, Stone J, Franks C, Mendenhall A, Follett R, Kimble J, Lal R 2001: A broad-scale perspective on the extent, distribution, and characteristics of us grazing lands. In: The potential of us grazing lands to sequester carbon and mitigate the greenhouse effect, pp. 21-63. CRC Press.

Sorensen L 1975: The influence of clay on the rate of decay of amino acid metabolites synthesized in soils during decomposition of cellulose. Soil Biol. Biochem., 7, 171-177.

Sozanska M, Skiba U, Metcalfe S 2002: Developing an inventory of N_2O emissions from british soils. Atmos. Environ., 36, 987-998.

Spiegelhalter DJ, Best NG, Carlin BP, Van A 2002: Bayesian measures of model complexity and fit. J. Roy. Statist Soc. Ser., 64, 583-639.

Stanford G, Dzienia S, Vander Pol 1975: Effect of temperature on denitrification rate in soils. Soil Sci. Soc. Am. J., 39, 867-870.

Stange F, Butterbach -bahl K, Papen H, Zechmeister -boltenstern S, Li C, Aber J 2000: A process -oriented model of N_2O and NO emissions from forest soils: 2. sensitivity analysis and validation. J. Geophys. Res-OC Atm. (1984–2012), 105, 4385-4398.

Thorsen M, Refsgaard J, Hansen S, Pebesma E, Jensen J, Kleeschulte S 2001: Assessment of uncertainty in simulation of nitrate leaching to aquifers at catchment scale. J. Hydrol., 242, 210-227.

Tiedje JM 1988: Ecology of denitrification and dissimilatory nitrate reduction to ammonium. Biology of anaerobic microorganisms, 717, 179-244.

Toma Y, Kimura SD, Hirose Y, Kusa K, Hatano R, 2007: Variation of emission factor of N_2O derived from chemical N fertilizer and organic matter-A case study of onion fields in Mikasa, Hokkaido, Japan. Soil. Sci. Plant. Nutr., 53, 692-703.

Tonitto C, David MB, Drinkwater, Li C 2007: Application of the DNDC model to tile-drained illinois agroecosystems: model calibration, validation, and uncertainty analysis. Nutr. Cycl. Agroecosyst., 78, 51-63.

Trasar-cepeda C, Gil-sotres G, Leirós M 2007: Thermodynamic parameters of enzymes in grassland soils from galicia, NW Spain. Soil Biol. Biochem., 39, 311-319.

Unep O 1995: IPCC guidelines for national greenhouse gas inventories. http://www.ipcc-tfi.iges.or.jp/meeting/pdfiles/Washington_Report.pdf. (July 2004)

Van Genuchten MT, Leij FJ, Lund LJ 1992: One estimating the hydraulic properties of unsaturated soils. In: Indirect methods for estimating the hydraulic properties of unsaturated soils, pp. 1-14. Univerisity of California, Riverside, CA.

Van oijen, Rougier J, Smith R 2005: Bayesian calibration of process-based forest models: Bridging the gap between models and data. Tree Physiol., 25, 915-927.

Vogt E, Braban CF, Dragosits U, Theobald MR, Billett M, Dore AJ, Tang Y, Van Dijk, Rees, RM, Mcdonald C 2013: Estimation of nitrogen budgets for contrasting catchments at the landscape scale. Biogeosciences, 10, 119.

Wang G, Chen S 2012: A review on parameterization and uncertainty in modeling greenhouse gas emissions from soil. Geoderma, 170, 206-216.

Wang G, Xia J, Chen J 2010: A multi-parameter sensitivity and uncertainty analysis method to evaluate relative importance of parameters and model performance. Geogr. Res., 29, 263-270.

Wattenbach M, Sus O, Vuichard N, Lehuger S, Leip A, Gottschalk P, Smith P 2010: The carbon balance of european croplands: a trans-european, cross-site, multi model simulation study. EGU General Assembly Conference Abstracts. http://adsabs.harvard.edu/abs/2010EGUGA..12.6923W

Weier K, Doran J, Power J, Walters D 1993: Denitrification and the dinitrogen/nitrous oxide ratio as affected by soil water, available carbon, and nitrate. Soil Sci. Soc. Am. J., 57, 66-72.

Wheatley R, Williams B 1989: Seasonal changes in rates of potential denitrification in poorly-drained reseeded blanket peat. Soil Biol. Biochem., 21, 355-360.

Wrage N, Velthof GL. Van beusichem ML, Oenema O 2001: Role of nitrifier denitrification in the production of nitrous oxide. Soil Biol. Biochem., 33, 1723-1732.

Wu L, Mcgechan M 1998: A review of carbon and nitrogen processes in four soil nitrogen dynamics models. J. Agric. Eng. Res., 69, 279-305.

Xu C, Shaffer M, Al-kaisi M 1998: Simulating the impact of management practices on nitrous oxide emissions. Soil Sci. Soc. Am. J., 62, 736-742.

Xu M, Qi Y 2001: Spatial and seasonal variations of q 10 determined by soil respiration measurements at a sierra nevadan forest. Glob. Biogeochem. Cycles., 15, 687-696.

Xu T, White L, Hui D, Luo Y 2006: Probabilistic inversion of a terrestrial ecosystem model: analysis of uncertainty in parameter estimation and model prediction. Glob. Biogeochem. Cycles, 20. DOI: 10.1029/2005GB002468

Yang YM, Small MJ, Junker B, Bromhal GS, Strazisar B, Wells A 2011: Bayesian hierarchical models for soil CO_2 flux and leak detection at geologic sequestration sites. Environ. Earth Sci., 64, 787-798.

Yeluripati J, Van oijen, Wattenbach M, Neftel A, Ammann A, Parton W, Smith P 2009: Bayesian calibration as a tool for initialising the carbon pools of dynamic soil models. Soil Biol. Biochem., 41, 2579-2583.

Yokozawa M, Shirato Y, Sakamoto T, Yonemura S, Nakai M, Ohkura T 2010: Use of the rothc model to estimate the carbon sequestration potential of organic matter application in Japanese arable soils. Soil Sci. Plant Nutr, 56, 168-176.

Zhang F, Li C, Wang Z, Wu H 2006: Modeling impacts of management alternatives on soil carbon storage of farmland in northwest china. Biogeosci. Discuss., 3, 409-447.

Zimmermanm M, Leifeld J, Schmidt M, Smith P, Fuhrer J 2007: Measured soil organic matter fractions can be related to pools in the rothc model. Eur. J. Soil Sci., 58, 658-667.